INFORMATION TO USERS

This manuscript has been reproduced from the microfilm master. UMI films the text directly from the original or copy submitted. Thus, some thesis and dissertation copies are in typewriter face, while others may be from any type of computer printer.

The quality of this reproduction is dependent upon the quality of the copy submitted. Broken or indistinct print, colored or poor quality illustrations and photographs, print bleedthrough, substandard margins, and improper alignment can adversely affect reproduction.

In the unlikely event that the author did not send UMI a complete manuscript and there are missing pages, these will be noted. Also, if unauthorized copyright material had to be removed, a note will indicate the deletion.

Oversize materials (e.g., maps, drawings, charts) are reproduced by sectioning the original, beginning at the upper left-hand corner and continuing from left to right in equal sections with small overlaps. Each original is also photographed in one exposure and is included in reduced form at the back of the book.

Photographs included in the original manuscript have been reproduced xerographically in this copy. Higher quality 6" x 9" black and white photographic prints are available for any photographs or illustrations appearing in this copy for an additional charge. Contact UMI directly to order.

UMI

A Bell & Howell Information Company
300 North Zeeb Road, Ann Arbor MI 48106-1346 USA
313/761-4700 800/521-0600

^{13}C, ^{15}N AND ^{31}P NMR STUDY OF THE SCRAMBLING AND THE REDOX REACTIONS OF SOME GOLD(I) COMPLEXES

BY

MUHAMMAD NASEEM AKHTAR

A Dissertation Presented to the

FACULTY OF THE COLLEGE OF GRADUATE STUDIES

KING FAHD UNIVERSITY OF PETROLEUM & MINERALS

DHAHRAN, SAUDI ARABIA

In Partial Fulfillment of the
Requirements for the Degree of

DOCTOR OF PHILOSOPHY

In

CHEMISTRY

SEPTEMBER, 1996

In The Name of Allah
The Most Merciful
The Most Gracious

KING FAHD UNIVERSITY OF PETROLEUM AND MINERALS DHAHRAN 31261, SAUDI ARABIA

COLLEGE OF GRADUATE STUDIES

This dissertation, written by Mr. Muhammad Naseem Akhtar under the direction of his Dissertation advisor and approved by his Dissertation Committee, has presented to and accepted by the Dean of College of Graduate Studies, in partial fulfillment of the requirements for the degree of DOCTOR OF PHILOSOPHY in chemistry.

Dissertation committee:

Dr. A. A. Isab
Dissertation Advisor

Professor M. I. M. Wazeer
Member

Professor S. A. Ali
Member

Dr. H. P. Perzanowski
Member

Dr. E. Z. Hamad
Member

Dr. A. R. Al-Arfaj
Dissertation Co-Advisor
and Department Chairman

Dean, College of Graduate Studies

Date: 19-11-96

Dedicated to my wife and daughter "Arfah"

ACKNOWLEDGMENT

All praise for **Allah** who, guides us in darkness and helps us in difficulties and all respects are for his holy prophet **Hazrat Muhammad** (peace be upon him) who, enabled us to recognize our creator.

I would like to express my sincere gratitude and appreciation to my dissertation advisor Dr. A. A. Isab, for his versatile and learned guidance during the research work. His generous cooperation, erudite suggestions, invigorating encouragement and patience have always remained a source of inspiration for me.

I am also very grateful to Dr. A. R. Al-Arfaj as co-advisor and as department chairman for his helpful suggestions and cooperation. My sincere gratitudes go to the other members of my dissertation committee, Prof. S. A. Ali, Prof. M. I. M. Wazeer, Dr. H. P. Perzanowski and Dr. E. Z. Hamad for their constructive suggestions.

I am thankful to Prof. M. S. Hussain for carrying out X-ray structure of some of the complexes. I am thankful to central analytical laboratory of Research Institute of KFUPM for performing elemental analysis and NMR of the complexes. I am also thankful to Chemistry Department of KFUPM for providing all research facilities.

I am thankful to Mazhar Hussain, M. Arab and S. Fayaz for their help during this research work.

My sincere thanks also go to my colleagues and friends especially Shakil Ahmed, Azfar Hassan and Syed Zaka Ahmed.

Finally, my thanks and appreciation go to my wife who, supported, helped and encouraged me throughout this study, and who shared with the

difficult times. I am also grateful to my parents and all my family members for their encouragement and support. May God bless them and they live long.

TABLE OF CONTENTS

LIST OF TABLES

LIST OF FIGURES

LIST OF PUBLICATIONS

1. A. A. Isab, A. R. Al-Arfaj and **M. N. Akhtar**, "The redox reaction of gold(I)thiomalate in the presence of selenourea", *J. Coord. Chem.*, **33**, 287-294, 1994.
2. A. A. Isab, **M. N. Akhtar** and A. R. Al-Arfaj, "Carbon-13 nuclear magnetic resonance studies of the redox reaction of aurothiomalate with selenocyanate in aqueous solution", *J. Chem. Soc. Dalton Trans.*, 1483-1487, 1995.
3. **M. N. Akhtar**, H. Ghazi, A. A. Isab, A. R. Al-Arfaj, M. I. M. Wazeer and M. S. Hussain, "^{15}N and ^{31}P NMR studies of cyano (trialkyl/triaryl)phosphine gold(I) complexes", *J. Coord. Chem.*, **36**, 149-157, 1995.
4. A. R. Al-Arfaj, M. S. Hussain, A. A. Isab, and **M. N. Akhtar**, "Bromo[tris(2-cyanoethyl)phosphine]gold(I), [(CEP)AuBr]", *Acta Cryst,*, **C(52)**, 550-553, 1996.
5. A. A. Isab and **M. N. Akhtar**, "Comparative ^{13}C NMR studies of complexation of imidazolidine-2-selenone and its analogous thione to gold(I) thiomalate", *J. Coord. Chem.*, **39**, 21-31, 1996.
6. M. S. Hussain, A. R. Al-Arfaj, **M. N. Akhtar**,and A. A. Isab "$[\{(CEP)_2Au\}^+\{Au(CN)_2\}^-]$: A compound with gold-gold bonds", *Polyhedron*, **15**, 2781-2785, 1996, .
7. **M. N. Akhtar**, A. A. Isab and M. I. M. Wazeer, "Characterization of polymeric gold(I)captopril complex using viscosity and various spectroscopic techniques", *J. Inorg. Biochem.*, **64**, 37-53,1996.
8. **M. N. Akhtar**, A. A. Isab, M. S. Hussain and A. R. Al-Arfaj, "Synthesis of thionato(trimethylphosphine) gold(I) complexes", *Tansition Met. Chem.*, 1996, (in press).
9. A. A. Isab, **M. N. Akhtar**, A. R. Al-Arfaj and M. S. Hussain, "Synthesis and spectroscopic characterization of (trialkyl/triaryl) phosphine gold(I) thiocyanate complexes", *Polyhedron*, 1996, (in press).
10. **M. N. Akhtar**, A. A. Isab and A. R. Al-Arfaj, "^{13}C and ^{15}N NMR studies of gold(I) captopril with selenocyanate, selenourea and thiourea in aqueous solution" *J. Inorg. Biochem.*, (accepted, 1996).

DISSERTATION ABSTRACT

NAME	MUHAMMAD NASEEM AKHTAR
TITLE OF STUDY	^{13}C, ^{15}N AND ^{31}P NMR STUDY OF THE SCRAMBLING AND THE REDOX REACTIONS OF SOME GOLD(I) COMPLEXES
MAJOR FIELD	CHEMISTRY
DATE OF DEGREE	September, 1996

The interaction of antiarthritic drug aurothiomalate $(Autm)_n$ with thiourea, selenourea, imidazoildine-2-selone, SCN^- and $SeCN^-$ in aqueous solution has been studied using ^{13}C NMR spectroscopy. It has been observed that the thiourea forms a 1:1 complex with $(Autm)_n$, SCN^- causes an increase in the polymerization of $(Autm)_n$, while, selenourea, imidazolidine-2-selone and $SeCN^-$ cause redox reactions with $(Autm)_n$ to form metallic gold, metallic selenium and thiomalic disulfide.

The characterization of polymeric gold(I)captopril $(Aucap)_n$ has been carried out using viscosity and electronic, mass, ^{13}C and ^{15}N NMR spectroscopies. It was observed that the degree of polymerization in $(Aucap)_n$ is much higher than that of $(Autm)_n$. Mass spectroscopy has shown two characteristic routes of fragmentation. It has been observed that $(Aucap)_n$ also forms 1:1 complex with thiourea, while it undergo a redox reaction with selenourea and $SeCN^-$ to produce metallic gold, metallic selenium and captopril disulfide.

The ligand scrambling reaction of $R_3PAu^{13}C^{15}N$ complexes to form $[(R_3P)_2Au]^+$ and $[Au(^{13}C^{15}N)_2]^-$ species has been studied using ^{13}C, ^{15}N and ^{31}P NMR spectroscopy in a series of complexes. We have reported $^1J_{(^{31}P-^{13}C)}$, $^1J_{(^{13}C-^{15}N)}$, $^2J_{(^{31}P-^{13}C)}$ and $^3J_{(^{31}P-^{15}N)}$ coupling constants in these complexes and have observed various trends in them with respect to basicity of phosphine ligands. The free energy of activation in these complexes is also measured using ^{31}P NMR band shape analysis.

The antisymbiotic *trans* effect in a series of $R_3PAuS^{13}C^{15}N$ complexes has been studied using infrared, ^{13}C, ^{15}N and ^{31}P NMR spectroscopies. It has been observed that unlike $R_3PAu^{13}C^{15}N$ complexes, the $R_3PAuS^{13}C^{15}N$ complexes do not undergo ligand scrambling reactions.

DOCTOR OF PHILOSOPHY DEGREE

KING FAHD UNIVERSITY OF PETROLEUM AND MINERALS

DHAHRAN, SAUDI ARABIA

خلاصة الرسالة

اسم الطالب	:	محمد نسيم أختر
عنوان الدراسة	:	دراسة تفاعلات تبادل وتأكسد بعض مركبات الذهب بواسطة مطيافية الرنين النووي المغناطيسي ^{31}P و ^{15}N و ^{13}C .
التخصص	:	كيمياء
تاريخ الدرجة	:	سبتمبر ١٩٩٦ م – جمادى الأولى ١٤١٧ هـ

تمت دراسة تفاعل العقاقير المثبطة للالتهابات المفصلية مع ثيوريا وسلينويوريا وأميدازولين -٢ - سيلون و مجموعات SCN^- و $SeCN^-$ في المحاليل المائية باستعمال مطيافية الرنين النووي المغناطيسي ^{13}C. وقد لوحظ أن الثيوريا تكون مركب بنسبة ١ : ١ مع $(Autm)_n$ و SCN^- وتسبب ازدياد بلمرة $(Autm)_n$ بينما تسبب السلينويوريا والأميدازوليدين -٢-سيلون و $SeCN^-$ تفاعلات أكسدة مع $(Autm)_n$ ويتكون نتيجة لذلك الذهب المعدني والسلينيوم المعدني وكبريتيد الثيومماليك .

اختبرت خصائص اللزوجة والكتلة الالكترونية ومطيافية الرنين النووي المغناطيسي ^{13}C و ^{15}N لكابتوبريل ا لذهب البولمري $(Aucap)_n$ فلوحظ أن درجة التبلمر في $(Aucap)_n$ أعلى منها في $(Autm)_n$ كما أظهرت مطيافية الكتلة وجود مسارين في طريقة تحطم $(Aucap)_n$. كما لوحظ أيضاً أن $(Aucap)_n$ تكون مركب بنسبة ١ : ١ مع الثيوريا بينما يحدث تفاعل أكسدة مع السيلينويوريا و $(SeCN^-)$ لانتاج ذهب معدني وسيلينيوم معدني وكبريتيد الكابتوبريل .

وتفاعلات التبادل لمركبات $(R_3PAu^{13}C^{15}N)$ لتكوين $[(R_3P)_2Au]^+$ و $[Au(^{13}C^{15}N)_2]^-$ تم دراستها باستخدام مطيافية الرنين النووي المغناطيسي ^{31}P و ^{15}N و ^{13}C في مجموعة من المركبات . كما تم دراسة ثابت الازدواج (J) في هذه المركبات كالتالي : $^1J(^{31}P^{13}C)$ و $^1J(^{13}C^{15}N)$ و $^2J(^{31}P^{13}C)$ و $^3J(^{31}P^{15}N)$ ولوحظ اختلافات متعددة تعتمدعلى قاعدية متصلة الفوسفين . وقد قيست الطاقة الحرة في هذه المركبات باستخدام التحليل الشكلي (المظهري) لمطيافية الرنين النووي المغناطيسي ^{31}P .

كما درس تأثير متصلات الفوسفين على قاعدية في مركبات $R_3PAuS^{13}C^{15}N$ باستخدام الأشعة تحت الحمراء ومطيافية الرنين النووي ^{31}P و ^{15}N و ^{13}C. كما تم ملاحظة أنه على خلاف مركبات $R_3PAu^{13}C^{15}N$ فان مركبات $R_3PAuS^{13}C^{15}N$ لا تقوم بتفاعلات التبادل .

درجة الدكتوراة في الفلسفة

جامعة الملك فهد للبترول والمعادن

الظهران ، المملكة العربية السعودية

CHAPTER 1

INTRODUCTION

Since earliest recorded times, gold has captured the attention and imagination of men and women. Its beauty, luster, malleability, resistance to corrosion and natural occurrence in the elemental state led to its being one of the first metals discovered [1]. Its beauty, scarcity and inertness made it a prized possession resulting in its utilization in jewelry, coinage and as monetary standard [2]. Today gold is still used in jewelry and as a monetary standard, but its high thermal and electrical conductivity along with its inertness make it ideal for employment in the electronics and aerospace industries [3]. Gold also has applications in the area of medicine including dentistry, for the treatment of rheumatoid arthritis, for anti tumor activity and for the treatment of pemphigus, a skin disorder [4].

1.1 MEDICINAL USE OF GOLD

Gold complexes have been used for a half century with mixed success in the treatment of rheumatoid arthritis and recently for pemphigus. The use of

gold complexes as medicine is called chrysotherapy. This name chrysotherapy is derived from chrysos, the Greek word for gold.

1.1.1 Rheumatoid arthritis

Rheumatoid arthritis is a disease of the joint, which seems to start with an attack on the synovial membrane which spreads to the lining on the top of the bone, resulting in irreparable joint damage. The cause of disease is unknown, with various factors such as heredity, physical stress, viruses , accidents etc., all suggested as playing a part in its commencement. The disease is systematic, affecting many joints and is an autoimune process in which the presence of large number of white blood cells for long period of time in synovial tissue seems to destroy it. This damage results in very swollen and painful joints which contain large amounts of fluid.

The use of gold complexes for the treatment of rheumatoid arthritis was first reported in 1929 [5]. Since that time there have been a number of controlled studies which indicate that gold can provide effective and long lasting relief [6,7].

Several gold(I) complexes are used for the treatment of rheumatoid arthritis, which are shown in Figure 1.1 with their trade names. Most important of them are gold(I) thiomalate (myochrysine) and auro thioglucose (solganal) which are water soluble and are administered intramuscularly. These gold complexes are polymeric in nature [8] by sulfur bridging. Recently it has been reported that 2,3,4,6-tetra-*o*-acetyl-1-thio-β-D-glucose (triethyl phosphine) gold(I), with trade name "auranofin" is very effective anti-arthritic agent [9]. Auranofin is monomeric in nature and is lipophilic, therefore it is taken orally.

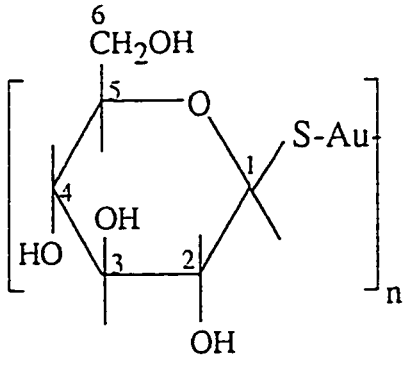

Gold(I) thioglucuse (Solganal)

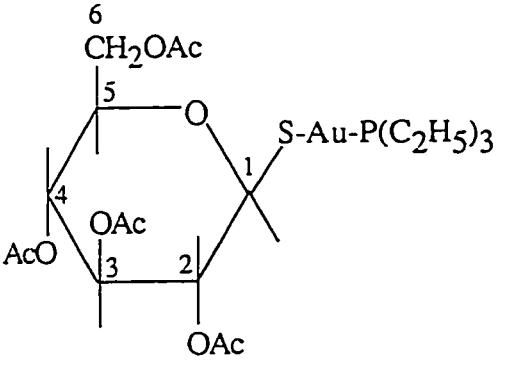

Auranofin

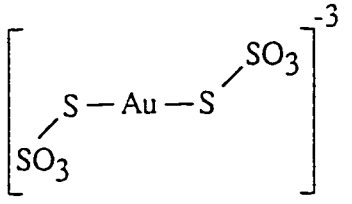

Gold(I) thiosulfate (Sanochrysine)

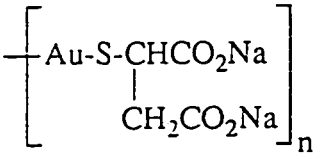

Gold(I) thiomalate (Myochrysine)

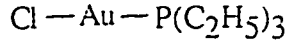

Chloro(triethylphosphine)gold(I)

Figure 1.1 Structure of some important gold drugs.

Extensive pharmacological investigations and clinical tests have been conducted and gold complexes are considered to have intracellular sites of action, since the gold becomes localized in intracellular organelles [10], but there is as yet no accepted mechanism of gold therapy.

Some speculations about the mechanism are given below.

1. Inhibition of lysosomal enzymes in phagocytic cells, which are responsible for causing joint inflammation [11], it is supported by the accumulation of gold in synovium during chrysotherapy.
2. Stops the growth of the infectious agent (bacteria, mycoplasma, virus etc.) responsible for the disease.
3. Affects joint structure through stabilization of collagen by cross linking or altering abnormal disulfide bonding in proteins. The known reactivity of gold(I) with protein sulphydral groups may indicate that gold modulates sulphydral equilibria [12]. Depletion of protein SH groups may be contributing factor to the destruction of connective tissue.
4. Gold is known to inhibit the enzymes for prostaglandin synthesis [13] leading to its anti inflammatory effect.

One of the factor that makes it difficult to assess these mechanisms is the limited amount of information available on the transport and metabolism of the gold drugs. Since gold(I) complexes normally undergo ligand exchange reactions quite readily and rapidly, the gold species that exerts the therapeutic effect may be very different from the drug itself.

It is well known that gold(I) thiolate drugs (polymers) do not enter into red blood cells [14,15]. However tobacco smoking is known to increase the concentration of gold in red blood cells during chrysotherapy. These

polymeric gold(I) thiolates react with the cyanide ion to yield the aurocyanide complex ion, $[Au(CN)_2]^-$, which is readily taken up by red blood cells [16-21]. Thus chrysotherapy patients who are tobacco smokers accumulate gold in their red blood cells from injectable drugs, while non smokers do not [22]. Cyanide is probably acting as a shuttle to carry gold into red blood cells, and it is unlikely that the aurocyanide complex ion is bound within the cell, as a result cyanide from the inhaled smoke alters the metabolism of gold and therefore reaction of the cyanide with gold(I) thiolates in vivo are therapeutically significant [19-21]. It was found that thiolate complexes react with cyanide (CN^-) even at the low concentration forming intermediate $[RS\text{-}Au\text{-}CN]^-$, which disproportionate to give $[Au(CN)_2]^-$ that enters the red blood cells and changes the metabolism of the gold drugs [16,18].

1.1.2 Pemphigus

Pemphigus is an autoimune disorder of the skin, which if untreated may become fatal. Pennys *et.al.* [23-25] have reported that it responds to chrysotherapy and that use of gold salts have significant advantages over corticosteroids, which can themselves be fatal.

1.2 GOLD METABOLISM

Gold is an element which is present in the body in sub-trace levels, but which can be accumulated upon environmental exposure or due to deliberate introduction to the organism.

The distribution of gold following injections of its compounds has been thoroughly investigated and it appears to be widely dispersed throughout the body. In a systematic study using rats [26,27] soluble compounds such as $(Autm)_n$, $Na[Au(tg)_2]$ and $Na_3[Au(S_2O_3)_2]$ were found to concentrate in the liver, spleen and kidney, with the greatest concentration in the kidney. These compounds were eliminated primarily via urinary excretion [26]. Insoluble compounds, such as colloidal gold and gold sulfide, accumulate in the same organs, but with the greatest concentration in the liver and with fecal excretion as the primary rout of elimination. A much larger percentage of the gold remained localized at the site of injection [26]. Gold calcium thiomalate, which has a limited solubility, has a distribution and elimination pattern intermediate between the soluble and insoluble complexes [27]. The concentration of gold in the liver, kidneys and spleen following injection of various gold compounds has also been observed in rabbits [28], mice [29] and humans [30,31].

Other sites of gold localization are the bone marrow [32] and synovia [33-35]. The synovial accumulation of gold has been extensively investigated for a possible role in the therapeutic action of gold. The concentration can be as high as 30 μM in patients undergoing gold therapy [35].

Recent examination of tissues from patients undergoing long term chrysotherapy demonstrate that accumulation of gold occurs in muscles, bones, and fats [36].

The natural accumulation of gold in the blood is known to be so small that it cannot be detected by spectrophotometric or atomic absorption techniques, but neutron activation analysis shows a concentration below 1 ng/g tissue [37,38]. A value of 3.5×10^{-10} g/g wet weight has been obtained for healthy

persons. During gold chemotherapy this value increases dramatically. Serum concentrations of 20 to 50 μM gold are obtained during the days immediately following a $(Autm)_n$ injection, and levels of 10-15 μM are routinely maintained during the course of therapy [35,39].

1.3 OXIDATION STATES OF GOLD

Compounds of gold having the formal oxidation states -I, 0, I, II, III and V have been characterized and reported. However among all these oxidation states 0, I and III are the most common oxidation states while other are rare.

1.3.1 Gold (-I, II and V)

The oxidation states of -I, II and V for gold are uncommon, but several complexes in these states have been reported. Only three examples of Au(-I) are known, CsAu and RbAu, which are ionic crystal containing auride ions [40,41]. In these compounds high electronegativity of gold causes the electropositive Cs and Rb to loose one electron. Liquid ammonia solution of Au(-I) is also prepared by dissolving colloidal gold in liquid ammonia solution of alkali metals [42].

Gold(II) complexes usually exist as dimers that contain a gold-gold bond. The $\{Au(Ph_2P(CH_2)S)I\}_2$ [43] and $\{AuCH_2.Et_2PCH_2Cl\}_2$ [44] are known gold(II) complexes as shown in Figure 1.2.

A gold(V) fluoride complex, $\{Xe_2F_{11}\}^+\{AuF_6\}^-$ has been prepared [45] in which $[AuF_6]^-$ ion has the expected octahedral geometry for six

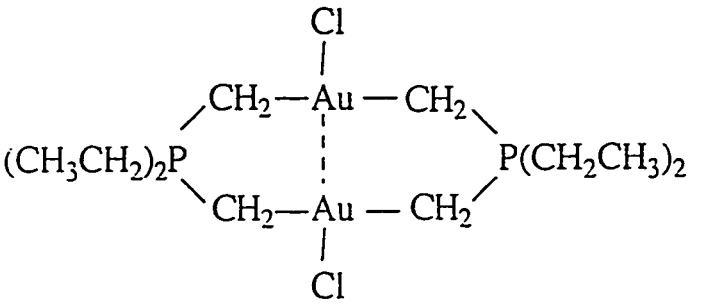

$[AuCH_2.Et_2PCH_2Cl]_2$

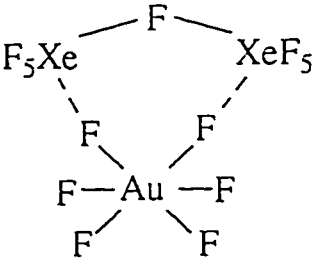

$[\ Xe_2F_{11}]^+[AuF_6]^-$

Figure 1.2 Structure of some gold(II and V) complexes.

coordinate species (Fig.1.2). However, the reduction potentials of these oxidation states are undoubtedly sufficient For Au(-I) to be rapidly oxidized and Au(V) to be rapidly reduced in aqueous solutions.

1.3.2 Gold(0)

Gold is known as noble metal because it does not react with either oxygen or sulfur at any temperature, nor is it oxidized unless there are suitable ligands present. Gold in earth's crust can be extracted by reaction of cyanide to form $[Au(CN)_2]^-$ which is then reduced to Au^0 by Zn^0. When gold compounds are reduced to metallic gold, colloidal solutions are frequently formed. Number of methods are available to prepare gold solutions of varying degrees of dispersion. Gold solutions are usually very stable and depending on reaction condition, have colors ranging from red, violet to blue.

This colloidal gold is used as radioisotope for diagnostic scans and has been used for rheumatoid arthritis treatment on a limited basis [46].

1.3.3 Gold(III)

Gold(III) generally form square planer four coordinate complexes which are typical of d^8 metal ions of the second and third row transition metal elements. Typical complexes which have been characterized crystallographically include $\{AuCl_4\}^-$ [47,48], $\{Au(en)(SO_3)_2\}^-$ [49]. The tendency to form four coordinate complexes is so strong that complexes of empirical formula L_3Au such as $\{Me_2Au(OH)\}$, $AuBr_3$, $AuCl_3$ in fact contain bridging groups to complete the four coordination about the gold

and are correctly formulated as $\{Me_2Au\text{-}\mu\text{-}OH\}_4$ [50], $\{Au_2Br_6\}$ [51] and $\{Au_2Cl_6\}$ [52] as shown in Figure 1.3.

Although five and six coordinate complexes are rare but they have been prepared including *trans*-diiodobis(o-phenylenedimethylarsine) gold(III) six coordinated [53] and chloro(tetraphenylporphinato) gold(III) [54], trichloro(orthophenanthroline) gold(III) [55] five coordinated as shown in Figure 1.4.

Since focus of this study involves the synthesis and characterization of Au(I) complexes, therefore chemistry of other oxidation states will not be discussed further.

1.3.4 Gold(I)

Gold(I) is a $5d^{10}$ metal ion and is considered as 'soft acid' or class 'b' metal. It can form two, three and four coordinate complexes, but two coordinate complexes, usually resulting in linear structure, are most common and most stable. The true salts of gold(I) such as halides are unstable in the presence of moisture and disproportionate to elemental gold and gold(III). However gold(I) is stabilized by complexing with 'soft ligands' such as thiolates [56-58], thioethers [59], phosphines [56,60] and cyanide [61] etc.

There is a vast amount of literature dealing gold(I) complexes and several crystallographic reviews have been published [62]. Large number of compounds with coordination number two have been prepared for example Ph_3PAuCN [63] Et_3PAuCN [64], auranofin (Et_3PAutg) etc. are shown in Figure 1.5. Similarly a number of gold(I) thiolates have been prepared with ratio of 1:1, which exist in polymeric form using sulfur as bridging

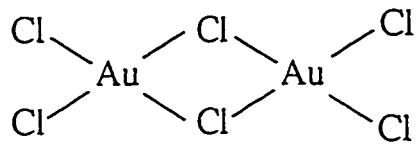

Au_2Cl_6

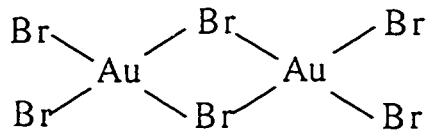

Au_2Br_6

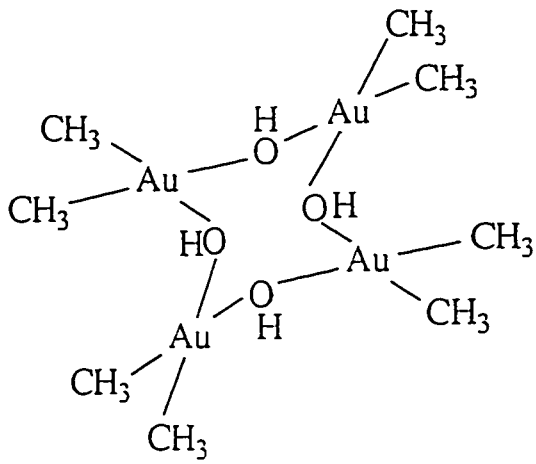

$[(CH_3)_2Au\text{-}\mu\text{-}OH]_4$

Figure 1.3 Structure of some gold(III) complexes with four coordination number.

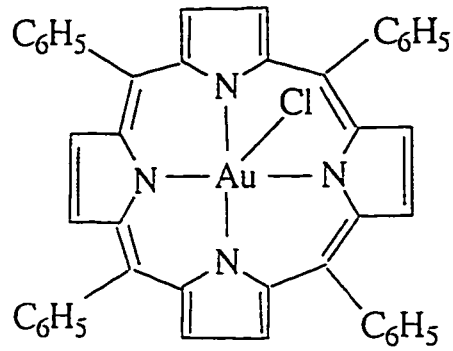

Chloro(tetraphenylporphinato)gold(III)

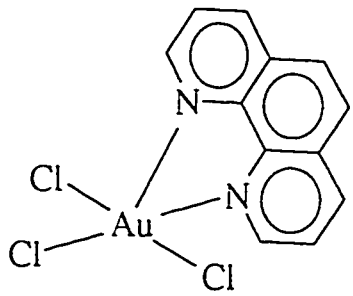

Trichloro(orthophenanthroline)gold(III)

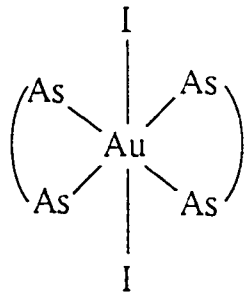

Diiodobis(o-phenylenedimethylarsine)gold(III)

Figure 1.4 Structure of some gold(III) complexes with coordination number five and six.

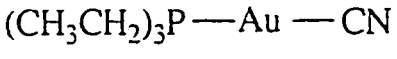

Et_3PAuCN

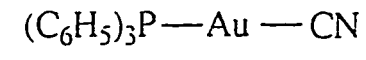

Ph_3PAuCN

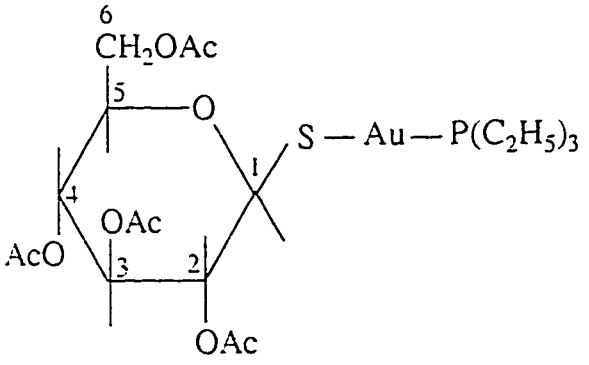

Auranofin

Figure 1.5 Structure of some gold(I) complexes with coordination number two.

element for example $(Autm)_n$, $(Autg)_n$ [65] etc. However some gold(I) complexes with gold-gold interactions have been characterized. Examples of such complexes are $\{RNCS_2Au\}_2$ [66] where R=n-pr and $\{AuSCH_2CH_2PEt_2\}_2$ [67] shown in Figure 1.6.

Gold(I) complexes with three and four coordination are also known, most of which have one or more tertiary phosphine ligands. Examples of three coordinate complexes are chlorobis(triphenylphosphine)gold(I) [68] and tris(triphenylphosphine)gold(I) cation [69] having regular trigonal planar geometry (Fig.1.7). Four coordinate complexes include $\{Au(PPh_2Me)_4\}^+$ [70] with nearly tetrahedral geometry (Fig.1.7).

1.4 BONDING IN GOLD(I) COMPLEXES

Gold(I) is $5d^{10}$ system with empty 6s and 6p orbitals. There are two different approaches to explain the bonding in linear two coordinate gold(I) complexes. In both approaches the ligand-gold-ligand axis is treated as Z-axis.

The first simplest approach is based on valence bond treatment with sp hybridization of 6s and $6p_z$ orbitals and ligands donate electron pairs to these hybrid orbitals of gold [71]. The degree of hybridization for the gold will be dependent upon the electronegativity of the two ligands. In agreement to the Bent's rule, that maximum 's' character will be present in the bond to the least electronegative element [72]. In the case of Ph_3PAuCN, the phosphine-gold bond has predominantly 's' character while the cyanide-gold bond has predominantly 'p' character [71].

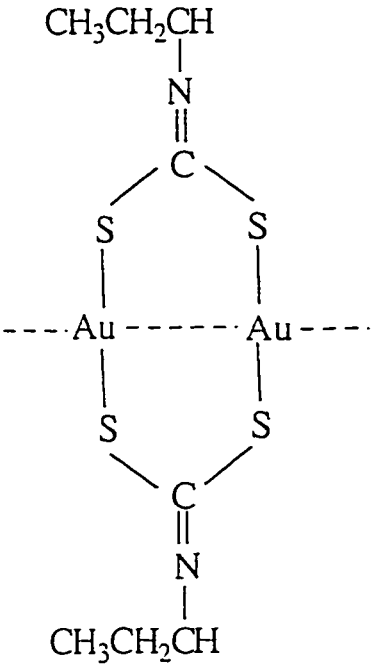

$[CH_3CH_2CHNCS_2Au]_2$

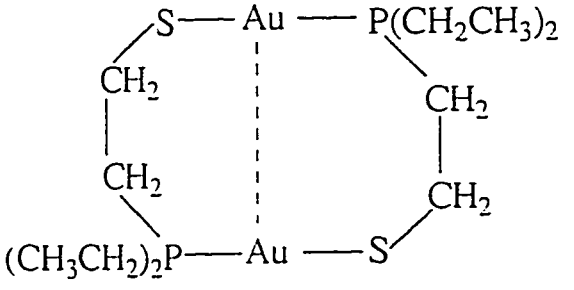

$[AuSCH_2CH_2PEt_2]_2$

Figure 1.6 Structure of some gold(I) complexes with gold-gold interaction.

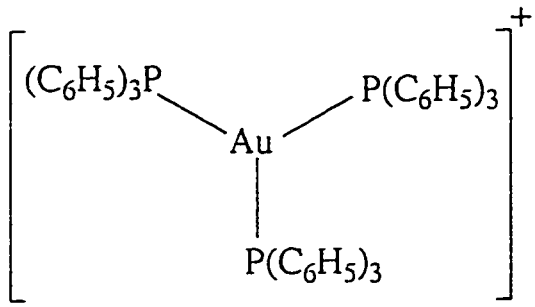

$[Au(PPh_3)_3]^+$

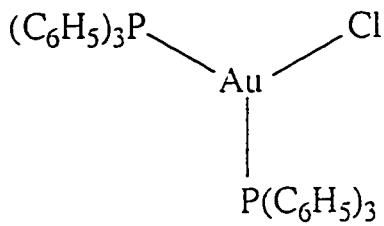

$[(PPh_3)_2AuCl]$

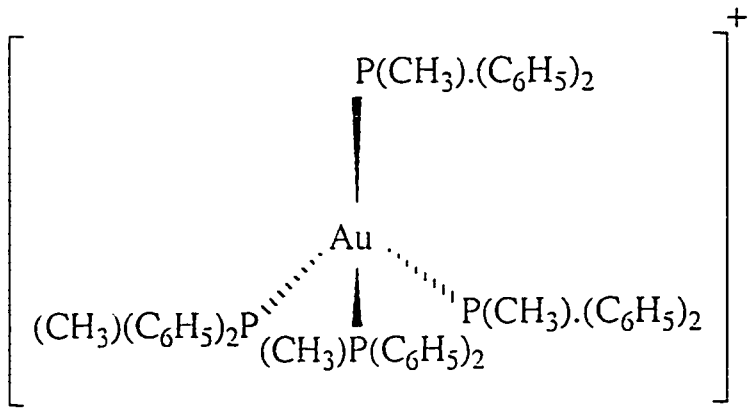

$[Au(PPh_2Me)_4]^+$

Figure 1.7 Structure of some gold(I) complexes with coordination number three and four.

The second interpretation of bonding which is based on linear combination of atomic orbitals (LCAO), and differs from the first due to the involvement of 5d orbitals. The 5d orbitals are certainly not core orbitals because gold(I) complexes, with linear geometry often undergo oxidative addition to give square planner gold(III) complexes with $5d^8$ electron configuration at gold [73]. The mixing of $5d_{z^2}$ and 6s orbitals on the gold produces two new molecular orbitals ψ_1 and ψ_2 (Fig. 1.8) [74]. The electron pair initially present in $5d_{z^2}$ orbital can occupy ψ_1 molecular orbital whose lobes are concentrated in X-Y plane away from the ligands. While further hybridization of ψ_2 molecular orbital with the $6p_z$, gives two empty orbitals directed along the Z-axis that are suitable for bonding. A molecular orbital diagram [75] using this approach is shown in Figure 1.9.

Out of two models presented, the sp hybridization model is a more likely explanation for σ-bonding in the linear two coordinate complexes, although $5d_{z^2}$ orbital may participate slightly [75,76].

Depending upon the nature of ligands gold(I) can also form π-bonds with π-acceptor ligands, which split the degeneracy of $\pi_g(d_{xz},d_{yz})$ and $\delta_g(d_{xy},d_{x^2-y^2})$ molecular orbitals. It is common in R_3PAuCN complexes. In which phosphine groups are σ-donor ligands which increase the electron density on the gold atom. Therefore d_{xz} or d_{yz} orbitals of gold can overlap with the π^* anti bonding orbitals of CN^- ligand and back donation occurs, thus decreasing the electron density on the gold atom and stabilizing it. This back donation is shown in Figure 1.10.

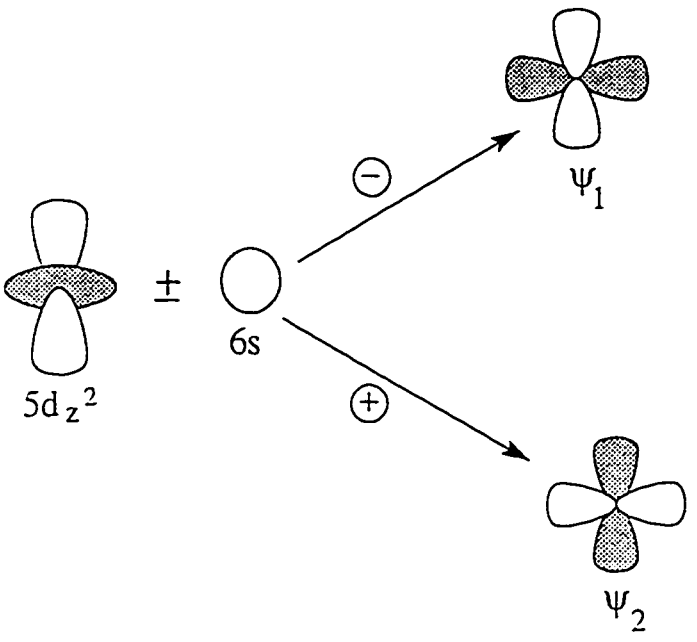

Figure 1.8 Linear combination of $5dz^2$ and 6s orbitals of gold(I)

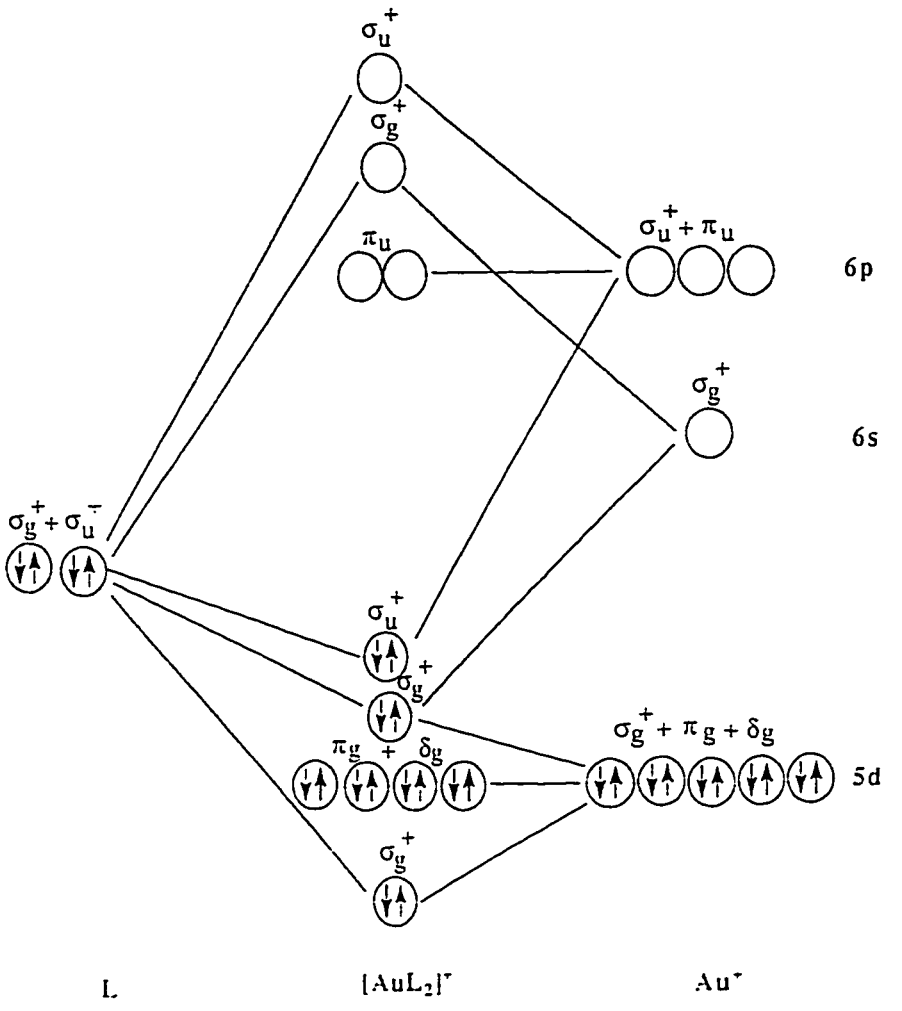

Figure 1.9 Qualitative MO diagram for a σ-bonded complex $[AuL_2]^+$.

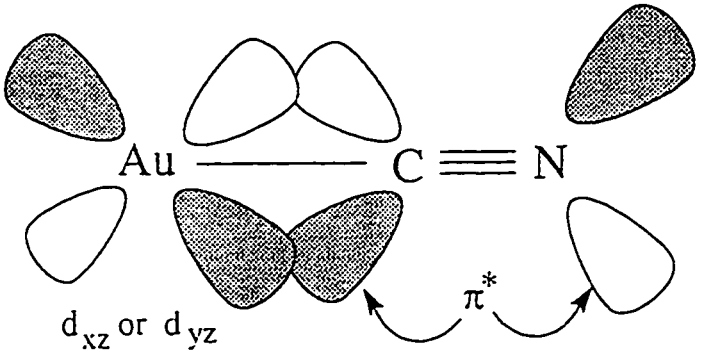

Figure 1.10 Representation of backbonding in R_3PAuCN complex.

1.5 OBJECTIVES OF THE PROPOSED RESEARCH

The goals of this study are to enhance our knowledge of gold(I) chemistry and to gain insight into the metabolism and mechanism of action of gold drugs. The objectives are identified as below.

- Comparative ^{13}C NMR study of interaction of gold(I) thiomalate with selenium containing ligands, and their analogous sulfur containing ligands.
- Characterization of polymeric gold(I)-captopril complex using viscosity and various spectroscopic techniques.
- Synthesis of $R_3PAuCN/R_3PAu^{13}C^{15}N$ complexes and their redistribution studies using ^{13}C, ^{15}N and ^{31}P NMR spectroscopy.
- Synthesis and spectroscopic characterization of $R_3PAuS^{13}C^{15}N$ complexes.

CHAPTER 2

^{13}C NMR STUDY OF THE INTERACTION OF $(Autm)_n$ WITH 'Se' AND 'S' CONTAINING LIGANDS.

Gold(I) thiolate complexes are widely used in the treatment of rheumatoid arthritis [77,78]. The most widely used gold(I) complex, myochrisin or gold(I) thiomalate is a 1:1 complex of gold to thiomalate, as shown below.

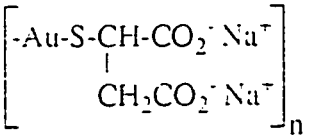

Gold(I) thiomalate

Gold(I) thiomalate can be prepared by the addition of thiomalic acid (RSH) to aqueous sodium tetrachloroaurate(III) either directly, or with prior reduction to gold(I) using bis(2-hydroxyethyl) sulfide as shown by the following equations *2.1* and *2.2*. [79].

$$3RSH + [AuCl_4] \longrightarrow 1/n[AuSR]_n + RS\text{-}SR + 3HCl + Cl^- \qquad 2.1$$

$$[AuCl_4]^- + 2(HOCH_2CH_2)_2S \xrightarrow{H_2O} [ClAuS(CH_2CH_2OH)_2] + HCl + (HOCH_2CH_2)_2SO + Cl^- \qquad 2.2a$$

$$[ClAuS(CH_2CH_2OH)_2] + RSH \longrightarrow 1/n[AuSR]_n + (HOCH_2CH_2)_2S + HCl \quad 2.2b$$

Gold(I) complexes usually form linear two coordinate complexes but not in the case of gold(I) thiolates. In order to attain linear coordination these drugs exist as polymers [4,14,77].

Gold(I) thiomalate is amorphous in nature, therefore its structure cannot be determined by x-ray crystallography. However Elder [80] and Sadler [8] independently have determined the structure of solid myochrisin with the help of extended x-ray absorption fine structure (EXAFS) and wide angle x-ray scattering (WAXS). Gold(I) thiomalate (Myochrisin) exists in solution in different polymeric forms depending upon the method of preparation [81]. The degree of association is known to be dependent on the ionic strength of the solution, concentration of $(Autm)_n$, and pH of the solution [82]. Elder [83,84] has examined its one form using solution x-ray methods and concluded that it is a linear polymer with a centrosymmetric structure. It has a basic 'A-frame' unit with a short gold-gold distance and a thiomalate bridge with a formula of $[Au_8tm_9]^{-8}$. This structure is shown in Figure 2.1.

The interaction of $(Autm)_n$ with various ligands for example CN^- [16,85], disulfides [86], thiols [87,88], thiones [89,90], bovine serum albumin [91] and human red blood cells [92] etc. has been reported in the literature. Most of these ligands, except CN^-, contain a thiol or thione group which act as a binding site for gold(I). In presence of excess of thiols [87,88], CN^- [16,85] and selenols [93,94] $(Autm)_n$ undergoes ligand exchange reaction to form $[Au(SR)_2]^-$, $[Au(CN)_2]^-$ and $[Au(selenol)_2]^-$ respectively, with ejecting free thiomalic acid tm^{-}. This reaction is shown below in equation *2.3*.

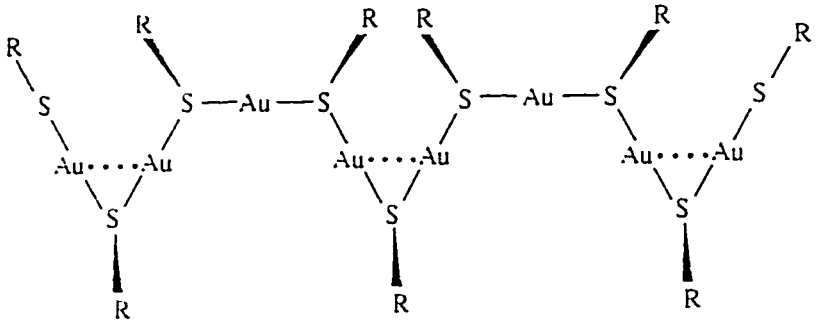

Figure 2.1 Structure of gold(I) thiomalate

$$[Autm]_n + nHL \rightleftharpoons n[L\text{-}Au\text{-}tm] + nH^+ \qquad 2.3a$$

$$[L\text{-}Au\text{-}tm] + HL \rightleftharpoons [L\text{-}Au\text{-}L] + Htm \qquad 2.3b$$

Where $L = RS^-, CN^-$ & RSe^-

However in the presence of thiones, $(Autm)_n$ forms only a ternary complex of the type >C=S-Autm [89,90] as shown below in equation *2.4*.

$$R_2C{=}S + 1/n[Autm]_n \longrightarrow [R_2C{=}S\text{-}Au\text{-}tm] \qquad 2.4$$

The reactions of CN^-, SCN^- with gold(I)-thiolate are important since it has been reported that chrysotherapy patients who are tobacco smokers accumulate gold in their red blood cells from gold-based drugs, while non-smokers do not [20,21]. This was attributed to cyanide from the inhaled smoke which alters the metabolism of gold containing drugs, because it binds with gold(I) forming $[Au(CN)_2]^-$ complex. The log β_2 for $[Au(CN)_2]^-$ complex is reported to be 36.6 [95]. The CN^- is known to undergo two reactions: reversible binding to met-hemoglobin and irreversible oxidation to thiocyanate [96]. If the CN^- generated by smokers in the red blood cells and is oxidized to thiocyanate, it is important to know whether the interaction of $(Autm)_n$ with SCN^- will occur or not and as such we investigated the interaction of KSCN with $(Autm)_n$. Comparative reactions between KSeCN with $(Autm)_n$ and $KSe^{13}CN$ with $[Au(tm)_2]^-$ using ^{13}C NMR spectroscopy are also studied. To the best of our knowledge this is the first study in which disproportionation and redox reactions of [NCSe-Au-tm]$^-$ complex are reported.

Although a large amount of work has been done on the complexation of $(Autm)_n$ with sulfur containing ligands, very little is known about the interaction of selenol or selenone containing ligands. It has been reported

that $(Autm)_n$ and gold(I) thioglucose inhibit glutathione peroxidase[97,98] present in human red blood cells (having seleno-cysteine as an active binding site), which affects its ability to protect the cells from peroxidative damage.

Since there is very little information available regarding the interaction of selenol or selenone containing ligands with gold(I), it should be of interest to study the interaction of $(Autm)_n$ with selenone containing ligands using ^{13}C NMR spectroscopy and to compare the results with their sulfur analogs.

2.1 RESULTS

^{13}C NMR studies of interaction of $(Autm)_n$ and $[Au(tm)_2]^-$ with thiourea (TU), selenourea (SeU), imidazolidine-2-selone (SeImt), thiocyanate (SCN^-) and selenocyanate ($SeCN^-$) has been carried out. The details are given below.

2.1.1 Resonance assignment

The ^{13}C NMR resonance assignments of gold(I) thiomalate $(Autm)_n$, gold(I)bisthiomalate $[Au(tm)_2]^-$, thiomalic disulfide $(tm)_2$, free thiomalate (tm^-), thiourea (TU), selenourea (SeU), Imidazolidine-2-thione (Imt), Imidazolidine-2-selone (SeImt), $[tm\text{-}Au\text{-}SeCN]^-$ and glycerol are shown in Figure 2.2 with their chemical shifts.

Resonance assignments of various gold(I) complexes and ligands

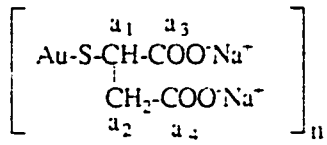

$(Autm)_n$

-*C*H- (a_1=47.9), -CH_2- (a_2=47.9), -CH-CO_2^- (a_3=182.2), -CH_2-CO_2^- (a_4=179.6)

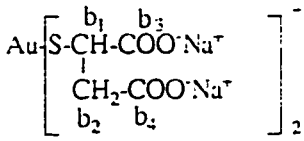

$[Au(tm)_2]^-$

-*C*H- (b_1=43.3), -CH_2- (b_2=47.7), -CH-CO_2^- (b_3=184.7), -CH_2-CO_2^- (b_4=184.8)

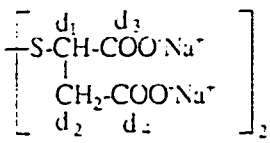

$(tm)_2$

-*C*H- (d_1=54.3,54.0), -CH_2- (d_2=41.1), -CH-CO_2^- (d_3=180.0), -CH_2-CO_2^- (d_4=179.1)

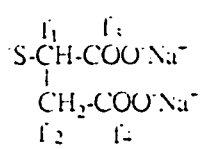

tm^-

-*C*H- (f_1=42.2), -CH_2- (f_2=45.1), -CH-CO_2^- (f_3=181.4), -CH_2-CO_2^- (f_4=180.4)

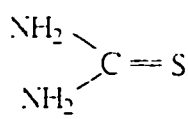

Tu

δ (^{13}C) 182.6

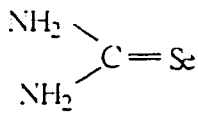

SeU

δ (^{13}C) 176.6

Figure 2.2 (continued)

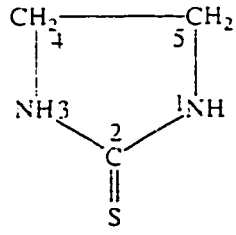

Imidazolidine-2-thione (Imt)

C_2 =182.1, C_4 & C_5 =45.38

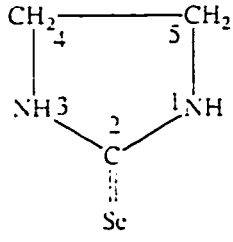

Imidazolidine-2-selone (SeImt)

C_2 =163.0, C_4 & C_5 =46.21

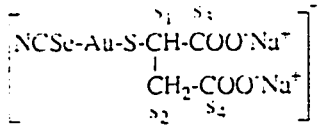

[tm-Au-SeCN]$^-$

-CH- (s_1=42.0), -CH_2- (s_2=52.8), -CH-CO_2^- (s_3=180.0), -CH_2-CO_2^- (s_4=179.1)

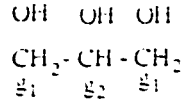

Glycerol

-CH-(g_1=72.88) and -CH-(g_2=63.35)

Figure 2.2

2.1.2 ^{13}C NMR study of interaction of $(Autm)_n$ with Selenourea and Thiourea.

0.274g of $(Autm)_n$ was dissolved in D_2O to prepare 2.0 ml of 0.30 M solution, which was pale yellow in color. The pH* of the solution was adjusted at 7.40. Then thiourea (TU) was added as a solid to this $(Autm)_n$ solution at various molar ratios and their ^{13}C NMR spectra were recorded and are shown in Figure 2.3 and ^{13}C chemical shifts for various resonances are given in Table 2.1. The pale yellow colored solution became colorless on addition of thiourea (TU). From Figure 2.3B to 2.3E it is clear that addition of thiourea results in a upfield shift of the a_1 resonance from 47.81 to 46.50 ppm, while the a_2 resonance remained almost unshifted. The a_3 resonance was shifted from 181.98 to 183.08 ppm and the a_4 resonance shifted from 179.44 to 181.22 ppm. The thione carbon resonance of thiourea moved from free chemical shift of 182.64 to 180.30 ppm at a 1:1 ratio of $(Autm)_n$:TU and to 181.22 at 1:2 ratio of $(Autm)_n$:TU.

Same experiment was repeated with selenourea and $(Autm)_n$ at a pH* of 7.40. The solution was kept under nitrogen atmosphere and it became colorless on first addition of selenourea. When the ratio of $(Autm)_n$:selenourea was 1.0:0.5, some metallic gold was formed in the NMR tube. When this ratio was increased to 1.0:1.0, a colorless ppt was formed in the NMR tube. It is important to note that no metallic selenium was formed during this titration. The ^{13}C NMR spectra of this experiment are shown in Figure 2.4 and chemical shifts for various resonances are given in Table 2.2.

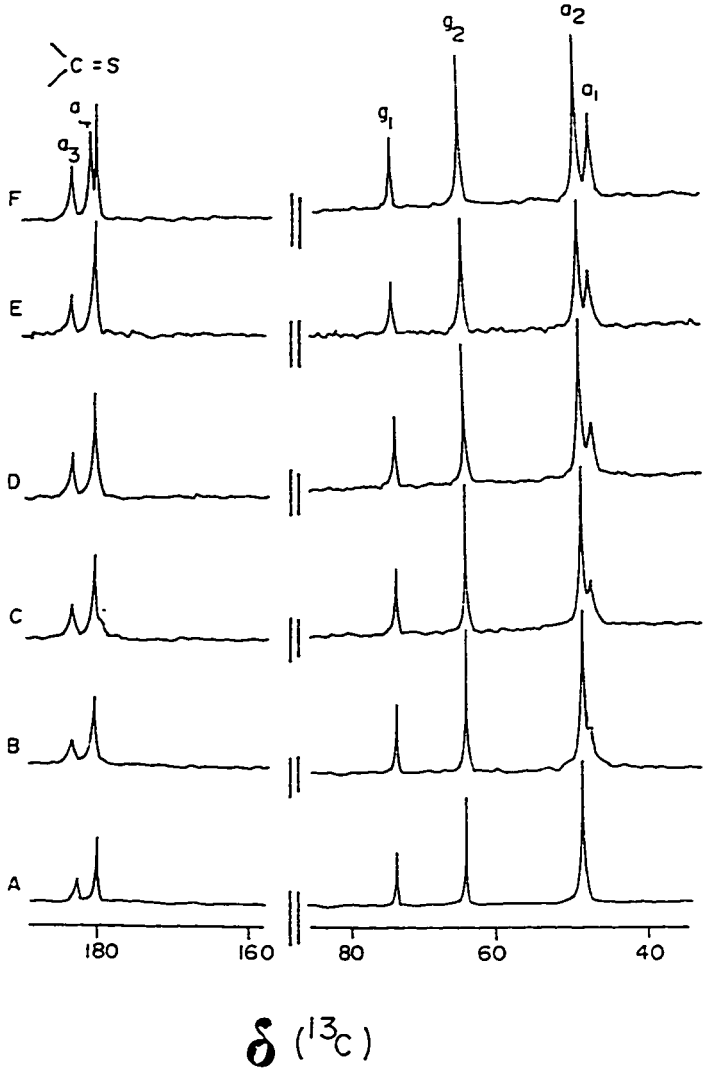

Figure 2.3 The 50 MHz ^{1}H noise-decoupled ^{13}C NMR spectra of 0.30 M $(Autm)_n$: x TU at pH* 7.40, where 'x' is (A) 0.000, (B) 0.075, (C) 0.150, (D) 0.225, (E) 0.300 and (F) 0.600

TABLE 2.1 ^{13}C NMR chemical shifts of $(Autm)_n$:thiourea(TU) at various molar ratios. The values are taken from Figure-2.3

Figure 2.3	$(Autm)_n$:TU	a_1	a_2	a_3	a_4	C of TU
-	0.00:1.00	-	-	-	-	182.64
A	1.00:0.00	47.81	47.81	181.98	179.46	[a]
B	1.00:0.25	47.00	47.86	182.65	179.85	[a]
C	1.00:0.50	46.79	47.87	183.02	180.09	179.27
D	1.00:0.75	46.58	47.85	183.23	180.22	179.88
E	1.00:1.00	46.50	47.86	183.37	180.30	180.30
F	1.00:2.00	46.13	47.82	183.62	180.41	181.22

[a] The resonance is too small to detect or may be overlapped with other resonances.

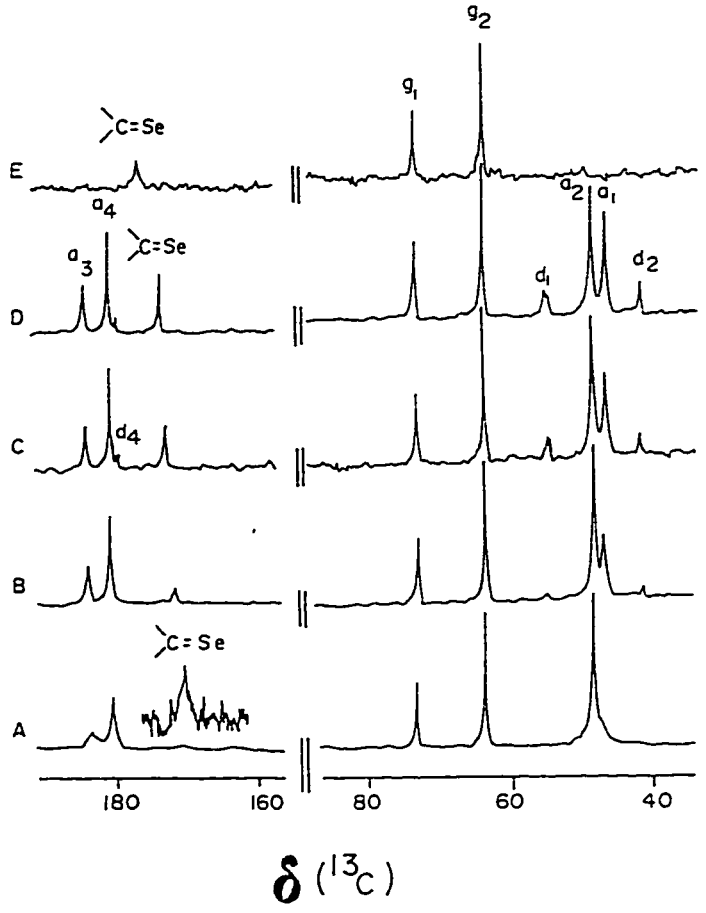

Figure 2.4 The 50 MHz ^{1}H noise-decoupled ^{13}C NMR spectra of 0.30 M $(Autm)_n$: x SeU at pH* 7.40, where 'x' is (A) 0.075, (B) 0.150, (C) 0.225, (D) 0.300 and (E) 0.000 : 0.300

TABLE 2.2 ^{13}C NMR chemical shifts in ppm of $(Autm)_n$:selenourea(SeU) at various mole ratios.

Figure 2.4	$(Autm)_n$:SeU	a_1	a_2	a_3	a_4	d_1	d_2	C of SeU
	1.00:0.00	47.81	47.81	181.98	179.46	-	-	-
A	1.00:0.25	46.99	47.87	182.74	179.93	-	-	169.94
B	1.00:0.50	46.61	47.84	183.33	180.28	54.42 54.07	41.13	171.15
C	1.00:0.75	46.10	47.82	183.72	180.47	54.41 54.05	41.11	172.68
D	1.00:1.00	45.96	47.85	183.92	180.60	54.42 54.07	41.13	173.43
E	0.00:1.00	-	-	-	-	-	-	176.55

Figure 2.4A shows the ^{13}C NMR spectrum of $(Autm)_n$:selenourea at a 1.0:0.25 ratio. In this spectrum a_2 resonance remains unshifted whereas the a_1 resonance was shifted to higher field of 46.99 ppm. The selone resonance of selenourea appeared at 169.44 ppm. Figure 2.4B shows the spectrum of $(Autm)_n$:selenourea at a 1.0:0.50 ratio. The a_1 resonance is shifted further up field whereas a_2 resonance remain almost unshifted. At this ratio some metallic gold was formed in the NMR tube and two thiomalic disulfide resonances d_1 and d_2 appeared at 54.42(54.42 and 54.07 as a doublet) and 41.11 ppm respectively. The a_3 and a_4 resonances appeared at 183.33 and 180.28 ppm respectively. The selone resonance of selenourea was shifted toward a free position at 171.15 ppm. When the concentration of selenourea was further increased the d_1 and d_2 resonances of thiomalic disulfide were increased in intensity and the amount of metallic gold also increased in the NMR tube.

2.1.3 ^{13}C NMR study of interaction of $(Autm)_n$ and $[(Autm)_2]^-$ with Imidazolidine-2-Selone (SeImt).

0.183g of $(Autm)_n$ was dissolved in D_2O to prepare 2.0 ml of 0.20M solution, which was pale yellow in color. The pH* of the solution was adjusted at 7.40 and nitrogen gas was bubbled through the solution during whole experiment. Then imidazolidine-2-selenone(SeImt) was added as solid to $(Autm)_n$ solution at various molar ratio and their ^{13}C NMR spectra were recorded which are shown in Figure 2.5 and the ^{13}C chemical shift of various resonances are given in Table 2.3.

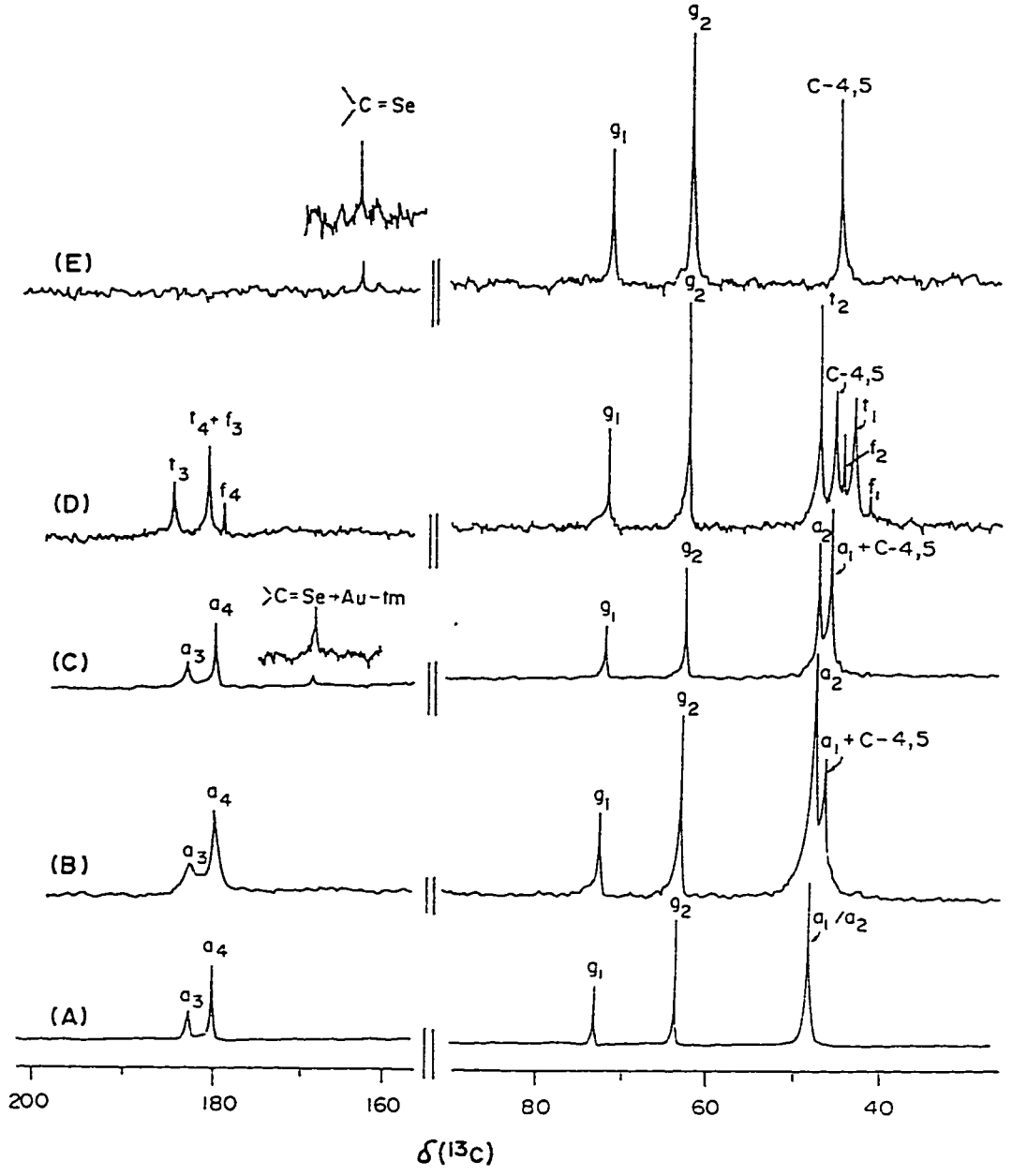

Figure 2.5 The 50 MHz ^{1}H noise-decoupled ^{13}C NMR spectra of 0.20 M $(Autm)_n$: SeImt at pH* 7.40 at various molar ratios: (A) 1.00:0.00; (B) 1.00:0.25; (C) 1.00:0.50; (D) 1.00:0.75; (E) 0.00:1.00.

TABLE 2.3 The ^{13}C NMR chemical shifts in ppm of $(Autm)_n$: SeImt at various molar ratios. The pH* of the solution was 7.40 throughout the titration.

Figure 2.5	$Au(tm)_n$:SeImt	a_1	a_2	a_3	a_4	f_1	f_2	f_3	f_4	C-2	C-4,5
A	1.00 : 0.00	47.81	47.81	181.98	179.46	-	-	-	-	-	-
B	1.00 : 0.25	46.51	47.79	182.57	179.91	-	-	-	-	*	46.51
C	1.00 : 0.50	46.51	47.84	183.28	180.26	-	-	-	-	168.92	46.51
D	1.00 : 0.75	44.08	48.06	184.84	181.07	42.17	45.42	181.07	180.39	*	46.23
E	1.00 : 1.00	-	-	-	-	-	-	-	-	162.97	46.21
	tm'	-	-	-	-	42.17	45.11	181.41	180.39	-	-

*The resonance was not observed.

The a_2 and a_1 resonances of $(Autm)_n$ appeared at 47.81 ppm, a_3 and a_4 resonances were observed at 181.98 and 179.46 ppm, respectively, as given in Table 2.3. When 0.050 M equivalent of SeImt was added as a solid to the $(Autm)_n$ solution, the solution remained pale yellow. The a_1 resonance was shifted to 46.51 ppm, also the C-4,5 resonance of SeImt overlapped with the a_1 resonance. No significant shift was observed in the other resonances except a slight broadening. The C-2 resonance of SeImt was not observed at this stage. When a further 0.05 M (0.10 M total) of SeImt was added to the $(Autm)_n$ solution, the solution became colorless. The a_1 resonance increased in intensity because of the overlapping C-4,5 resonance. At this point, the C-2 resonance of SeImt was observed at 168.92 ppm. There was no significant change in chemical shift of the other resonances. When 0.15 M (total) of SeImt was added to the $(Autm)_n$, the solution remained colorless. However, during the overnight run, some precipitates were observed in the NMR tube. The a_1 resonance was shifted further upfield and free thiomalate (tm^-) resonances (f_1, f_2, f_3 and f_4) were also observed in the spectrum.The C-2 resonance of SeImt was not observed at the 1:0.75 molar ratio of $(Autm)_n$:SeImt. Further titration was discontinued because of the precipitation at this molar ratio.

In second experiment $[Au(tm)_2]^-$ was generated by the addition of 0.18M thiomalic acid (Htm) as a solid to 0.20M $(Autm)_n$ solution. Since $(Autm)_n$ itself contains about 10% free tm^- as a free ligand, [107] therefore only 90% tm^- was added. The pH* of the solution was maintained at 7.40 and was purged with nitrogen gas throughout the titration. Then SeImt and KCN were added as solid to $(Autm)_n$ solution at various ratios and their

^{13}C NMR spectra were recorded which are shown in Figure 2.6 and ^{13}C chemical shifts of various resonances are given in Table 2.4.

The b_1, b_2, b_3 and b_4 resonances due to $[Au(tm)_2]^-$ appeared in the spectrum. There were no f_2 and f_1 resonances in the spectrum due to free tm^- in the spectrum. When 0.10 M equivalent of SeImt was added to the above solution to get the ratio of 1.0:0.5 of $[Au(tm)_2]^-$:SeImt the d_1, d_2, d_3 and d_4 resonances which are due to thiomalic disulfide $(tm)_2$ appeared in the spectrum as shown in Figure 2.6B. The C-4,5 resonance of SeImt also appeared at 46.48 ppm. Some metallic gold appeared in the NMR tube. When $[Au(tm)_2]^-$:SeImt ratio was further increased to 1.0:1.0 the disulfide resonances of $(tm)_2$ were increased in intensity compared to g_2 resonance of glycerol as shown in Figure 2.6C. It is to be noted that there is no C-2 resonance of SeImt observed in Figure 2.6B or 2.6C. After reaching the ratio of 1:1 of ($[Au(tm)_2]^-$: SeImt), solid KCN of 1 and 2 mole equivalents was added to the above solution. As shown in Figure 2.6D and 2.6E, the b_2 resonance was decreased and d_2 resonance was increased in intensity. The $[Au(CN)_2]^-$ resonance was also observed at 154.04 ppm [16,85].

2.1.4 ^{13}C NMR study of interaction of $(Autm)_n$ and $[(Autm)_2]^-$ with thiocyanate(SCN^-) and selenocyanate ($SeCN^-$) in aqueous solution.

A number of experiments were carried out for the comparative study of interaction of $(Autm)_n$ with KSCN and KSeCN using ^{13}C NMR spectroscopy which are described below.

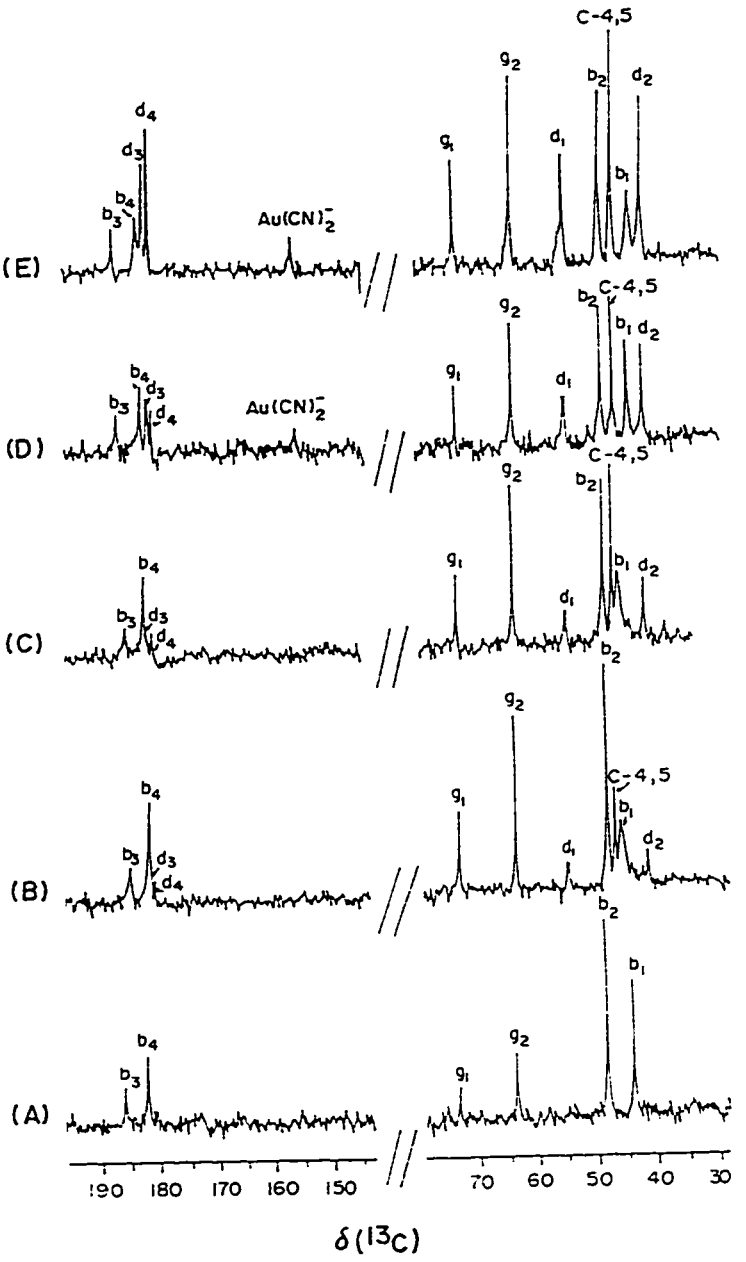

Figure 2.6 The 50 MHz ^{1}H noise-decoupled ^{13}C NMR spectra of 0.20 M (Autm)$_n$: Htm : SeImt : KCN (pH* 7.40) at various molar ratios: (A) 1.00 : 0.90 : 0.00 : 0.00; (B) 1.00 : 0.90 : 0.50 : 0.00; (C) 1.00 : 0.90 : 1.00 : 0.00; (D) 1.00 : 0.90 : 1.00 : 1.00; (E) 1.00 : 0.90 : 1.00 : 2.00.

TABLE 2.4 The ^{13}C NMR chemical shifts in ppm of $(Autm)_n$: Htm : Selmt : KCN at various molar ratios. The pH* of the solution was 7.40 throughout the titration.

Figure 2.6	b_1	b_2	b_3	b_4	C-4,5	d_1	d_2	d_3	d_4	$[Au(CN)_2]^-$
A	43.28	47.71	184.65	180.76	-	-	-	-	-	-
B	45.37	47.91	183.57	180.31	46.48	54.17 54.52	41.15	180.01	179.27	-
C	45.31	47.99	183.85	180.45	46.41	54.15 54.52	41.18	180.03	179.27	-
D	43.62	48.14	185.03	181.07	46.12	54.17 54.53	41.18	180.04	179.27	154.02
E	43.21	48.16	185.22	181.13	46.12	54.12 54.52	41.22	180.04	179.27	154.04

Experiment 1

0.183g of $(Autm)_n$ was dissolved in D_2O to prepare 2.0 ml of 0.20M solution, which was pale yellow in color. The pH* of the solution was adjusted at 7.40. Then KSCN was added as a solid to the $(Autm)_n$ solution at various ratios and their ^{13}C NMR spectra were recorded, which are shown in Figure 2.7 and the chemical shifts of various resonances are summarized in Table 2.5. When 0.20 M KSCN was added as a solid to the $(Autm)_n$ solution (not shown in the Fig.) no change in the spectrum was observed. The concentration of KSCN was then increased to 0.60 M and as shown in Fig.2.7B (pH*7.40), one resonance, labeled as p_1 at 49.0 ppm appeared and a slight shift of a_1 resonance (47.9 to 47.4 ppm) was observed. In low field region no change was observed in the chemical shifts of a_3 and a_4 resonances, however, a new p_2 resonance appeared at 180.8 ppm. The free SCN^- resonance appeared at 133.4 ppm and in the presence of Autm:SCN^- (1:3), the SCN^- resonance appeared at 134.2 ppm. The color of the solution remained pale yellow throughout the experiment .

Experiment 2

Same experiment was repeated to prepare 2.0 ml of 0.20 M $(Autm)_n$ in D_2O. This time KSeCN was added as a solid to $(Autm)_n$ solution at pH* of 7.40 to get various ratios. The solution was purged with nitrogen gas throughout the titration. When 0.0144 g (equivalent of 0.050 M) $SeCN^-$ was added as a solid to the $(Autm)_n$ solution (0.25:1 $SeCN^-$:$(Autm)_n$ equivalent ratio), the color of the solution changed to orange. The chemical shifts of various resonances are summarized in Table 2.6 and ^{13}C NMR spectra are presented in Figure 2.8. Note that two new resonances d_2 at 41.1 and d_1 at 54.3 and 54.0 ppm appeared. The two resonances of d_1 are attributed to the

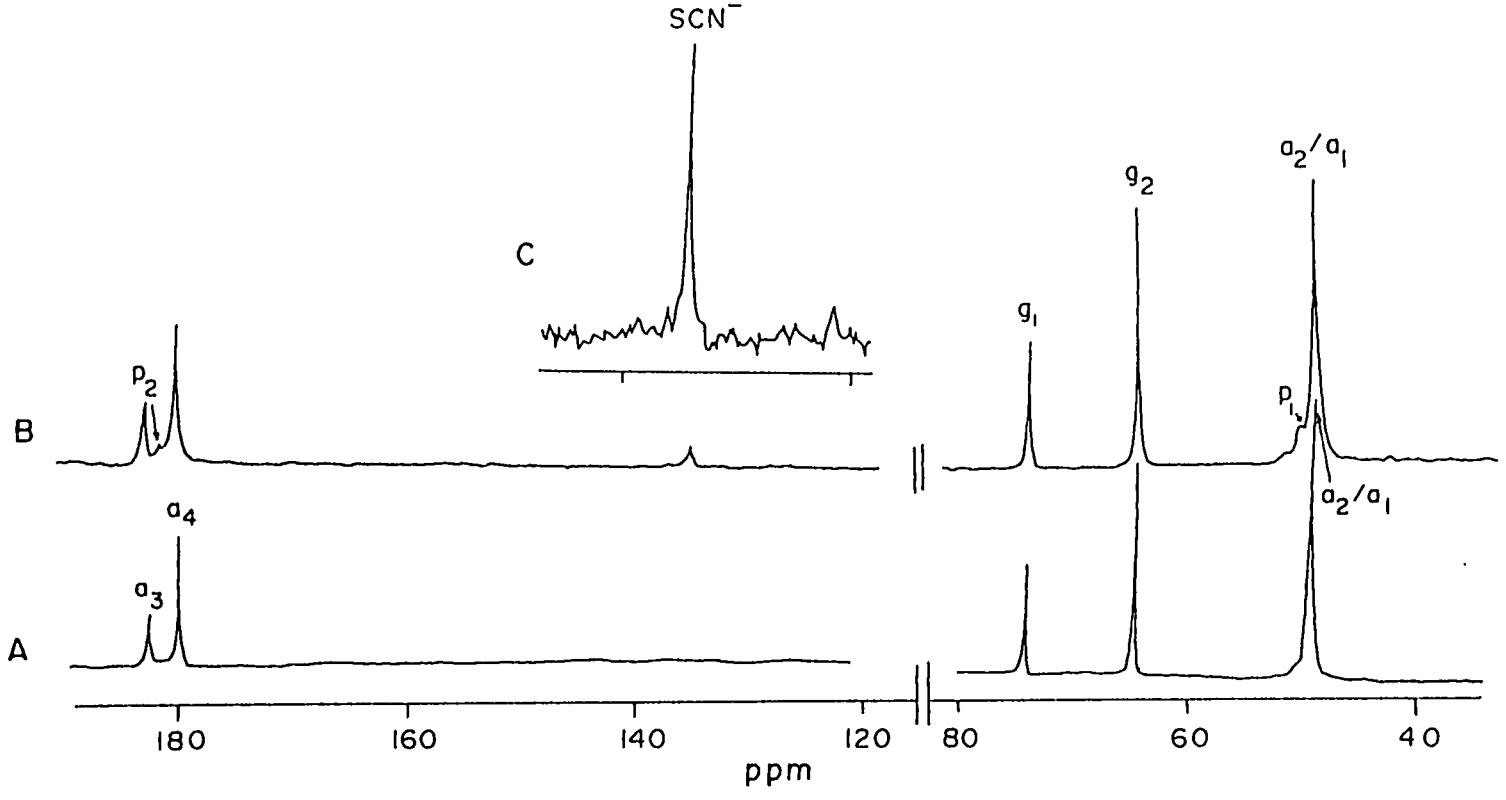

Figure 2.7 The 50 MHz ^{1}H noise-decoupled ^{13}C NMR spectra of (at pH* 7.40): (A) 0.20 M $(Autm)_n$ and (B) 0.20 M $(Autm)_n$: 0.60 M KSCN (C) 0.00 M $(Autm)_n$: 0.20 M KSCN

TABLE 2.5 The ^{13}C NMR chemical shifts in ppm of 0.20 M $(Autm)_n$ in the presence of KSCN.

Figure 2.7	$(Autm)_n$: KSCN	a_1	a_2	a_3	a_4	SCN^-	p_1	p_2
A	0.20 : 0.00	47.9	47.9	182.2	179.6	-	-	-
B	0.20 : 0.60	47.4	47.9	182.2	179.6	134.2	49.0	180.8
C	0.00 : 0.20	-	-	-	-	133.4	-	-

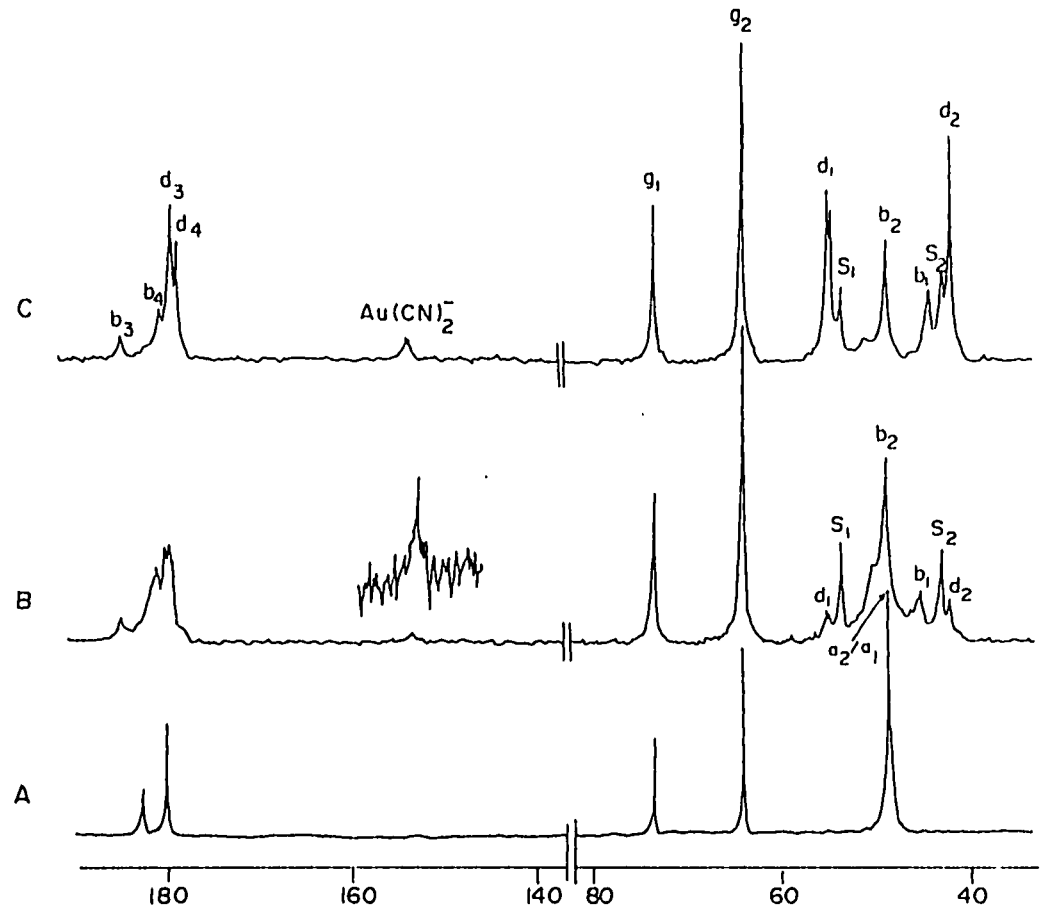

Figure 2.8 The 50 MHz ^{1}H noise-decoupled ^{13}C NMR spectra of (at pH* 7.40): (A) 0.20 M $(Autm)_n$, (B) 0.20 M $(Autm)_n$: 0.05 M KSeCN and (C) 0.20 M $(Autm)_n$: 0.10 M KSeCN

TABLE 2.6 The ^{13}C NMR chemical shifts in ppm of 0.20 M $(Autm)_n$ in the presence of KSeCN.

Figure 2.8	$(Autm)_n$:KSeCN	b_1	b_2	b_3	b_4	s_1	s_2	d_1	d_2	d_3	d_4	$[Au(CN)_2]^-$
A	0.20 : 0.00	47.9	47.9	182.2	179.6	-	-	-	-	-	-	-
B	0.20 : 0.05	43.3	47.9	185.0	181.0	52.8	42.0	54.3 54.0	41.1	180.0	179.1	155.3
C	0.20 : 0.10	43.3	47.9	185.0	181.0	52.8	42.0	54.3 54.0	41.1	180.0	179.1	155.3

diasterotopic -CH carbons of two thiomalic disulfide $(tm)_2$ diastereoisomers. These disulfides resonances are assigned to the spectrum of the disulfide obtained by oxidizing free thiomalate (tm^{-}) with O_2 at pH* 7.40.

The $[tm\text{-}Au\text{-}SeCN]^{-}$ complex aiso gave two resonances in the high-field region due to -CH (s_1) and $-CH_2$(s_2) resonances at 42.0 ppm and at 52.8 ppm respectively, while resonance due to $[Au(CN)_2]^{-}$ appeared at 155.3 ppm . The chemical shift of the free $SeCN^{-}$ resonance in D_2O (pH* 7.50), was observed at 121.1 ppm.

When the concentration of $SeCN^{-}$ was increased to 0.10 M, (0.5:1 $SeCN^{-}$:$(Autm)_n$ equivalent ratio), the solution became dark orange. The spectrum was recorded by an overnight accumulation. The mixture contained dark red precipitates (which is a characteristic of metallic selenium) and some metallic gold on the side of the NMR tube. As shown in Fig. 2.8C, the d_2 and d_1 resonances increased in intensity, while the opposite (a decrease in intensity) was observed for s_2, s_1, b_2 and b_1 resonances. The precipitation of selenium as well as the deposition of metallic gold is explained by the following equations *2.5* and *2.6*.

$$1/n[(Autm)_n] + SeCN^{-} \longrightarrow [tm\text{-}Au\text{-}SeCN] \qquad 2.5$$

$$2\,[tm\text{-}Au\text{-}SeCN]^{-} \longrightarrow \begin{cases} [Au(tm)_2]^{-} + [Au(SeCN)_2]^{-} \\ \quad\downarrow \\ [Au(CN)_2]^{-} + 2Se^{0} \\ (tm)_2 + 2Au^{0} + 2Se^{0} + 2CN^{-} \end{cases} \qquad 2.6$$

Experiment 3

In order to follow the time-dependent disproportionation of unstable [tm-Au-SeCN]$^-$ complex, the following experiment was carried out.

Nitrogen gas was passed through a 0.20 M $(Autm)_n$ solution in D_2O, pH* of the solution was 7.40. One equivalent of $SeCN^-$ solid was added to the $(Autm)_n$ solution. The solution was of slightly brown color and no precipitates were observed. The spectrum 2.9A was recorded after 6 hours. The b_4, b_3, b_2, b_1, s_4, s_3, s_2 and s_1 resonances appeared and their chemical shift values are given in Table 2.7. It should be noted that there are no signs of thiomalic disulfide $(tm)_2$ resonances in this spectrum. The spectrum 2.9B was recorded after 12 hours, the solution was dark brown and some mixture of precipitates was observed, which are due to metallic gold and selenium. This time thiomalic disulfide $(tm)_2$ resonances (d_2 and d_1) are also present in the spectrum. The resonance at 154.0 ppm is presumably due to $[Au(^{13}CN)_2]^-$ as described in equation 2.6. The resonance at 121.2 ppm is due to free $SeCN^-$ ligand. The spectrum 2.9C was recorded after 24 hours, the solution was still dark brown colored and more precipitates of metallic gold and metallic selenium appeared. The s_2 and s_1 resonances disappeared completely and the d_2, d_1 resonances were increased in intensity relative to g_2 resonance of glycerol.

Figure 2.10 shows the approximate percentage intensity of b_1, d_1 and s_1 resonances from the spectrum of Fig. 2.9A to 2.9C. These values are measured relative to g_2 resonance. We did not measure the T_1 values of these resonances because [tm-Au-SeCN]$^-$ complex is unstable. However, these percentage values show how the disproportionation or decomposition of the [tm-Au-SeCN]$^-$ complex proceeds with the time.

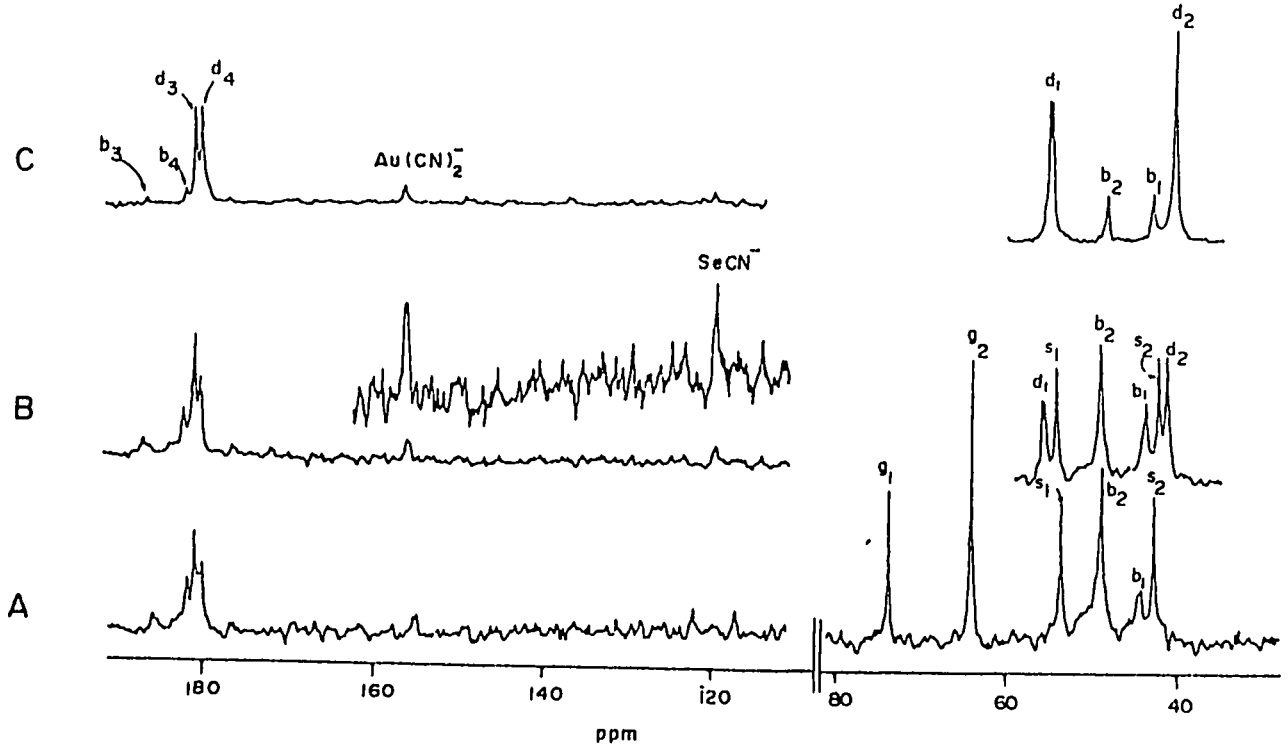

Figure 2.9 The 50 MHz ^1H noise-decoupled ^{13}C NMR spectra of (at pH* 7.40): (A) 0.20 M $(Autm)_n$: 0.20 M KSeCN at pH* 7.40 after 6 hrs (B) after 12 hrs and (C) after 24 hrs.

TABLE 2.7 The ^{13}C NMR chemical shifts in ppm of 0.20 M $(Autm)_n$: 0.20 M KSeCN after different time intervals.

Figure 2.9	t/h	b_1	b_2	b_3	b_4	s_1	s_2	s_3	s_4	d_1	d_2	d_3	d_4	$[Au(CN)_2]^-$
A	6	43.7	47.9	185.0	181.0	52.8	42.0	180.0	179.1	-	-	-	-	-
B	12	43.7	47.9	185.0	181.0	52.8	42.0	180.0	179.1	54.3 54.0	41.1	180.0	179.1	155.3
C	24	43.7	47.9	185.0	181.0	-	-	-	-	54.3 54.0	41.1	180.0	179.1	155.3

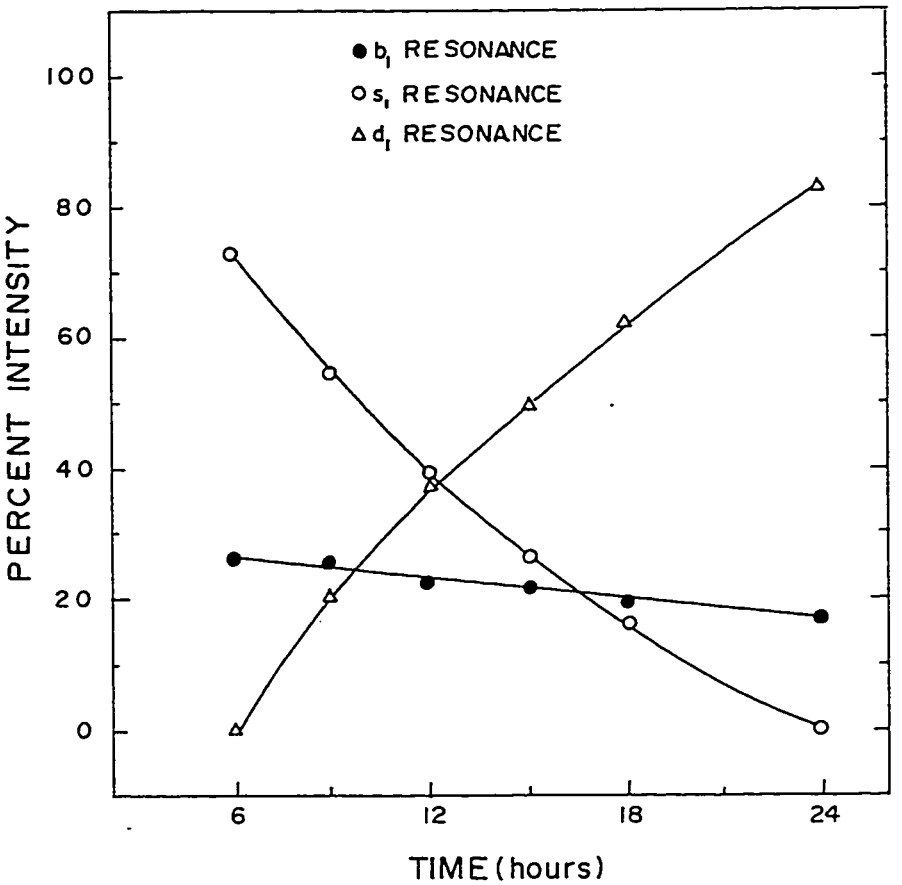

Figure 2.10 The (%) intensity of -CH resonance of $[Au(tm)_2]^-$, [tm-Au-SeCN]$^-$ and $(tm)_2$ species as a function of time (for resonance assignment see the text).

Experiment 4

In order to assign the resonance at 153.18 ppm, the following experiment was carried out. A 0.20 M $(Autm)_n$ solution was prepared in 1.0 ml D_2O under N_2 gas and 1 equivalent of $KSe^{13}CN$ (0.0290 g) was added. A broad resonance at 153.18 ppm and a sharp resonance at 121.16 ppm due to unreacted $Se^{13}CN^-$ appeared. Since the $Se^{13}CN^-$ used was labeled in this experiment, the higher-field resonances were very weak. Two separate resonances due to $[Au(SeCN)_2]^-$ and [tm-Au-SeCN]$^-$ species were anticipated, however, only one broad resonance at 153.18 ppm was observed. This may be due to the exchange between these two species. However, as explained in equation *2.6* both of these species eventually decomposed to give $[Au(CN)_2]^-$. Therefore 153.18 ppm resonance must be due to $[Au(CN)_2]^-$ because it did not disappear even after 24 hours of NMR data accumulation .

Experiment 5

To confirm the assignment of s_1 and s_2 resonances which are believed to be due to [tm-Au-SeCN]$^-$ species, the following experiment was carried out. $[Au(tm)_2]^-$ was generated by the addition of 0.18M Htm as a solid to a 0.20M $(Autm)_n$ solution. Since $(Autm)_n$ itself contains about 10% tm$^-$ as a free ligand, [107] therefore only 90% tm- was added. The pH* of the solution was maintained at 7.40 and was purged with nitrogen gas throughout the titration. As shown in Fig. 2.11A, no free tm$^-$ resonances appeared. The resonance assignments are given in Table 2.8. In this solution one equivalent of $KSe^{13}CN$ (0.0290 g) was added. The color did not change immediately, but after 12 hr's of NMR data accumulation, the color changed to dark brown. The spectrum is shown in Fig 2.11B. It should be

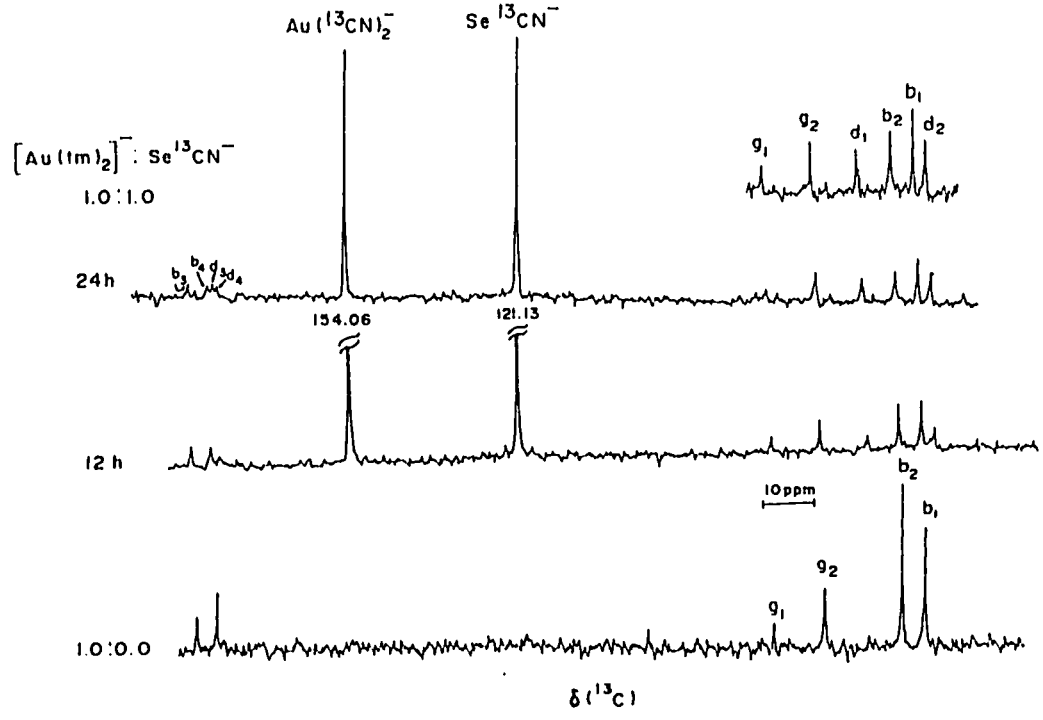

Figure 2.11 The 50 MHz ^{1}H noise-decoupled ^{13}C NMRspectra of (at pH* 7.40): (A) 0.20 M $(AuStm)_n$: 0.15 M Htm at pH* 7.40; (B) solution described as in (A) + 0.20 M labelled $KSe^{13}CN$, spectrum recorded after 12 hrs and (C) after 24 hrs of accumulation.

TABLE 2.8 The ^{13}C NMR chemical shifts in ppm of 0.20 M $[Au(tm)_2]^-$ in the presence of $KSe^{13}CN$.

Figure 2.11	$[Au(tm)_2]^-$: $KSe^{13}CN$	t/h	b_1	b_2	b_3	b_4	d_1	d_2	d_3	d_4	$[Au(CN)_2]^-$	$Se^{13}CN^-$
A	0.20:0.00	-	43.28	47.71	184.65	180.76	-	-	-	-	-	-
B	0.20:0.20	12	43.68	48.12	184.65	180.76	54.46 54.11	41.07	180.0	179.1	154.06	121.13
C	0.20:0.20	24	43.68	48.12	184.65	180.76	54.46 54.11	41.07	180.0	179.1	154.06	121.13

noted that no s_1 or s_2 resonances appeared in the spectrum, only d_1 and d_2 resonances appeared. A sharp resonance appeared at 154.06 ppm, due to $[Au(CN)_2]^-$ and a resonance at 121.13 ppm due to free $Se^{13}CN^-$ is observed. Another spectrum was recorded after 24 hours of accumulation as shown in Fig. 2.11C. Note that compared to g_2 resonance, the d_1, d_2 resonances increased in intensity and b_1, b_2 resonances decreased in intensity.

2.2 DISCUSSION

From the interaction of $(Autm)_n$ and thiourea it is clear that even at the ratio of 1:2 of $(Autm)_n$:thiourea , no free thiomalate (tm^-) resonance appeared, indicating that it only forms [tm-Au-TU] complex and excess thiourea is in fast exchange with bound thiourea. However in the presence of selenourea, some thiomalate (tm^-) is ejected as a free ligand in the solution and is consequently oxidized to thiomalic disulfide $(tm)_2$ and gold(I) is reduced to metallic gold. These results indicate that a redox reaction of $(Autm)_n$ takes place in the presence of selenourea, because only metallic gold appeared in the NMR tube and no selenium metal was formed. However in the presence of other ligands such as CN^- or thiols, tm^- was ejected as a free ligand but was never oxidized to thiomalic disulfide $(tm)_2$. As noted in Tables 2.2 and 2.3 the a_1 resonance is shifted by 1.68 ppm at a 1:1 ratio of $(Autm)_n$:TU, whereas for SeU system at same ratio it is shifted by 1.85 ppm. Similarly thione chemical shift difference between free thione and the complex $(Autm)_n$:TU at a 1.0:0.5 ratio is found to be 3.37 ppm, while that for $(Autm)_n$:SeU at the same ratio is found to be 5.40 ppm.

A comparison of chemical shift difference in thiones and selone resonance of selenourea on complexation with $(Autm)_n$ at a 1:1 ratio, shown in Figure 2.12 and Table 2.9. indicates that selone resonance of selenourea is shifted more than thione resonances (Where thiones are thiourea, imidazolidine-2-thione and 1,3-diazinine-2-thione). The ^{13}C chemical shifts of Diaz and Imt are reported earlier [89, 90].

In previous studies [90] it has been observed that during the ^{13}C NMR interaction of $(Autm)_n$ with Imt a ternary complex of type [>C=S-Au-tm] is formed without ejection of tm^- as free ligand, which is known in case of other thiones [89,90]. However, in the present study it is shown that SeImt behaves differently from Imt and analogous thione ligands; it ejects tm^- as a free ligand at a 1:0.75 ratio of $(Autm)_n$:SeImt. This observation indicates that SeImt binds to $(Autm)_n$ more strongly than all other thiones reported in the literature [18, 89, 90]. As noted in Table 2.10, the C-2 chemical shift difference between the free thione and the complex $(Autm)_n$:Imt at a 1.0:0.5 ratio is found to be 3.65 ppm [90], whereas that for $(Autm)_n$:SeImt at the same ratio is 5.95 ppm. These chemical shift differences between Imt and SeImt bound to $(Autm)_n$ also support our conclusion that SeImt binds to $(Autm)_n$ more strongly than Imt. The a_1 resonance of $(Autm)_n$ shifts by 1.11 ppm at a 1:0.75 ratio of $(Autm)_n$:Imt whereas for SeImt system at the same ratio it is shifted by 3.73 ppm. The C-4,5 resonance of SeImt did not shift much during the titration which indicates that the NH group of the ligand is not involved in binding to gold(I).Thus the electron withdrawal effect for SeImt is much greater than that for Imt when it binds to $(Autm)_n$.

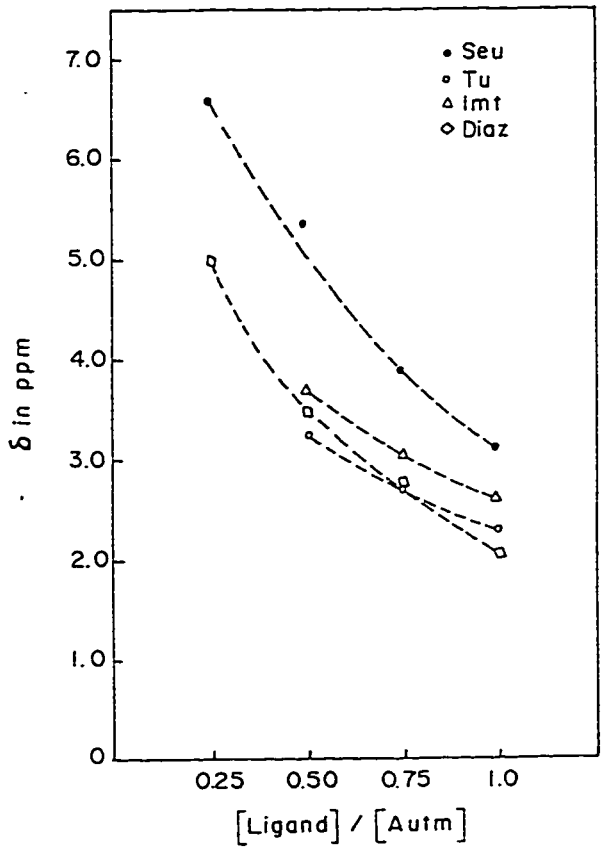

Figure 2.12 The ^{13}C NMR chemical shift differences (in ppm) of C-2 resonance between free and bound ligand after binding with $(Autm)_n$ as a function of concentration. The Imidazolidine-2-thione (Imt) and diazinine-2-thione (Diaz) data are taken from reference 90.

TABLE 2.9 The ^{13}C NMR chemical shift difference (Δ) of C-2 resonance between the free ligand and $(Autm)_n$ complex at a 1.00:0.50 ratio of $(Autm)_n$:ligand at pH* 7.40.

$(Autm)_n$: Ligand	Δ(ppm)	Reference
$(Autm)_n$: Ergothionine(Erg)	3.92	18
$(Autm)_n$: Imidazolidine-2-thione(Imt)	3.65	90
$(Autm)_n$: 1,3-Diazinine-2-thione(Diaz)	3.40	90
$(Autm)_n$: Thiourea(TU)	3.37	This work
$(Autm)_n$: Imidazolidine-2-selenone(SeImt)	5.95	-do-
$(Autm)_n$: Selenourea(SeU)	5.4	-do-

As shown in Figure 2.6, the $[Au(tm)_2]^-$ reacts differently with SeImt than $(Autm)_n$. When both sites of gold(I) are blocked by tm^-, the SeImt replaces tm^- which is then oxidized to thiomalic disulfide and some metallic gold appears in the NMR tube. This observation indicates that SeImt acts as a catalyst for a redox reaction of gold(I) to metallic gold and tm^- to $(tm)_2$.

This redox reaction is not observed when $(Autm)_n$ reacts with SeImt. In this case formation of only ternary complex of [ImtSe-Au-tm] was observed and some free tm^- was ejected in solution which remained in thiol (tm^-) form and did not oxidize to disulfide $(tm)_2$. This redox reaction was expediated when CN^- was added to the solution as shown in Fig.2. Since the formation constant of $[Au(CN)_2]^-$ is 36.6, [95] the CN^- binds to gold(I) leaving tm^- as a free ligand which is oxidized to $(tm)_2$. The reactions of $[Au(tm)_2]^-$ with H^+ and CN^- catalyzed by SeImt can be explained as below:

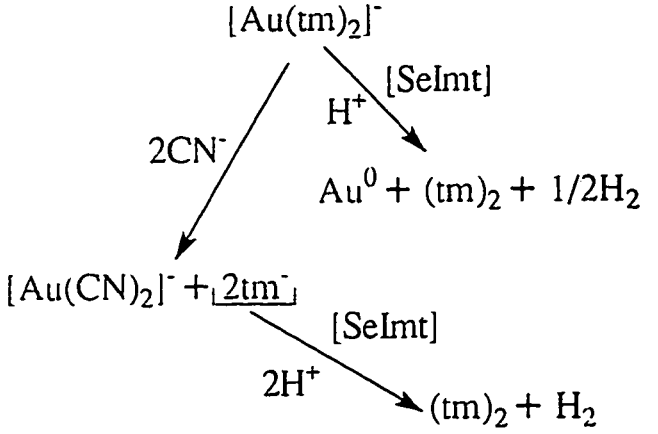

However this redox reaction is observed in case of selenourea with $(Autm)_n$ which can be explained on the basis of the fact that selenourea has a $-NH_2$ group, which might be supporting 'Se' to act as a catalyst. This conclusion is based on previous studies of redox reactions of $[AuCl_4]^-$ with L-methionine and N-acetyl-L-methionine [100]. It was observed that when

-NH_2 group was blocked with acetyl group the rate of redox reaction of gold(III) to gold(I) and oxidation of -S-CH_3 to O=S-CH_3 (i.e. methionine to sulfoxide) was reduced considerably. In Selmt, the -NH group is a secondary amine and therefore not expected to involve in the redox reaction.

Godderd *et al* [101,102] have determined the stability of metal complexes of selenourea as well as thiourea. They have reported that order of affinity towards a class 'b' metal like Hg(II) is more for selenium than for sulfur. Isab [103,104] has also found, while studying the binding of Hg(II) with L-methionine and D,L-slenomethionine, that ^{13}C NMR chemical shift of methyl resonance was shifted by 3.56 ppm in the presence of L-methionine and was shifted by 9.29 ppm in the presence of D,L-slenomethionine. Log K_f values of $CH_3Hg(II)$ for L-methionine and D,L-slenomethionine are reported to be 1.94 and 3.73 respectively in an acidic aqueous solution [105,106].

Arnold *et al* [108] studied the formation constants of $CH_3Hg(II)$ with thiols and its analogous selenols. They reported that the formation constants for selenol-containing ligands are much higher than their analogous thiols. Formation constants K_f of selenocysteine, cysteine, selenopenicillamine and penicillamine are found to be 17.38, 16.67, 17.40 and 16.94 respectively. Also the formation constant for $CH_3HgSeCN$ is determined to be larger than that for CH_3HgSCN [109]. Structural data also suggests that Hg-Se binding in $CH_3HgSeCH_2CH(NH_2)CO_2H_2O$ ($CH_3Hg(II)$-selenocysteinate) complex is stronger than the Hg-S binding in the analogous cysteine complex [110]. These studies also support the fact that selenium-containing ligands bind more strongly to class 'b' metal ions compared to the analogous sulfur-

containing ligands.Since gold(I) is isoelectronic with Hg(II), hence it is not surprising that gold(I) binds more strongly to selenourea than thiourea.

During the interaction of $Au(tm)_n$ with SCN^- in experiment 1 two extra peaks p_1 and p_2 appeared in the ^{13}C NMR spectrum. Similar peaks were observed when NaCl and Na_2SO_4 were added to $Au(tm)_n$ solution. This shows that SCN^- is increasing ionic strength and is polymerizing $Au(tm)_n$ solution further as described earlier.[82]

The results described in experiment 2 indicate that the reactions of $SeCN^-$ with $(Autm)_n$ generate $[tm\text{-}Au\text{-}SeCN]^-$ complex in aqueous solution as shown in equation 2.5. The resonance assignments of b_1,b_2, b_3 and b_4 has been described previously [87]. The d_1, d_2, d_3 and d_4 resonance assignments were confirmed by dissolving Htm in D_2O at pH* 7.4 and oxidizing it with air. The d_2 and d_1 resonances were assigned by off-resonance decoupling and s_1 and s_2 resonances, which appeared after the addition of $SeCN^-$ to $(Autm)_n$ solution, have to be from the $[tm\text{-}Au\text{-}SeCN]^-$ complex as described in equation 2.5. As reported in the literature [111], most $SeCN^-$ containing complexes decompose in aqueous solution in the presence of a majority of metal ions. The s_3 and s_4 resonances of $[tm\text{-}Au\text{-}SeCN]^-$ complex could not be observed, this may be due to overlapping with d_3 and d_4 resonances.

The attempt to generate $[Au(SeCN)_2]^-$ by reducing gold(III) to gold(I) in aqueous solution and then adding $SeCN^-$ ligand failed and only brown precipitates with gold (I) were observed.

The disproportionation of the unsymmetric linear gold(I) complexes are known, [16,85,112,113] as shown in equation 2.7.

$$2\,[RS\text{-}Au\text{-}CN]^- \rightleftharpoons [Au(RS)_2]^- + [Au(CN)_2]^- \qquad 2.7$$

(where RS^- = thiomalate, thioglucose, glutathione etc.)

Similarly the disproportionation reactions of cyano(trialkylphosphine) gold(I) complexes have also been reported by ^{13}C, ^{15}N and ^{31}P NMR spectroscopy.[17,114,115]

$$2\,[R_3P\text{-}Au\text{-}CN] \rightleftharpoons [(R_3P)_2Au]^+ + [Au(CN)_2]^- \qquad 2.8$$

(where R = methyl, ethyl, phenyl group etc.)

However, the unsymmetric complex described in this report [tm-Au-SeCN]$^-$ does not disproportionate according to the reaction described in equation 2.7 because, if it did, the increase in the intensity of the b_1 resonance and decrease in s_1 resonance should have been observed. However, as shown in Figure 2.11 and 2.12 and described in experiment 3 and 4 the intensity of the b_1 resonance does not change, but s_1 transforms directly to d_1. Moreover the intensity of the b_1 resonance of $[Au(tm)_2]^-$ did not change significantly which indicates that $[Au(tm)_2]^-$ species is stable for 6 to 24 hr's period.

Recently a study on the exchange reactions of $(Autm)_n$ with selenopropionate in water was reported.[93] At a 1:2 ratio $(Autm)_n$:selenopropionate the bis [Au(Seleno-propionate)$_2$]$^-$ complex is formed. The tm$^-$ was ejected as a free ligand and unlike the present study, it did not oxidize to $tm)_2$. This observation suggests that selenol simply binds to gold(I) and no redox reaction takes place. Similar reactions were observed with other selenols [94].

The s_1 and s_2 resonances were confirmed (experiment 5) by reacting $Se^{13}CN^-$ with $[Au(tm)_2]^-$ in which the intermediate specie [tm-Au-SeCN]$^-$ was not generated because the Au(I) was blocked from both sides with tm$^-$ however, only the disulfide resonances of thiomalic disulfide appeared as shown in Fig. 2.13A to 2.13C. The sharp resonance at 154.06 ppm in

Figure 2.13C is due to $[Au(^{13}CN)_2]^-$ species [16,85,112-114]. This is simply because no [tm-Au-Se^{13}CN]$^-$ was generated and $[Au(Se^{13}CN)_2]^-$ is unstable and could not be observed even after 24 hr's as shown in Fig. 2.13C. The $[Au(^{13}CN)_2]^-$ may be generated as described in equation 2.6. The $[Au(^{13}CN)_2]^-$ resonance was observed at 154.00 ppm in various studies of gold(I) drugs with CN^- interactions [16,85,112-114].

In all our studies we observed an orange color solution during interaction of $(Autm)_n$ with $SeCN^-$, this color may be due to the generation of Se_2^{2-} species which is known to have orange color as reported in the literature [116-118].

The reaction between $[Au(tm)_2]^-$ and $SeCN^-$ without forming [tm-Au-SeCN]$^-$ intermediate species is explained by the following equation *2.9*

$$[Au(tm)_2]^- + 2SeCN^- \longrightarrow (tm)_2 + Se_2^{2-} + [Au(CN)_2]^- \qquad 2.9$$

As shown in this equation $[Au(CN)_2]^-$ and Se_2^{2-} species are generated which explain the orange color solution as well as a sharp resonance (Fig. 2.13B and 2.13C) at 154.00 ppm which is clearly due to $[Au(CN)_2]^-$ species [16,85,112-114].

The reactions 2.6 to 2.9 are summarized in scheme I which shows the redox cum decomposition of [tm-Au-SeCN]$^-$ and $[Au(SeCN)_2]^-$ species. The final products lead to thiomalic disulfide, $[Au(CN)_2]^-$, orange color solution (due to Se_2^{2-}), metallic gold, metallic selenium and free CN^-. This free CN^- which may be generated in small concentration may exchange further with $[Au(CN)_2]^-$. This exchange reaction will lead to the slight shift of $[Au(CN)_2]^-$ resonance between 153.0 to 155.0 ppm as well as broadening of the $[Au(CN)_2]^-$ resonance [85,112,113].

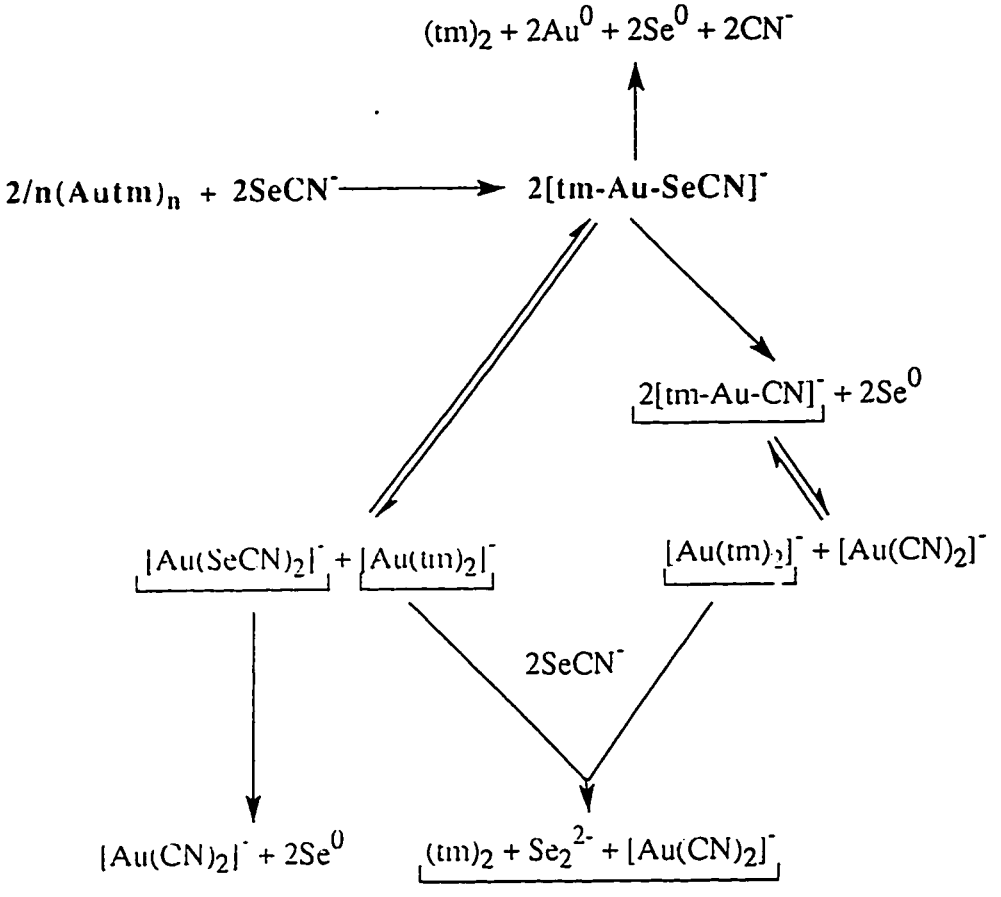
(tm)2 + 2Au0 + 2Se0 + 2CN-
2/n(Autm)n + 2SeCN-
2[tm-Au-SeCN]-
2[tm-Au-CN]- + 2Se0
[Au(SeCN)2]- + [Au(tm)2]-
[Au(tm)2]- + [Au(CN)2]-
2SeCN-
[Au(CN)2]- + 2Se0
(tm)2 + Se2 2- + [Au(CN)2]-

Scheme I

From the results presented above it is clear that selenium-containing ligands bind more strongly to gold(I) drugs than that of the analogous sulfur-containing ligands. If the gold drug enters the red blood cells, it is expected to bind glutathione peroxidase, consequently causing some of the side effects of the drug.

2.3 CONCLUSION

The following conclusions can be madefrom this study.

i. Selenourea and SeImt ligands, acting as a monodentate ligands, bind to $(Autm)_n$ via Se atom only.

ii. The large ^{13}C chemical shift differences of the selone resonance between free and bound ligand indicates that SeU and SeImt binds more strongly to $(Autm)_n$ as compared to their analogous thiones.

iii. The larger shift in a_1 resonance of $(Autm)_n$ in the presence of SeU and SeImt than their analogous thiones also indicate the stronger binding of selone containing ligands than that of thione containing ligands.

iv. The free tm^- from $(Autm)_n$ was ejected in the presence of SeImt, while in presence of SeU it was oxidized to $(tm)_2$, which is never observed in the presence of any analogous thiones.

v. The bis gold(I) thiomalate reacts differently with SeImt than with gold(I) thiomalate.

vi. The reduction of gold(I) to metallic gold and oxidation of thiomalic acid to disulfide is observed only in the presence of selone containing ligands, not in the presence of analogous thiones.

vii. The present study shows that SCN^- increases the polymerization of $Au(tm)_n$ complex. However, $SeCN^-$ oxidizes thiomalic acid (Htm) to thiomalic disulfide $(tm)_2$ and reduces gold(I) to metallic gold in both $Au(tm)_n$ and $[Au(tm)_2]^-$ complexes.

CHAPTER-3

CHARACTERIZATION OF POLYMERIC GOLD(I) CAPTOPRIL COMPLEX

Captopril, 1-[2(S)-3-mercapto-2-methyl-1-oxopropyl]-L-proline, is a recently developed orally active drug for the treatment of high blood pressure [119,120]. High blood pressure can result from the overproduction of angiotension II from inactive angiotension I, the conversion being catalyzed by angiotension-converting enzyme, which is a zinc metalloenzyme [121,122]. The antihypertensive activity of captopril is considered to result from the inhibition of angiotension-converting enzyme, presumably through interaction of thiol group with the enzyme at its active site [119,120]. The thiol group is also the key functional group in the metabolism of captopril, the major metabolites being captopril-disulfide and mixed disulfide with thiols containing aminoacids, peptides and proteins [123,124]. More recently captopril has been used with some success for the treatment of Rheumatoid Arthritis [125] and Migraine [126].

It is well known that proline-containing peptides normally exist as equilibrium mixture of *trans*- and *cis*- isomers with respect to peptide bond involving the proline amino group [127]. The captopril is also expected to

be present in aqueous solution as the *trans-* and *cis-* forms I and II, respectively with their relative population dependent on the protonation state of the molecule [128,129].

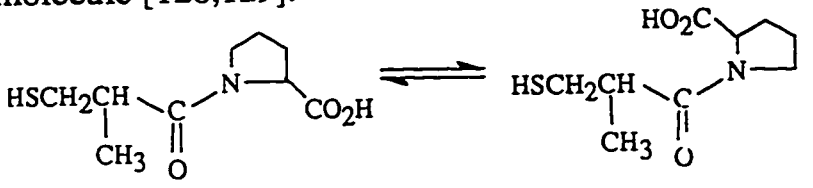

I II

It has been observed that the conformationally restricted angiotension-converting enzyme inhibitors require a *trans-* amide bond of captopril when binding to the enzyme [130]. Since the rate of interchange between the *cis-* and *trans-* conformation by rotation around the C-N bond of the peptide linkage is slow on the NMR time scale [128,129], therefore NMR provides a convenient method for detection of the *cis-* and *trans-* isomers. It has been found that *trans-* isomer is more abundant than that of *cis-* isomer [131].

The captopril has two acidic protons i.e. of carboxylic group and sulfahydral group and is represented as H_2A. When it looses carboxylic proton it is represented as HA^- and with loss of both protons as A^{2-}. Acid dissociation constant for the carboxylic acid and sulfahydral groups of *trans-* and *cis-* isomers has been determined using ^{13}C NMR spectroscopy [132]. The average values obtained for pK_1 of the *trans-* and *cis-* isomers are 3.52 and 2.86 respectively, where K_1 is the acid dissociation constant for carboxylic group as shown in equation *3.1*:

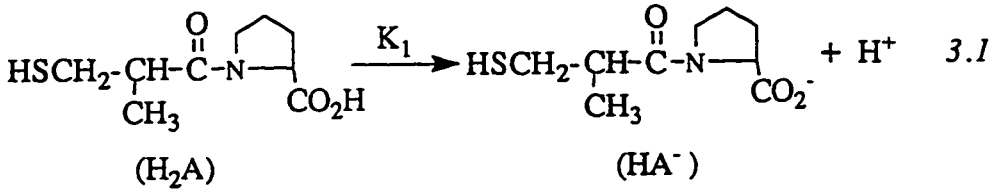

(H_2A) (HA^-) 3.1

The average values for pK_2 have been found to be 9.71 and 9.99 for the *trans-* and *cis-* isomers respectively. Where K_2 is acid dissociation constant of sulfahydral group as shown in equation *3.2*:

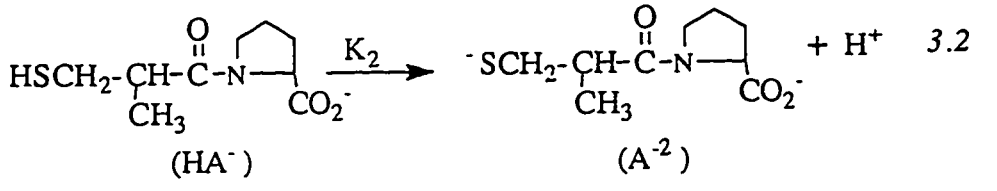

(HA^-) (A^{-2}) 3.2

The *trans-* isomer stability is enhanced in H_2A form of captopril by the intramolecular hydrogen bonding as observed in the other *trans-* isomers of the carboxylic acid forms of the related small peptides as shown below.

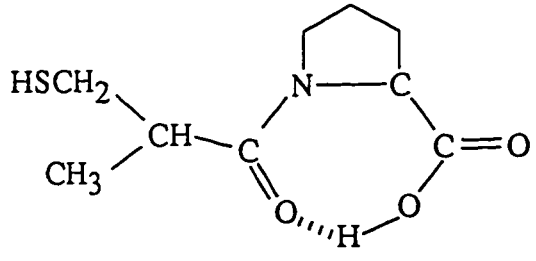

Since the hydrogen involved in the proposed hydrogen bonding is the one being titrated, when the *trans* isomer goes from H_2A to HA^-, the carboxylic group of the *trans* isomer is expected to be some what less acidic than that of *cis-* as observed [131]. Since the *cis* isomer of A^{2-} form is less

stable than that of *trans* isomer due to increased charge-charge repulsion between deprotonated carboxylic group and sulfahydral group, the sulfahydral group of *cis* isomer is expected to be less acidic than that of *trans* which is also observed.

The binding of captopril with heavy metal ions e.g. Zn^{2+}, Cd^{2+}, Pd^{2+} and Cu^{2+} has been reported [133,134]. Since these studies were carried out by potentiometric titration, the *trans*- and *cis*- isomers were not resolved. Complexation of $CH_3Hg(II)$ with captopril has also been studied using ^1H and ^{13}C NMR spectroscopy [135]. It is observed that captopril, like other thiols, reacts with Au^+ to form $(AuSR)_n$ polymers [4,46,82,136,137]. This polymer is insoluble in water except at high pH (~12). While the other anti-arthritic Au(I)-thiolate drugs, like Au(I)-thiomalate $(Autm)_n$, and Au(I)-thioglucose $(Autg)_n$, exist in powder form, Au(I)-captopril remains in the crystalline form. However, due to its polymeric nature we were unable to get reflections for X-ray diffraction. By using various physical techniques, it has been established that these gold(I) drugs have AuS_2 coordination environments formed by bridging of the thiolate ligands between gold(I) ions to form oligomers and these oligomers may be upto octamers [4,46,82,137,138]. However, Au(I)-captopril complex, forms polymers of much higher degree in aqueous solution .

3.1 RESULTS

The characterization of gold(I) captopril $(Aucap)_n$ has been carried out using viscosity, electronic, mass, ^{13}C and ^{15}N NMR spectroscopies. The

interaction of gold(I) captopril $(Aucap)_n$ with CN^-, $SeCN^-$, thiourea (TU) and selenourea (SeU) is also carried out using ^{13}C and ^{15}N NMR spectrosopy. The details are given below.

3.1.1 Preparation of solutions

The preparation of Au(I)-captopril $(Aucap)_n$ is given in full detail in chapter six. In all experiments a desired aqueous solution of $(Aucap)_n$ was prepared at a pH of 12.0 and then various reagents such as potassium cyanide, potassium thiocyanate, potassium selenocyanate, labeled cyanide ($K^{13}CN$, $KC^{15}N$), thiourea (TU) and selenourea (SeU) were added as solids to the aqueous solution.

3.1.2 Mass spectroscopy of gold(I) captopril

The mass spectrum of $(Aucap)_n$ is shown in Figure 3.1. Since electron impact ionization source is highly energetic, we were unable to find molecular ion (equation *3.3*).

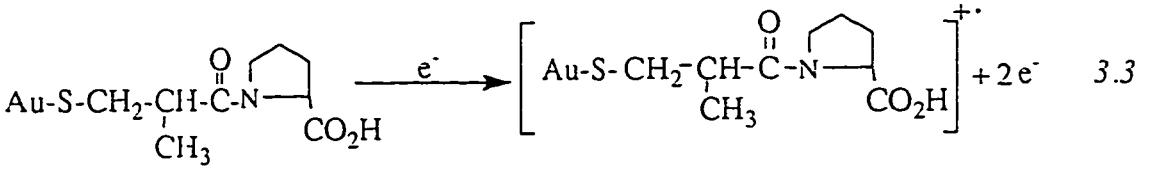

3.3

It was observed that $(Aucap)_n$ on fragmentation follows two characteristic routes as shown in scheme 3.1 and 3.2. In scheme 3.1, $(Aucap)_n$ undergoes gold-sulfur bond cleavage and produces an even electron ion of captopril at a m/z of 216 (equation *3.4*).

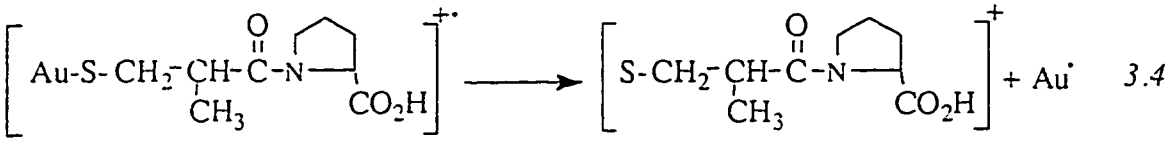

3.4

This captopril ion then undergoes further fragmentation which is

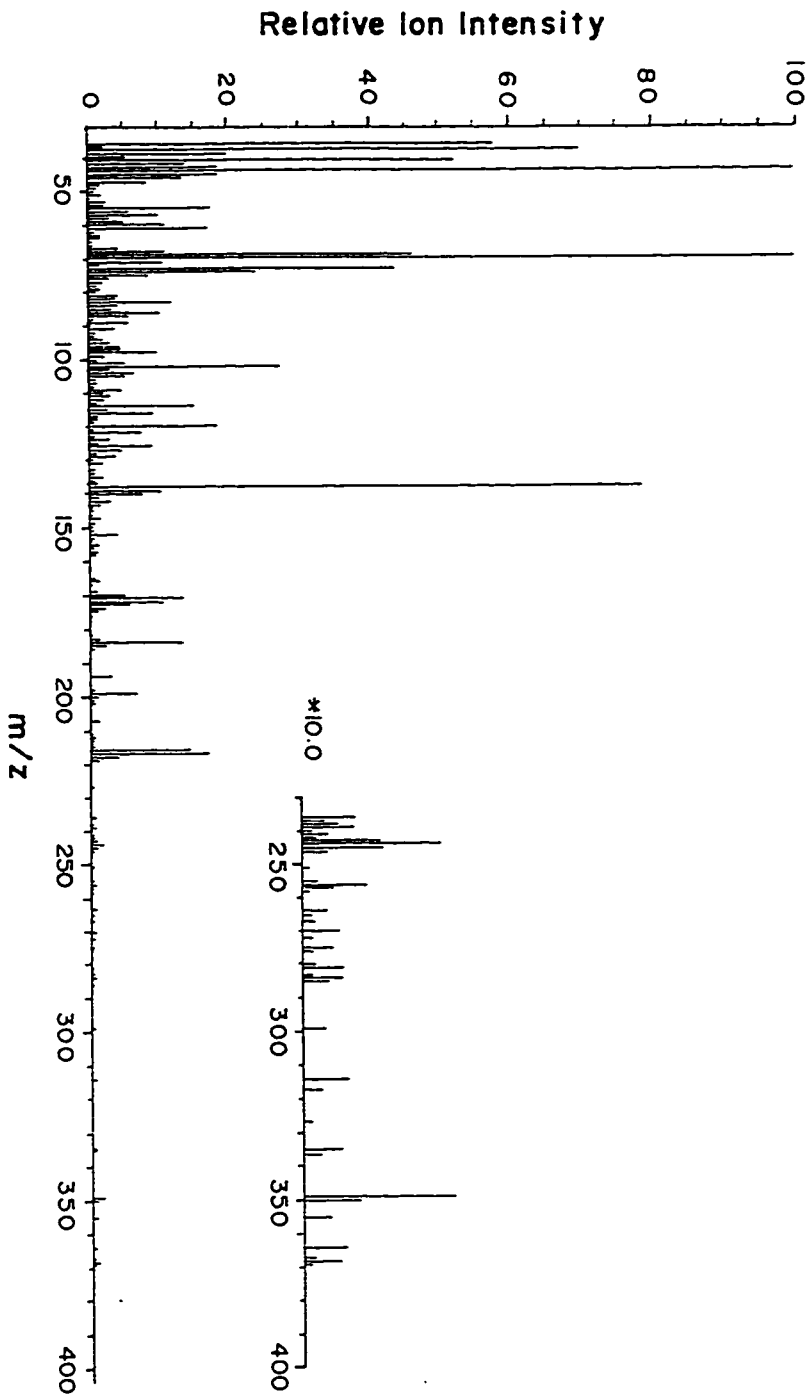

Figure 3.1. Mass spectrum of $(Aucap)_n$ complex.

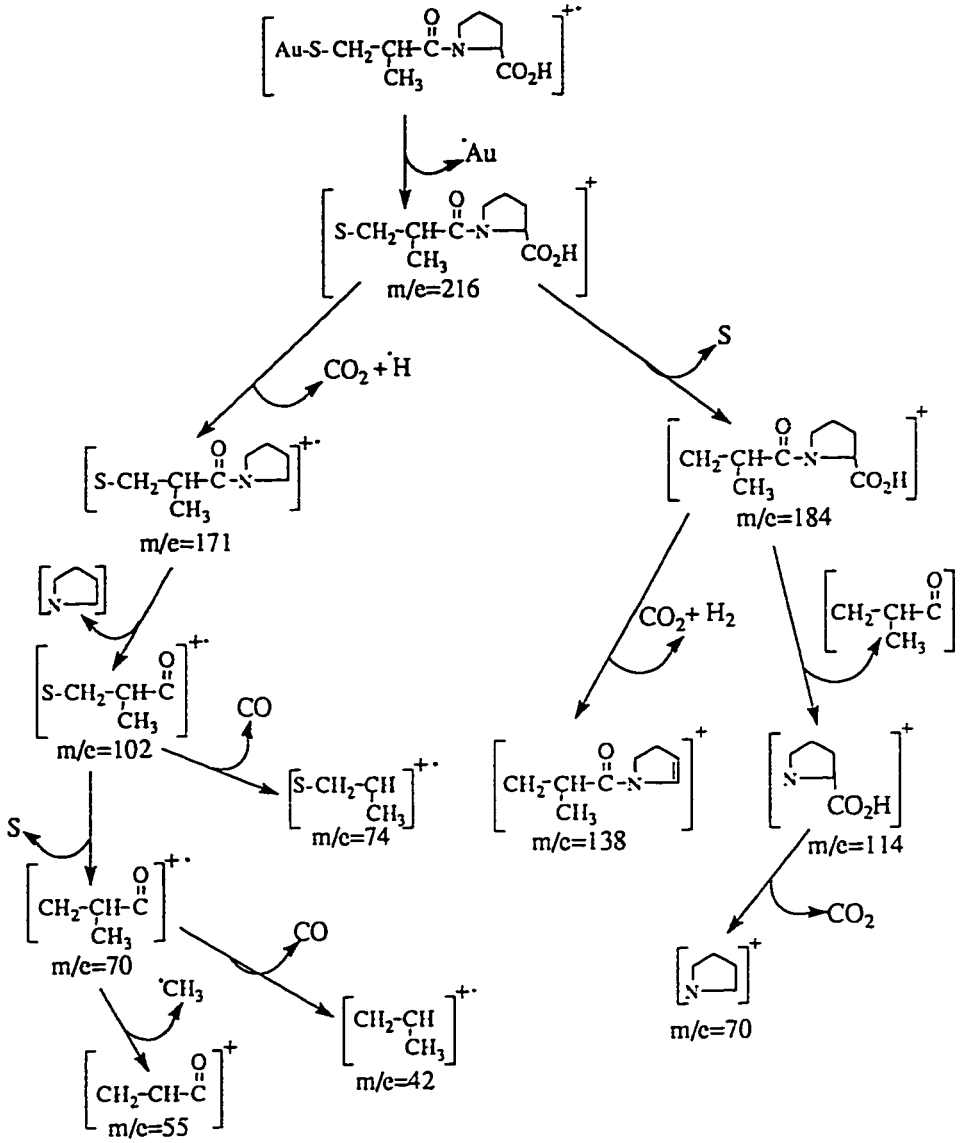
Au-S-CH2-CH(CH3)-C(=O)-N-CO2H
Au
S-CH2-CH(CH3)-C(=O)-N-CO2H
m/e=216
CO2 + H
S
S-CH2-CH(CH3)-C(=O)-N
m/e=171
CH2-CH(CH3)-C(=O)-N-CO2H
m/e=184
S-CH2-CH(CH3)-C(=O)
m/e=102
CO
S-CH2-CH(CH3)
m/e=74
CO2 + H2
CH2-CH(CH3)-C(=O)
S
CH2-CH(CH3)-C(=O)-N
m/e=138
N-CO2H
m/e=114
CH2-CH(CH3)-C(=O)
m/e=70
CO
CH3
CH2-CH(CH3)
m/e=42
CO2
CH2-CH-C(=O)
m/e=55
N
m/e=70

Scheme-3.1

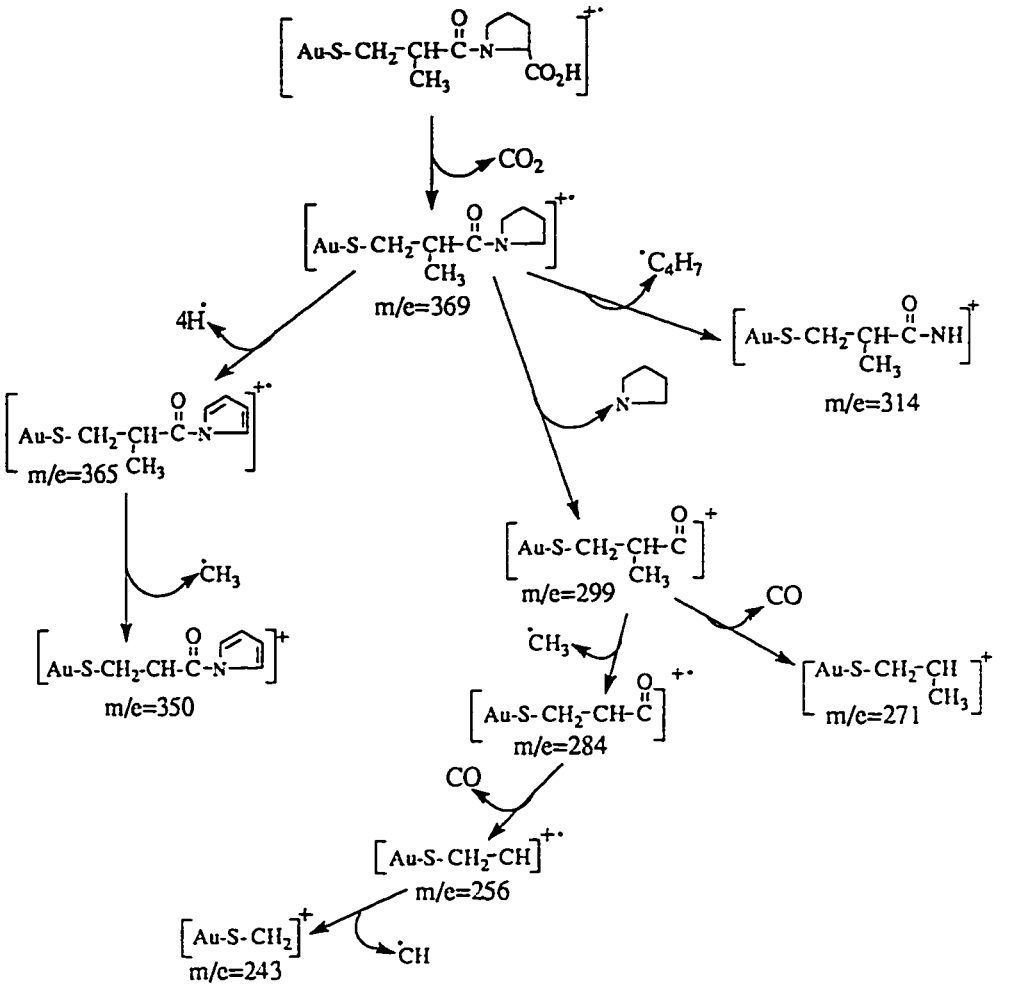
Au-S-CH2-CH-C-N
CH3
CO2H
CO2
m/e=369
C4H7
4H
Au-S-CH2-CH-C-NH
CH3
m/e=314
Au-S-CH2-CH-C-N
m/e=365 CH3
CH3
Au-S-CH2-CH-C
CH3
m/e=299
CO
Au-S-CH2-CH-C-N
m/e=350
CH3
Au-S-CH2-CH-C
m/e=284
Au-S-CH2-CH
CH3
m/e=271
CO
Au-S-CH2-CH
m/e=256
Au-S-CH2
m/e=243
CH

Scheme-3.2

shown in scheme 3.1. The ions arising from the fragmentation of captopril are in very high relative abundance.

In scheme 3.2 monomer Aucap itself undergoes fragmentation. The first fragment is formed with the removal of CO_2 and H· at a m/z of 368 (equation *3.5*).

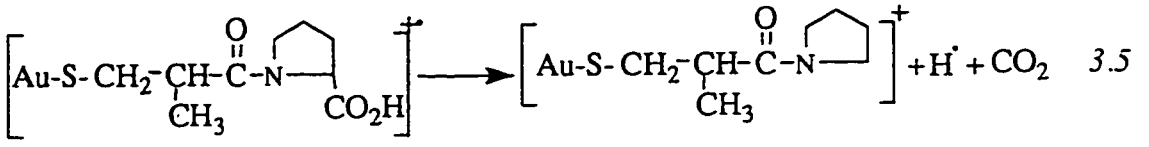

3.5

This ion further undergoes fragmentation as shown in scheme 3.2. The fragments arising from Aucap molecule itself are in very low relative abundance. Carbon dioxide is produced in both fragmentation routes with a very high relative abundance for CO_2^+ ion at a m/z of 44.

3.1.3 Viscosity measurements

A solution of $(Aucap)_n$ was prepared by dissolving it (0.67357g) in water (25.0 ml) at a pH of 12.0 which was highly viscous. The rate of flow of this solution was then measured with the help of Ubbelohde KPG viscometer. The solution was then diluted by addition of water to get various concentrations and time of flow was measured for these diluted solutions. The results are given in Table 3.1 and are plotted in Figure 3.2. The intrinsic viscosity of the solution was obtained from the intercept of the graph as 0.968. This high value of intrinsic viscosity suggests that $(Aucap)_n$ is a high molecular weight polymer [140].

Gold(I) thiomalate $(Autm)_n$ solutions of same concentrations as of $(Aucap)_n$ were prepared and their time of flow was measured to compare the degree of association in $(Aucap)_n$ and $(Autm)_n$. The data is given in Table 3.2 and is presented in Figure 3.3. It was observed that time of flow

TABLE 3.1. $\eta_{reduced}$ for various concentrations of $(Aucap)_n$

Concentration(g/100ml)	$\eta_{reduced}$(dl/g)
0.335	2.90
0.670	3.69
1.340	5.73
1.790	7.13
2.680	12.37

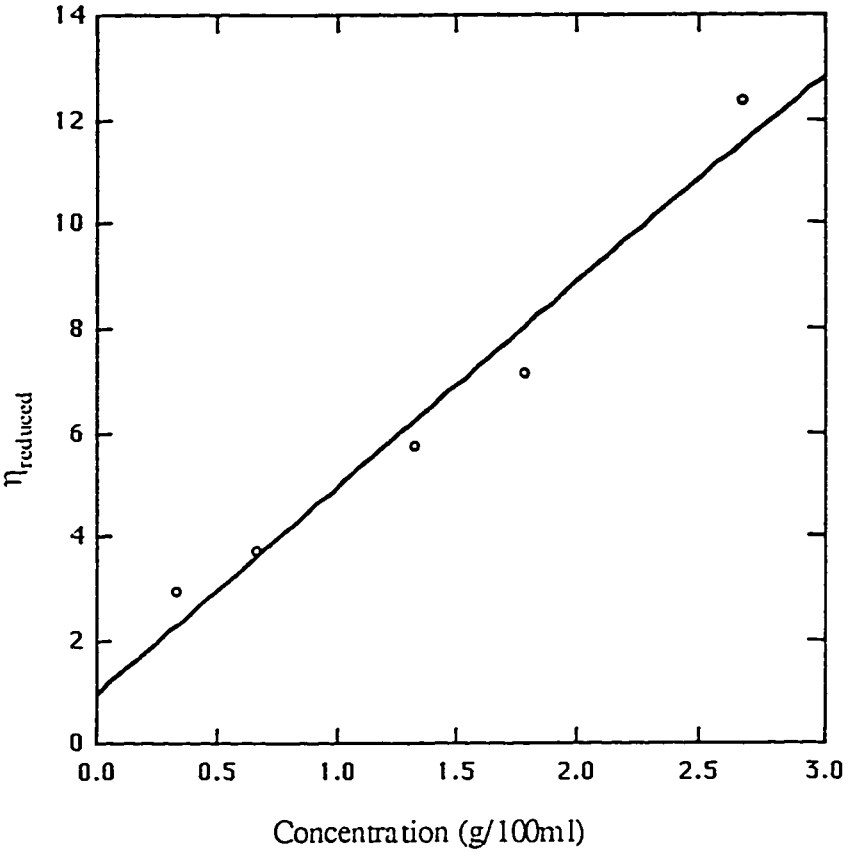

Figure 3.2 Plot of reduced viscosity ($\eta_{reduced}$)vs concentration (g/100ml) of 1/n[(Aucap)$_n$], where solid line is the regresion line.

TABLE 3.2 Time of flow of $(Aucap)_n$ and $(Autm)_n$ at various concentrations.

Concentration(M)	Time of flow(seconds) $(Aucap)_n$	$(Autm)_n$
0.0000	30.30	30.30
0.0077	59.56	30.35
0.0150	105.14	30.49
0.0310	263.00	30.94
0.0410	417.78	31.38
0.0610	1034.63	32.19

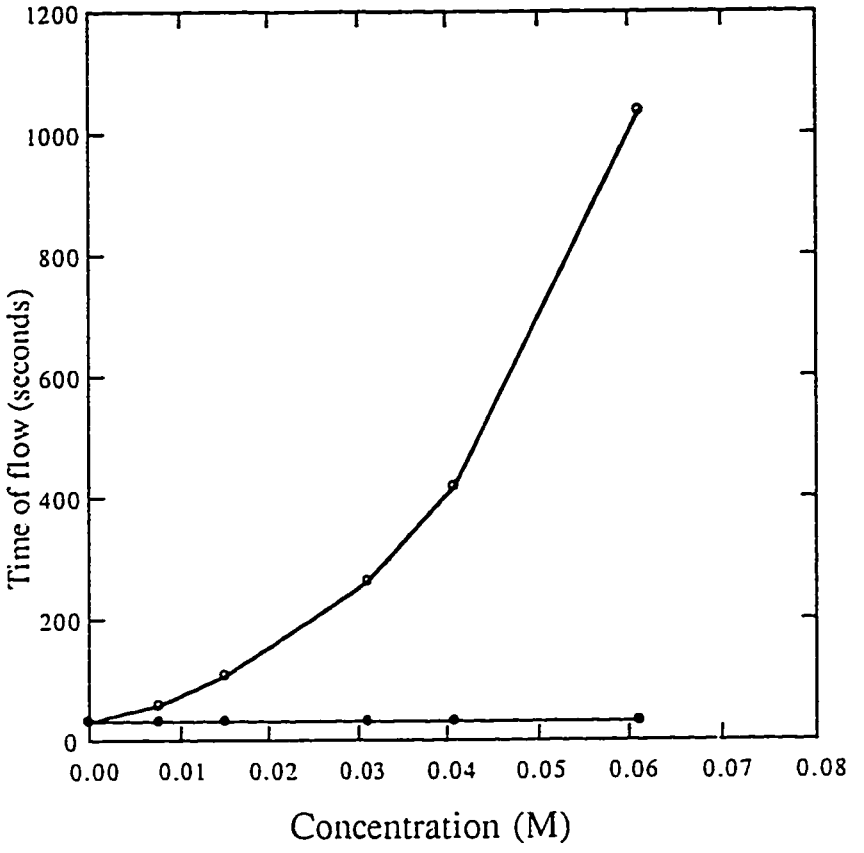

Figure 3.3 Time of flow of $(Aucap)_n$ and $(Autm)_n$ vs their molar concentration.

for $(Autm)_n$ was very low as compared to $(Aucap)_n$. The intrinsic viscosity of $(Autm)_n$ was also determined to be 0.0036, which is very small as compared to that of $(Aucap)_n$.

To study the effect of interactions of CN^-, SCN^- and $SeCN^-$ on the viscosity of gold(I) captopril the following experiment was carried out. A 0.01M $(Aucap)_n$ solution was prepared in water at pH of 12.0. Then KCN, KSCN and KSeCN were added as solid in separate solutions to get various ratios and their time of flow was measured. The data is presented in Table 3.3 and Figure 3.4. It was observed that time of flow of $(Aucap)_n$ decreased with increase in concentration of KCN, while it increased with increase in concentration of KSCN and KSeCN. When the time of flow of solutions was measured after 12h, it was observed that time of flow for $(Aucap)_n$:KCN solution remained constant, while for $(Aucap)_n$:KSCN it increased and for $(Aucap)_n$:KSeCN solution it decreased and selenium metal was found settled down in the solution.

3.1.4 UV spectroscopic measurements

A Gold(I)-captopril $(Aucap)_n$ solution of 1.66×10^{-5} molarity was prepared in water at a pH of 12.5. The potassium cyanide was then added in this solution to get the Au-cap : CN^- ratio of 1:0, 8:1, 4:1, 2:1, 1:1 and 1:2.

The UV spectrum of pure $(Aucap)_n$ (Fig. 3.5A) shows one absorption peak at 196.5 nm and a shoulder at 230.0 nm. When cyanide was added to this solution at a $(Aucap)_n$:CN^- ratio of 8:1 (Fig. 3.5B) there was a sharp change in the spectrum and shoulder of $(Aucap)_n$ at 230.0 nm disappeared completely. Further addition of CN^- showed no prominent change in the spectra up to the ratio of 2:1 [$(Aucap)_n$: CN^-] (Not shown in the figure). At a ratio of 1:1 (Fig. 3.5C) there was little change in the

TABLE 3.3 Time of flow of $(Aucap)_n$ with various ratios of KCN, KSCN and KSeCN.

	Time of flow(Seconds)		
$(Aucap)_n$[a]:L	KCN	KSCN	KSeCN
1 : 0	87.40	64.49	60.35
12 : 1	74.83	68.18	67.77
10 : 1	56.50	71.23	79.70
8 : 1	46.61	74.45	83.71
6 : 1	39.51	77.05	86.64
4 : 1	34.48	78.78	88.37
2 : 1	32.73	83.12	90.46
1 : 1	32.43	89.38	96.24

Where L= KCN, KSCN AND KSeCN.

[a]$(Aucap)_n$=0.01 M

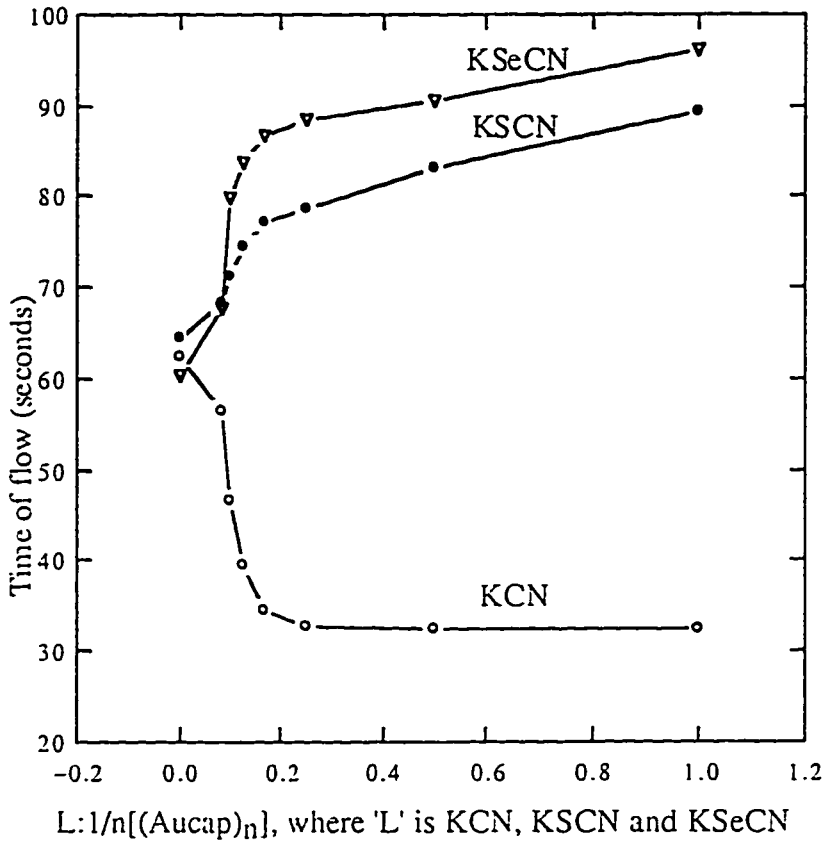

Figure 3.4 Time of flow (seconds) vs L:1/n[(Aucap)$_n$], where 'L' is KCN, KSCN and KSeCN.

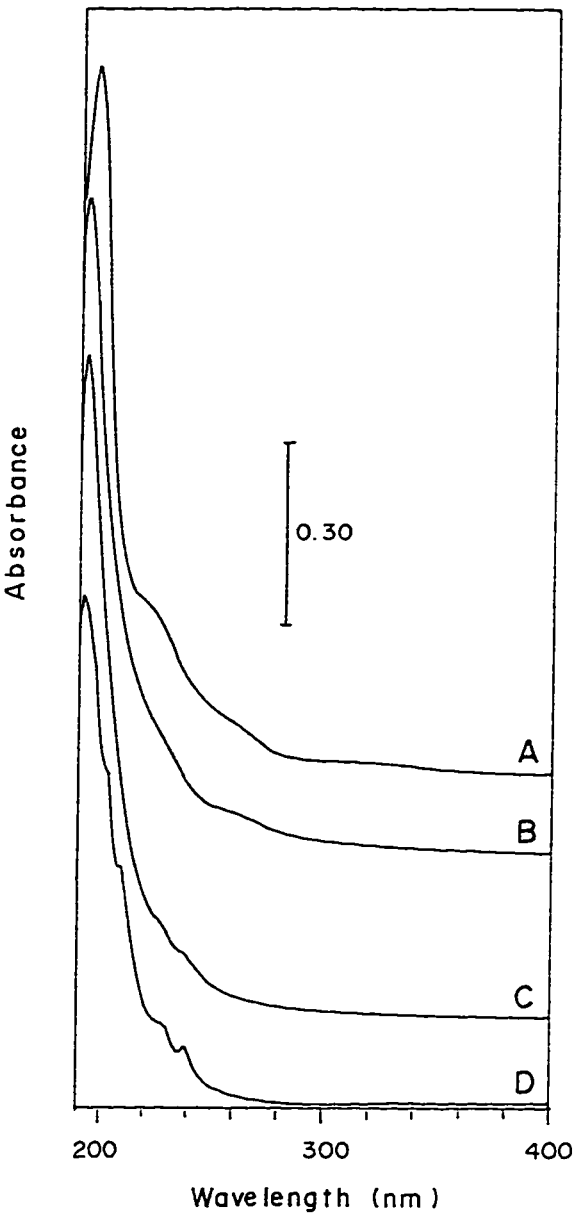

Figure 3.5. UV-visible spectra in solution of $1/n(Aucap)_n$: CN^- at (A) 8.0:0.0 (B) 8.0:1.0 (C) 8.0:8.0 (D) 8.0:16.0 ratios.

spectrum, while at ratio of 1:2 (Fig. 3.5D) the spectrum became almost identical to that of $[Au(CN)_2]^-$, except a band from $(Aucap)_n$ below 200 nm. The $[Au(CN)_2]^-$ solution exhibits absorption peaks at 210, 229 and 239 nm, which were also observed after addition of cyanide ion to $(Aucap)_n$ solution. Absorption due to $[Au(CN)_2]^-$ at 229 and 239 nm can also be seen in the spectrum of $(Aucap)_n$: CN^- at 1:1 ratio.

3.1.5 Interaction of $(Aucap)_n$ with $K^{13}CN$

The ^{13}C NMR spectra of $(Aucap)_n$ (0.20M in D_2O) is shown in Figure 3.6A. The complex is insoluble in D_2O below a pH* of 12.0. The colorless solution at high pH is highly viscous and the ^{13}C NMR spectrum is broad. When 0.065 mole equivalent of $K^{13}CN$ (30% labeled) was added to the aqueous solution of $(Aucap)_n$, its viscosity was decreased and number of resonances were observed in both low and high field region as shown in Figure 3.6B due to $[cap\text{-}Au\text{-}^{13}CN]^-$, $[Au(cap)_2]^-$ and $[Au(^{13}CN)_2]^-$ species. The generation of these species can be explained as shown in equation *3.6*.

$$(Aucap)_n + {}^{13}CN^- \longrightarrow (\text{-}cap\text{-}Au\text{-})_{n-1}\text{-}cap\text{-}Au\text{-}{}^{13}CN^- \quad 3.6$$

$$\downarrow$$

$$[cap\text{-}Au\text{-}{}^{13}CN]^- + (Aucap)_{n-1}$$

The asymmetric $[cap\text{-}Au\text{-}^{13}CN]^-$ complex undergoes disproportionation to produce $[Au(^{13}CN)_2]^-$ and $[Au(cap)_2]^-$ as shown in equation *3.7*.

$$2\,[cap\text{-}Au\text{-}{}^{13}CN]^- \longrightarrow [Au(^{13}CN)_2]^- + [Au(cap)_2]^- \qquad 3.7$$

In high field region all resonances due to $[Au(cap)_2]^-$ and $[cap\text{-}Au\text{-}^{13}CN]^-$ species were overlapped. In low field region a sharp resonance was observed at 154.44 ppm due to $[Au(^{13}CN)_2]^-$, while two broad

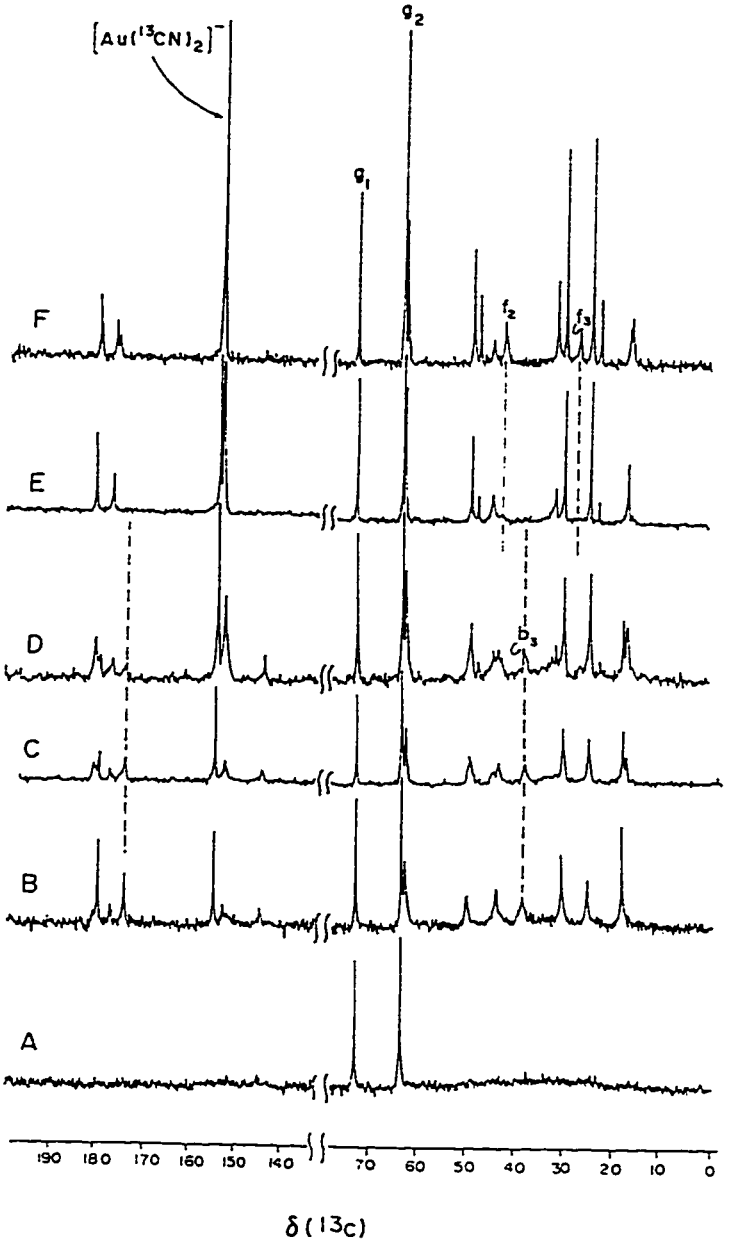

Figure 3.6. The 50.30 MHz ^{1}H noise-decoupled ^{13}C NMR spectra (at pH*12.0) of 0.20 M l/n[$(Aucap)_n$]:CN^- at (A) 1.000:0.000, (B) 1.000:0.065, (C) 1.000:0.125, (D) 1.000:0.250, (E) 1.000:0.500, (F) 1.000:0.750. [Note: f_2 and f_3 resonances are for free captopril and b_3 is for $[Au(cap)_2]^-$ or [cap-Au-CN]$^-$ species, see Table 3.4]

resonances at 152.15 and 143.98 were assigned on the basis of *cis*(c) and *trans*(t) isomers of captopril as [cap(t)-Au-^{13}CN]$^-$ and [cap(c)-Au-^{13}CN]$^-$ species respectively. The other resonances were observed due to 'CON' and 'CO_2^-' of both [Au(cap)$_2$]$^-$, and [cap-Au-^{13}CN]$^-$ species (see Table 3.4). Figure 3.6C and 3.6D show spectra of 1/n[(Aucap)$_n$] : ^{13}CN$^-$, at ratios of 1:0.125 and 1:0.25 respectively. All the resonances became sharper in these two spectra. At a ratio of 1:0.50 of 1/n[(Aucap)$_n$] : ^{13}CN$^-$, the ^{13}C NMR spectrum (Figure 3.6E), revealed prominent changes. The resonance at 38.45(b_3) belonging to [Au(cap)$_2$]$^-$ or [cap-Au-^{13}CN]$^-$ was not present. In low field region resonance at 143.90 ppm due to [cap(c)-Au-^{13}CN]$^-$ also disappeared while the resonance due to [cap(t)-Au-^{13}CN]$^-$ became more sharp and was shifted to low field. The spectrum of 1/n[(Aucap)$_n$] : CN$^-$ at 1:0.75 ratio (Figure 3.6F), is almost identical to the spectrum of free captopril. In high field region two sharp resonances at 27.47 and 42.00 were observed for C_3(f_3) and C_2(f_2) of free captopril. There was no resonance observed at 38.8(b_3) due to C_3 of [Au(cap)$_2$]$^-$ or [cap-Au-^{13}CN]$^-$ species. Resonance due to [cap(c)-Au-^{13}CN]$^-$ was not present in low field region. The resonance of [cap(t)-Au-^{13}CN]$^-$ was very sharp and was overlapped with the resonance of [Au(^{13}CN)$_2$]$^-$ species, which was increased in intensity. Four resonances were resolved in the region of 176-180 ppm due to 'CO_2^-' and 'CON' of [cap(t)-Au-^{13}CN]$^-$ and *cis* and *trans* forms of free captopril. The assignment of various resonances for various species discussed here are given in Table 3.4.

TABLE 3.4 ^{13}C NMR chemical shift resonances of various species present in Figure 3.6.

	cap$^-$	[Au(cap)$_2$]$^-$ or [cap-Au^{13}C^{15}N]$^-$	[Au(^{13}C^{15}N)$_2$]$^-$
C_3	27.47(t)[a] 27.56(c)	38.22(t)[c]	-
C_2	42.75(t)[b] 42.23(c)	43.87(t)	-
CH_3	17.39(t) 16.72(c)	18.34(t)	-
CON	176.51(t) 177.37(c)	174.95(t)	-
C_a	62.55(t) 63.18(c)	62.65(t) 63.26(c)	-
C_b	30.43(t) 32.14(c)	30.44(t) 32.32(c)	-
C_g	25.13(t) 23.24(c)	25.15(t) 23.23(c)	-
C_d	48.80(t) 47.92(c)	49.45(t)	-
CO_2	180.53(t) 180.32(c)	179.85(c) 180.46(t)	-
CN	-	152.15(t)[f] 143.98(c)	154.29

[a,b]= f_3 and f_2 resonances for C_3 and C_2 of free captopril.
[c]= b_3 resonance for C_3 of [Au(cap)$_2$]$^-$ or [cap-AuCN]$^-$ species.
[f]= Reference 33.

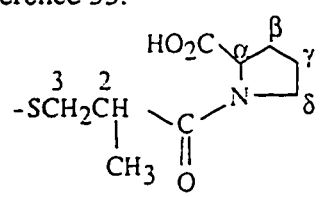

3.1.6 Interaction of $(Aucap)_n$ with $^{13}CN^-$ at different temperatures

Figure 3.7 represents the proton decoupled ^{13}C NMR spectra of the low field region of 0.298 M $(Aucap)_n$ with 0.0745 M $^{13}CN^-$ in D_2O at 3.0, 15.0, 25.0, 35.0 and 45.0 ^0C. The ^{13}C N.M.R. chemical shift resonances of various gold(I) complexes in Figure 3.7 at different temperatures are given in Table 3.5 . Three intense resonances, appeared in the low field region centered at d 144.09, 153.51 and 154.44 ppm, were assigned to the *cis* [cap-Au-$^{13}CN]^-$, *trans* [cap-Au-$^{13}CN]^-$ and $[Au(^{13}CN)_2]^-$, respectively. At low temperatures (15.0 and 3.0 ^0C) a broad resonance for *trans* [cap-Au-$^{13}CN]^-$ and a slightly broaden resonance with a shoulder for the *cis* [cap-Au-$^{13}CN]^-$ were resolved. With the increase in temperature the resonances due to the *trans* and *cis* isomers became broader with a decrease in their chemical shift differences along with the decrease in the intensity of the *cis* isomer. Finally at 45.0°C only one average resonance was observed at 151.96 ppm due to fast exchange of these two species.

3.1.7 Interaction of $(Aucap)_n$ with $C^{15}N^-$

Figure 3.8A shows the ^{15}N NMR spectrum of 0.400 M $(Aucap)_n$ with 0.2 mole equivalent of $C^{15}N^-$ in D_2O. Two resonances at 260.14 and 265.61 ppm are observed, which are assigned to *trans* [cap-Au-$C^{15}N]^-$ and $[Au(C^{15}N)_2]^-$, respectively. Then $(Aucap)_n$ concentration was increased to achieve a ratio of 3:1 of $(Aucap)_n$: $C^{15}N^-$ and the spectrum is shown in Figure 3.8B. A slightly down field shift of the resonance due to *trans* [cap-Au-$C^{15}N]^-$ was observed, however resonance due to $[Au(C^{15}N)_2]^-$ was shifted up field. At 8:1 ratio of $(Aucap)_n$:$C^{15}N^-$ (Fig.3.8C) the resonance due to *cis* [cap-Au-$C^{15}N]^-$ was observed at 269.32, while other

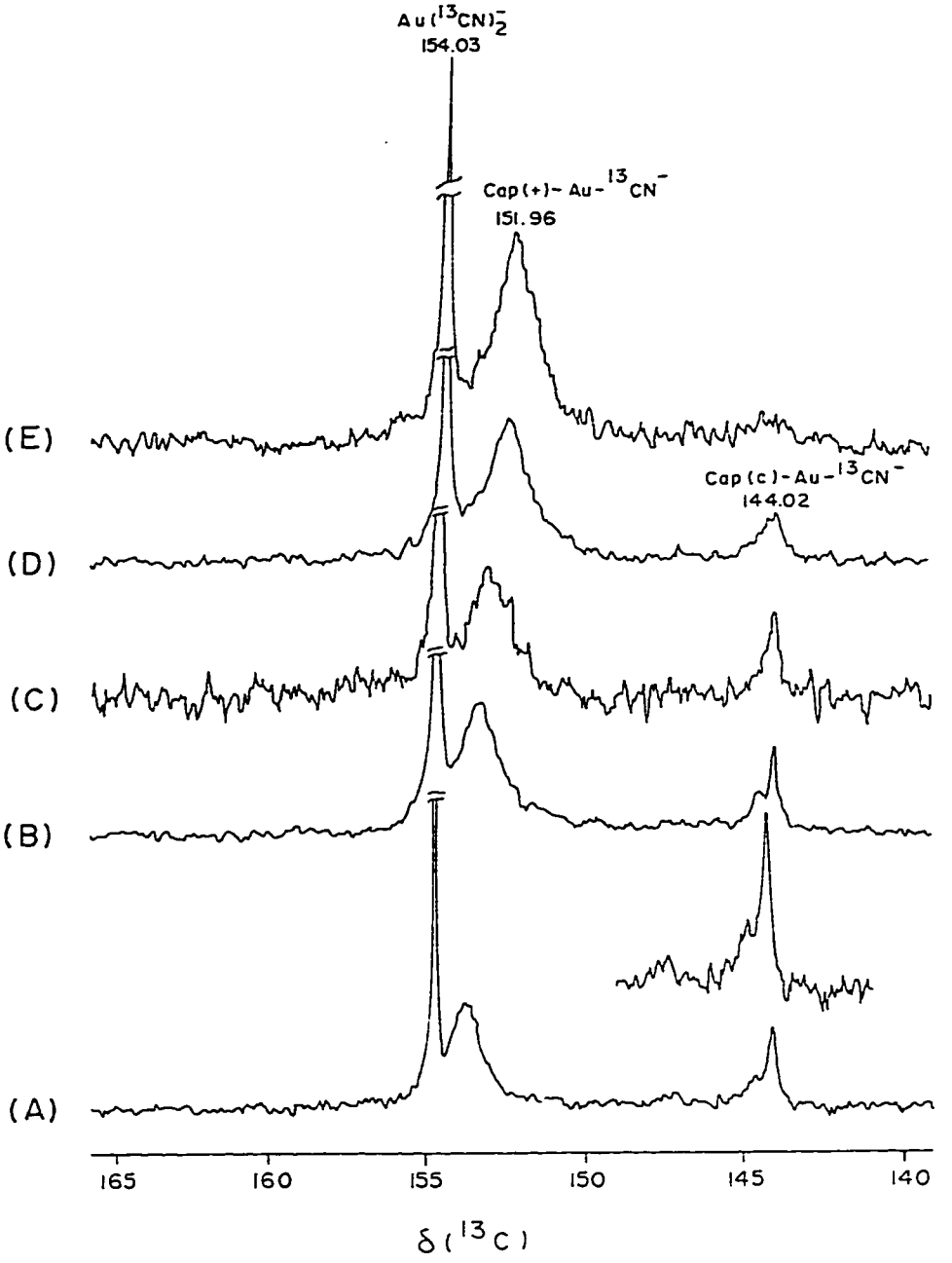

Figure 3.7. The 50 MHz ^{1}H noise-decoupled ^{13}C NMR spectra (at pH*=12.0) of 0.298 M $(Aucap)_n$: 0.074 M $^{13}CN^-$ at (A) 3.0°C (B) 15.0°C (C) 25.0°C (D) 35.0°C (E) 45.0°C.

TABLE 3.5 ^{13}C Chemical shifts of $(Aucap)_n$: $^{13}CN^-$ solution with 4:1 ratio at various temperatures.

Temp. (°C)	*cis*-[cap-Au-^{13}CN]$^-$	*trans*-[cap-Au-^{13}CN]$^-$	[Au(^{13}CN)$_2$]$^-$
3.0	144.09	153.51	154.44
15.0	144.0	152.94	154.35
25.0	144.02	152.76	154.28
35.0	143.96	152.24	154.18
45.0	-	151.96	154.03

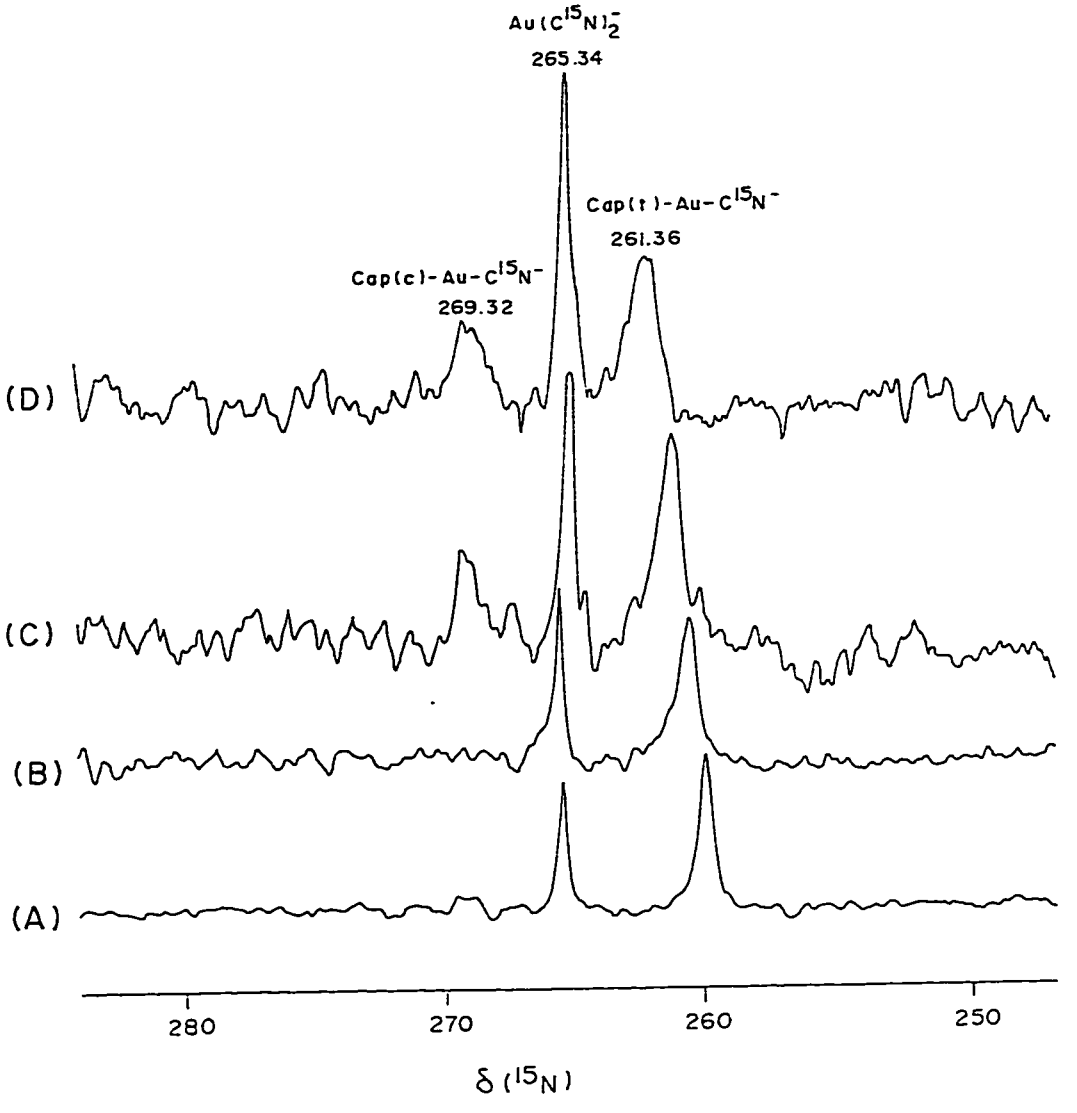

Figure 3.8. The 20 MHz ^{1}H noise-decoupled ^{15}N NMR spectra of $1/n(Aucap)_n : C^{15}N^-$ at various molar ratios (pH*=12.0) (A) 0.40:0.20 (B) 0.60:0.20 (C) 1.60:0.20 (D) 2.40:0.20 .

two resonances were increased in intensity. The $(Aucap)_n$ concentration was further increased to get a 12:1 ratio of $(Aucap)_n$:$C^{15}N^-$ and the spectrum is shown in Figure 3.8D. This time all resonances became broader. We did not measure temperature dependent experiment by ^{15}N spectroscopy because even after using label $C^{15}N^-$, it took about 36-48 hours to record each spectrum with reasonable signal to noise ratio. The ^{15}N chemical shifts for various resonances of gold(I) complexes at different concentrations are given in Table 3.6.

3.1.8 Interaction of $(Aucap)_n$ with $KSe^{13}C^{15}N$

The ^{13}C NMR spectrum of $(Aucap)_n$ (0.2M in D_2O) in low field region is shown in Figure 3.9A. The ^{13}C and ^{15}N NMR resonances of various species in Figures 3.9, 3.10 and 3.12 are given in Table 3.7. The $(Aucap)_n$ is insoluble in D_2O below pH* of 12.0 [113]. The colorless solution at high pH is highly viscous and its ^{13}C NMR spectrum is very broad. When one mol equivalent $KSe^{13}C^{15}N$ (0.2M) was added as a solid to the $(Aucap)_n$ solution under N_2 gas, color of the solution changed from colorless to light yellow immediately and its viscosity decreased, after 10h the color of solution was changed to bright yellow and only a resonance of free $Se^{13}C^{15}N^-$ was resolved (not shown in figure). After 24h the color of solution changed to orange and the resonances due to free $Se^{13}C^{15}N^-$ and $[Au(^{13}C^{15}N)_2]^-$ [16,64] were observed, two additional resonances were resolved at 153.74 and 154.64 ppm as doublets (Figure 3.9B). The resonance at 153.74 was more intense than the resonance at 154.64 ppm, which was overlapped with the $[Au(^{13}C^{15}N)_2]^-$ resonance. The resonances of captopril disulfide $(cap)_2$ were also identified in high field region from

TABLE 3.6 ^{15}N Chemical shifts of $(Aucap)_n$: $C^{15}N^-$ solution at various ratios.

$(Aucap)_n$:$C^{15}N^-$	*cis*-[cap-Au-$C^{15}N$]$^-$	*trans*-[cap-Au-$C^{15}N$]$^-$	[Au($C^{15}N$)$_2$]$^-$
2 : 1	-	260.14	265.61
3 : 1	-	260.67	265.68
8 : 1	269.32	261.36	265.34
12 : 1	269.34	261.88	265.32

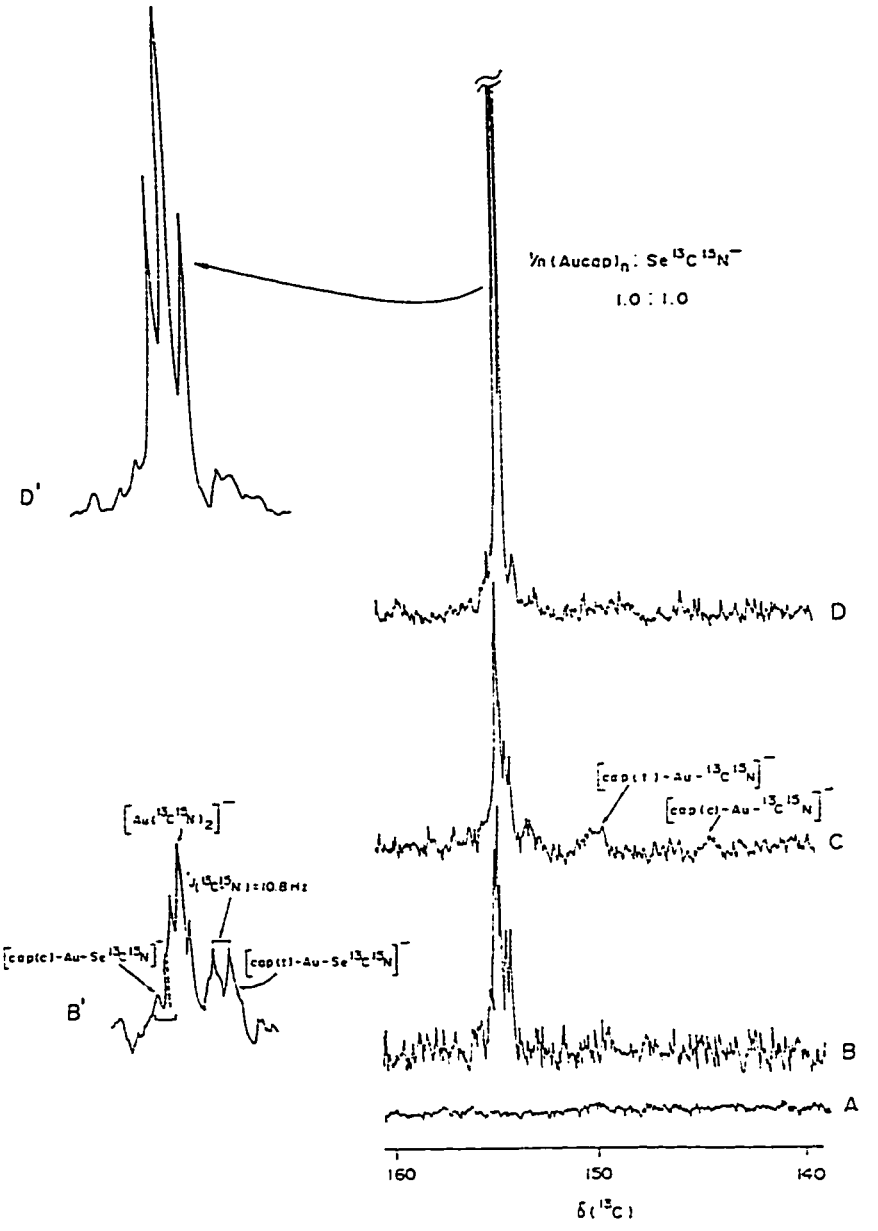

Figure 3.9 The 50.30 MHz ^{1}H noise-decoupled ^{13}C NMR spectra in low fields region (at pH* 12.0) of $(Aucap)_n$:$Se^{13}C^{15}N$ at (A) 1.0:0.0, (B) 1.0:1.0, after 24h, (C) 1.0:1.0, after 35h, (D) 1.0:1.0, after 143h, (B') expansion of 153 to 155 ppm region of spectrum 2B and (D') expansion of 153 to 155 ppm region of spectrum 2D.

TABLE 3.7 ^{13}C and ^{15}N NMR resonances of various species present in Figures 3.9, 3.10 and 3.12.

Species	δ (Resonance assignment)
$[Au(^{13}C^{15}N)_2]^-$	$\delta(^{13}C)$ =154.27; $\delta(^{15}N)$ = 264.82; $^1J_{(^{13}C-^{15}N)}$ = 6.3 Hz
$Se^{13}C^{15}N^-$	$\delta(^{13}C)$ = 121.36; $\delta(^{15}N)$ = 236.48; $^1J_{(^{13}C-^{15}N)}$ 10.3 Hz; $^1J_{(^{13}C-^{77}Se)}$ = 267.4 Hz
[cap(t)-Au-$Se^{13}C^{15}N$]$^-$	$\delta(^{13}C)$ = 153.74; $^1J_{(^{13}C-^{15}N)}$ 10.8 Hz
[cap(c)-Au-$Se^{13}C^{15}N$]$^-$	$\delta(^{13}C)$ = 154.64
[cap(t)-Au-$^{13}C^{15}N$]$^-$	$\delta(^{13}C)$ = 149.82*
[cap(c)-Au-$^{13}C^{15}N$]$^-$	$\delta(^{13}C)$ = 143.99*
$(cap)_2$	$\delta(^{13}C)$ $C_2(d_2)$ = 41.61(t-t), 41.44(t-c); $C_3(d_3)$ = 38.22 (t-t), 38.46(t-c)
[cap-Au-SeU]	$\delta(^{13}C)$ $C_2(t_2)$ = 45.23; C_3 = 30.58
[cap-Au-TU]	$\delta(^{13}C)$ C_2 = 45.32; C_3 = 30.60

* These resonances are broad (see the text for detail).

its C_2 and C_3 resonances (not shown in spectrum). The $(cap)_2$ resonances were identified by comparison with a spectrum of 0.10 M $(cap)_2$ alone at pH* 12.0 in D_2O. Figure 3.9B' shows the expansion of 153 to 155 ppm region from Figure 3.9B.

Figure 3.9C shows the low field region of ^{13}C NMR spectrum of same solution after 35h, the color of solution had changed to dark brown and some traces of metallic selenium and gold were observed in the solution. The resonance of $Se^{13}C^{15}N^-$ had decreased in intensity, and the resonance due to $[Au(^{13}C^{15}N)_2]^-$ increased in intensity. The resonance at 153.74 had also decreased in intensity and the resonance at 154.64 had disappeared. At this stage two new broad resonances were resolved at 149.82 and 143.99 ppm. The resonance at 143.99 was identified as $[cap(c)\text{-}Au\text{-}^{13}C^{15}N]^-$ [113].

Figure 3.9D shows the low field region of ^{13}C NMR spectrum of same solution after 143h. The color of the solution was changed to dark brown and more metallic selenium and gold were observed. The resonance due to $Se^{13}C^{15}N^-$ further decreased in intensity, the resonance due to $[Au(^{13}C^{15}N)_2]^-$ was increased in intensity, while resonance at 153.74 disappeared completely. Figure 3.9D' shows the expansion of 153-to-155 ppm region of Figure 3.9D.

A time dependent ^{13}C NMR study of $(Aucap)_n$:$Se^{13}C^{15}N^-$ system at ratio of 1:0.5, was also carried out in which the resonances due to $[Au(^{13}C^{15}N)_2]^-$ and $(cap)_2$ were resolved and metallic gold and selenium was observed, but resonances at 153.74 and 154.64 were not resolved. Figure 3.10A shows the ^{13}C NMR spectrum of $KSe^{13}C^{15}N$ as a doublet at 121.36 ppm with $^1J_{(^{13}C\text{-}^{15}N)}$ of 10.6 Hz, however, a

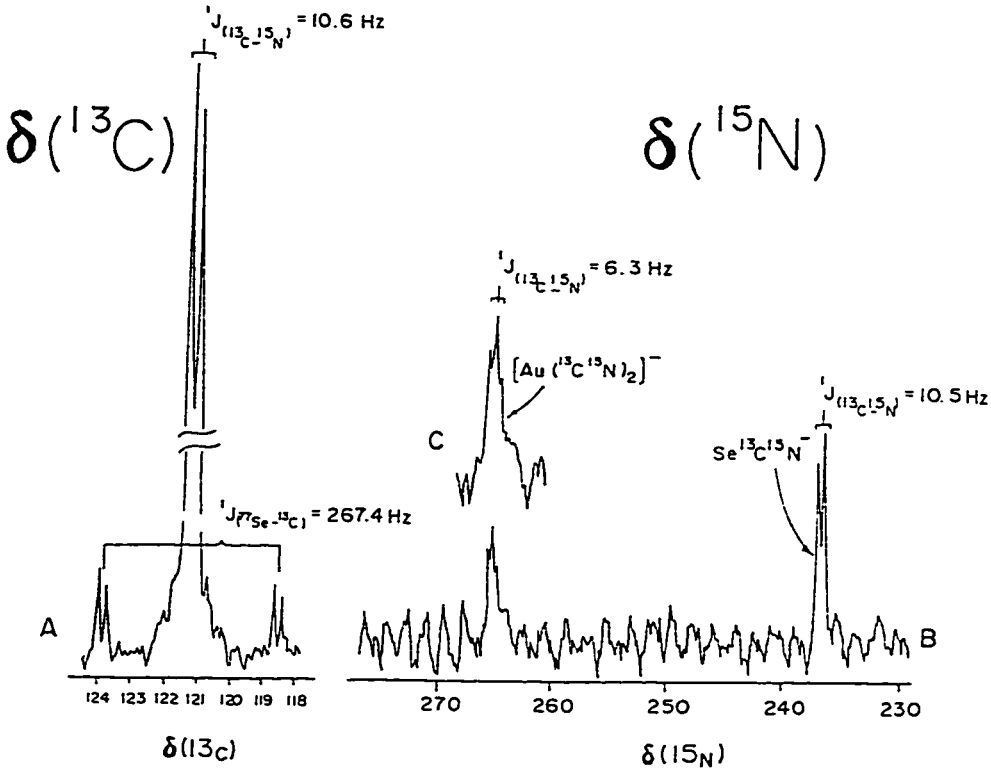

Figure 3.10 (A) The 50.30 MHz ^{1}H noise-decoupled ^{13}C NMR spectrum of $KSe^{13}C^{15}N$, (B) The 20.20 MHz ^{1}H noise-decoupled ^{15}N NMR spectrum of (Aucap)n:$KSe^{13}C^{15}N$ at a ratio of 1:1 after 96h and (C) expansion of ^{15}N NMR resonance of $[Au(^{13}C^{15}N)_2]^-$ species.

doublet of doublet is also observed with small intensity, around the central intense doublet. This doublet of doublet was observed due to coupling of ^{13}C with ^{77}Se(only 7% natural abundance). The $^{1}J_{(^{77}Se-^{13}C)}$ was resolved as 267.4 Hz.

Figure 3.10B shows the ^{15}N NMR spectrum of solution of $1/n[(Aucap)_n]$: $Se^{13}C^{15}N^-$ at 1:1 ratio after 96 hrs. Only two resonaces were resolved for $[Au(^{13}C^{15}N)_2]^-$ and free $Se^{13}C^{15}N^-$ species. The resonance at 236.48 ppm was resolved as a doublet for free $Se^{13}C^{15}N^-$ with $^{1}J_{(^{13}C-^{15}N)}$ of 10.3 Hz. The resonance at 264.82 ppm was resolved as a triplet for $[Au(^{13}C^{15}N)_2]^-$ due to virtual coupling with $^{1}J_{(^{13}C-^{15}N)}$ of 6.3 Hz. The resonance of $[cap\text{-}Au\text{-}^{13}C^{15}N]^-$ was not resolved due to low concentration.

Figure 3.11 shows % intensity of resonances due to 'CN' group of $[Au(^{13}C^{15}N)_2]^-$, $[cap\text{-}Au\text{-}Se^{13}C^{15}N]^-$ and free $Se^{13}C^{15}N^-$ species from the spectra of Figure 3.9. We assumed the 100% intensity of $Se^{13}C^{15}N^-$ is equivalent to its 0.2M initial concentration.The intensities for these resonances were measured with respect to the intensity of dioxane resonance (internal reference). The T_1 values of these resonances were not measured because of the redox reactions as well as decomposition of various species, however, it is assumed to be constant throughout the experiment. This figure shows slow decrease in intensity of free $Se^{13}C^{15}N^-$ and an increase in intensity of $[Au(^{13}C^{15}N)_2]^-$ species. There is also an increase in the intensity of $[cap(t)\text{-}Au\text{-}Se^{13}C^{15}N]^-$ (153.74 ppm) up to 29h, after which it decreases.

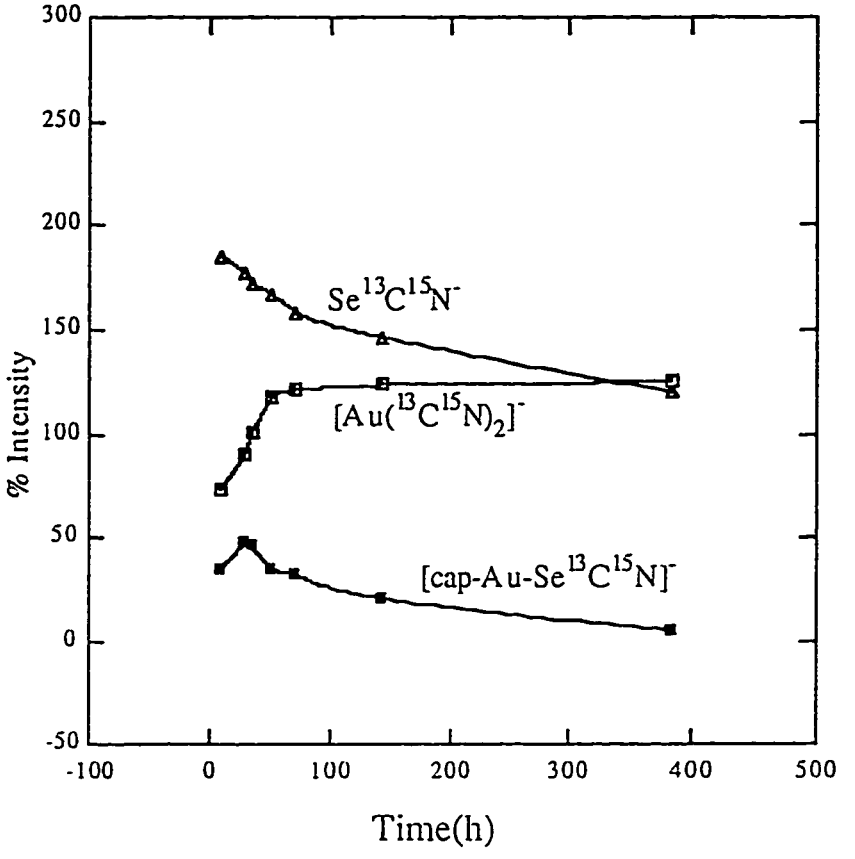

Figure 3.11 The % intensity of 'CN' group resonance of $[Au(^{13}C^{15}N)_2]^-$, $Se^{13}C^{15}N^-$ and $[cap\text{-}Au\text{-}Se^{13}C^{15}N]^-$ species as a function of time with respect to dioxane (internal reference), taken from Figure 3.9.

3.1.9 Interaction of $(Aucap)_n$ with selenourea and thiourea

Figure 3.12A shows a ^{13}C NMR spectrum of 1/n[$(Aucap)_n$] : SeU (selenourea) (0.1M:0.1M) in D_2O after 6 hours. The SeU was added as a solid to the highly viscous solution of $(Aucap)_n$ at pH* of 12.0 under N_2 atmosphere. The color of solution was changed to light orange immediately and its viscosity decreased. A number of resonances were observed in both low and high field regions of the ^{13}C NMR spectrum. The resonance due to free SeU was not observed.

Figure 3.12B shows a ^{13}C NMR spectrum of same solution after 20h, by that time the color of solution was turned dark brown and some precipitates due to metallic gold and selenium were observed in the solution. In high field region, the resonances due to $(cap)_2$ were identified from its C_2 and C_3 resonances while a resonance at 45.23 ppm was decreased in intensity.

Figure 3.12C shows ^{13}C NMR spectrum of the same solution after 54h. By this time the color of solution was an intense dark brown and more metallic gold and selenium was formed. The resonances due to $(cap)_2$ were increased in intensity , while resonance at 45.23 ppm disappeared completely.

We have also carried out the ^{13}C NMR study of SeU alone at pH 12.0, during which metallic selenium was observed and no ^{13}C resonance was resolved for SeU.

When thiourea (TU) was added as a solid to the highly viscous solution of $(Aucap)_n$ (pH* of 12.0) at a ratio of 0.1M:0.1M, the solution became less viscous immediately and after 6 hours, color of the solution changed from colorless to light yellow. Figure 3.12D shows a

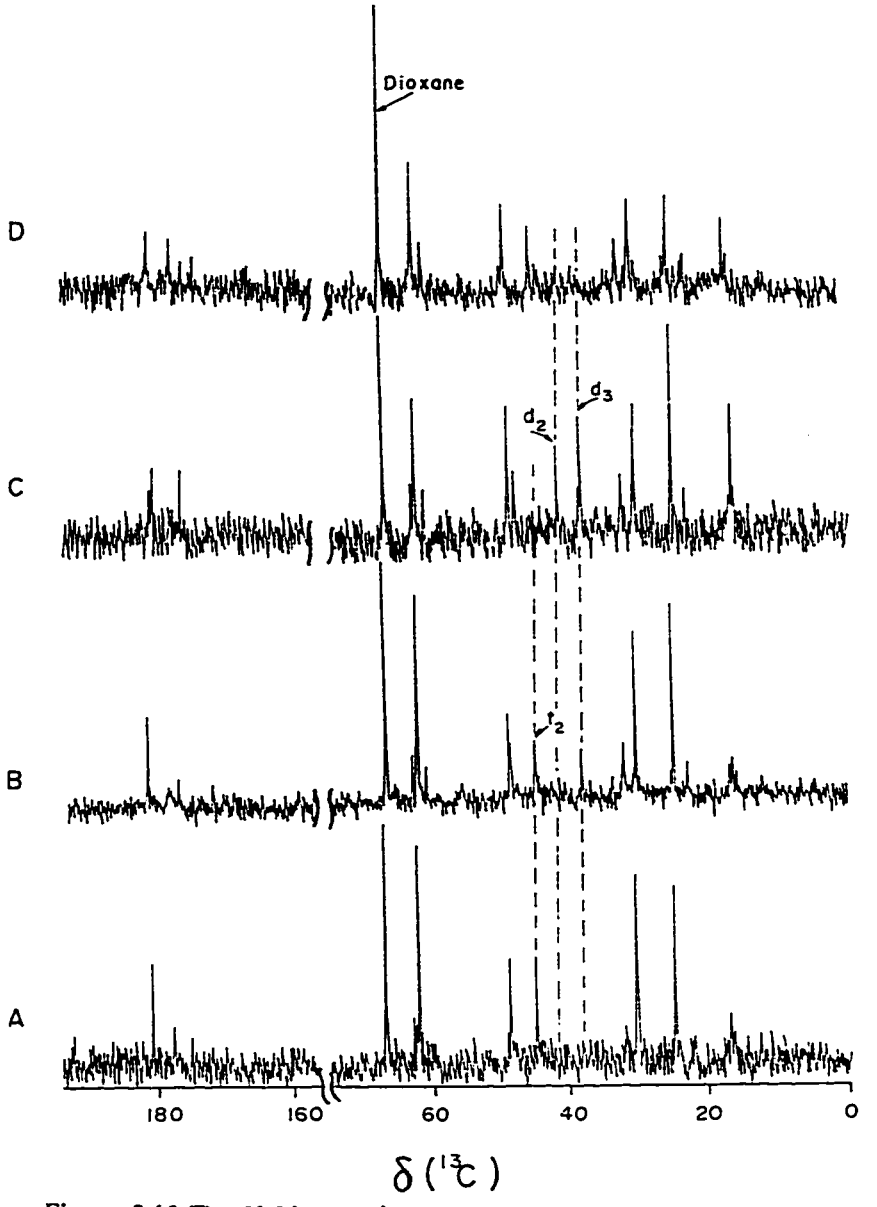

Figure 3.12 The 50.30 MHz ^{1}H noise-decoupled ^{13}C NMR spectra (at pH* 12.0) of $(Aucap)_n$:SeU at 1:1 ratio (A) after 6h, (B) after 20h, (C) after 54h and (D) ^{13}C NMR spectrum of $(Aucap)_n$:TU at 1:1 ratio after 70h.

^{13}C NMR spectrum of a solution containing $1/n[(Aucap)_n]$: TU (0.1M:0.1M) in D_2O after 70 hours. A number of resonances were observed in both low field and high field regions, which remained constant even after several weeks. There was no resonance due to $(cap)_2$ in the spectrum.

3.2 DISCUSSION

Gold(I) thiolates are known to exist as polymers from hexa- to octamers by bridging through sulfur atom [4,46,82,137,138]. Gold(I) captopril $(Aucap)_n$ is also considered to exist in polymeric form through bridging of sulfur atom. The probable structure of $(Aucap)_n$ is considered to be analogous to that of $(Autm)_n$ [8,83,84] as shown in Figure 2.1.

The intrinsic viscosity of $(Aucap)_n$ is found to be 0.968, which is characteristic of high molecular weight polymers [140]. The time of flow for $(Aucap)_n$ solution is found to be much higher than that of $(Autm)_n$ for same concentrations (Figure 3.3), which suggests that degree of association in $(Aucap)_n$ is much higher than in $(Autm)_n$. Decrease in viscosity of $(Aucap)_n$: CN^- solutions at various ratios indicates the binding of CN^- on the gold terminal to produce [cap-Au-CN]$^-$ as shown below in equation *3.8*

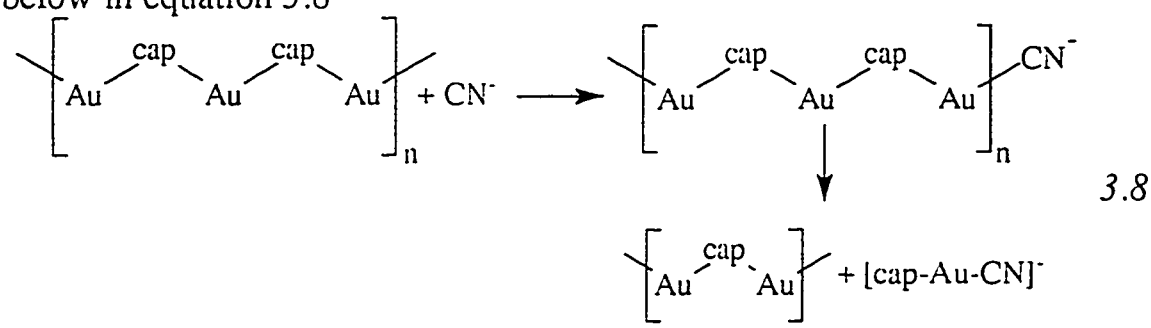

3.8

and the ensuing depolymerization decreases the viscosity with increase in

CN^- ion concentration. It is already known [16,19] that gold(I) thiols $(RS\text{-}Au)_n$ interact with CN^- ion to form $[RS\text{-}Au\text{-}CN]^-$ which undergoes disproportionation reactions to produce $[Au(CN)_2]^-$ as shown in equations *3.6* and *3.7*.

Viscosity measurements of $(Aucap)_n$:SCN^- and $SeCN^-$ at various ratios indicate that initially both SCN^- and $SeCN^-$ are acting like salts, which increase the ionic strength of the solution and in turn increase the degree of association as is already observed in the case of $(Autm)_n$ [82]. However with time (12 h) the behavior of these salts differed; while SCN^- was still acting as a salt, $SeCN^-$ afforded selenium metal and time of flow of the solution dropped. In chapter-2 it is shown that $(Autm)_n$ react with $SeCN^-$ to form an unstable complex $[tm\text{-}Au\text{-}SeCN]^-$ which readily undergoes decomposition to produce $[Au(CN)_2]^-$ and Selenium metal. The $SeCN^-$ is also presumed to react with $(Aucap)_n$ to form unstable $[cap\text{-}Au\text{-}SeCN]^-$ complex, which readily undergoes decomposition. All these different reactions are responsible for the breakdown of the polymeric $(Aucap)_n$ by $SeCN^-$.

UV spectroscopic study of solution containing various ratios of $(Aucap)_n$: CN^- also confirms the formation of $[Au(CN)_2]^-$ in the solution. From Figure 3.5, it can be seen that the changes in absorbance of $(Aucap)_n$ on the addition of cyanide ion are prominent but irregular. For example, there is a greater change in absorbance at 230 nm for $(Aucap)_n$: CN^- 8:1 solution. Then the spectra are almost same for 8:1, 4:1 and 2:1 solutions. A small change in spectrum in the region of 220-245 nm is observed at ratio of 1:1, which becomes pronounced further for the solution of 1:2 ratio and the spectrum become almost identical to that of $[Au(CN)_2]^-$ complex. These results indicate the production of at least one intermediate, with an

absorption spectrum different from that of $(Aucap)_n$ and $[Au(CN)_2]^-$, which might be $[Au(Cap)(CN)]^-$ complex as concluded by N.M.R. studies.

Grahm *et al* [16] have studied the interaction of $(Autm)_n$ with CN^- using ^1H, ^{13}C and UV spectroscopy. They have also observed the absorption peaks at 209.5, 228 and 238 nm owing to $[Au(CN)_2]^-$ complex on addition of CN^- ion to $(Autm)_n$ solution.

During mass spectroscopic studies $(Aucap)_n$ was subjected to fast atom bombardment mass spectroscopy to get some information about its polymeric nature, but it failed to produce any significant ions. Therefore it was subjected to electron impact mass spectroscopy. We couldnot observe the molecular ion due to high energy of electron ionization source. However, at very low relative abundance various fragments arising from Au-cap monomer molecule itself were detected which are presented in scheme 3.2.

The interaction of $^{13}CN^-$ with $(Aucap)_n$ indicates the formation of unsymmetric $[cap\text{-}Au\text{-}^{13}CN]^-$ complex as shown in equation *3.6*, which shows two broad resonances for *cis* and *trans* complexes at 145.26 and 149.02 ppm respectively.

The disproportionation in linear unsymmetric gold(I) complexes is well known [16,19,112,113]. The $[cap\text{-}Au\text{-}^{13}CN]^-$ also undergoes disproportionation to produce $[Au(cap)_2]^-$ and $[Au(^{13}CN)_2]^-$ species as shown in equation *3.7*. A sharp resonance at 154.44 ppm for $[Au(^{13}CN)_2]^-$ confirms this disproportionation [19]. However at higher concentration of $^{13}CN^-$ i.e. $1/n[(Aucap)_n]$: $^{13}CN^-$ 1.0:0.5 ratio, the resonances due to $[Au(cap)_2]^-$ disappear completely and at 1.0:0.75 ratio, resonances due to free captopril appear in the spectrum (Fig.

3.6F), which indicates that at higher concentration of $^{13}CN^-$, it interact with $[Au(cap)_2]^-$ and $[cap\text{-}Au\text{-}^{13}CN]^-$ to produce $[Au(^{13}CN)_2]^-$ and free captopril as shown in equation *3.9*

$$[Au(cap)_2]^- + {}^{13}CN^- \longrightarrow \underline{[cap\text{-}Au\text{-}^{13}CN]^-} + cap^- \qquad 3.9$$

$$\underline{[cap\text{-}Au\text{-}^{13}CN]^-} \xrightarrow{{}^{13}CN^-} [Au(^{13}CN)_2]^- + cap^-$$

This interaction causes decrease in concentration of $[Au(cap)_2]^-$ and $[cap\text{-}Au\text{-}^{13}CN]^-$ species.

From ^{13}C and ^{15}N NMR studies it is observed that ^{13}C chemical shift for the *cis* isomer of $[cap\text{-}Au\text{-}^{13}CN]^-$ is at higher field as compared to that of the *trans* isomer, while opposite is observed for ^{15}N chemical shift of $[cap\text{-}Au\text{-}C^{15}N]^-$ complex i.e. the *trans* isomer of $[cap\text{-}Au\text{-}C^{15}N]^-$ is present up field than that of *cis* isomer. Brown *et al* [141,142] have also made similar observations for ^{13}C and ^{15}N NMR chemical shifts of $^{15}N^{13}CCo(D_2H_2)L$ where L= pyridine, primary amine, 4-substituted aniline and their analogs. This inverse relationship between ^{13}C and ^{15}N chemical shifts could be explained due to metal-to-carbon π-bonding. Since the π-bonded species involves a transfer of electron density from a filled metal d-orbital into the carbon-centered member of the cyanide π*-anti bonding orbital, most of the electron density donated from the metal to the cyanide ligand would be expected to reside on the cyanide carbon. Thus stabilization of π-bonded species by increasing electron donation from different ligands should shift the cyanide ^{13}C resonance down field. Similarly the reduction in C-N bond order in the π-bonded species would be expected to be accompanied by an up field shift of the ^{15}N resonance. We have also

observed this inverse relationship for ^{13}C and ^{15}N chemical shifts of CN^- ion for R_3P-Au-CN complexes in chapter-4. It was observed that with increase in σ-donation of R_3P the ^{13}C chemical shift moved down field while the ^{15}N chemical shift moved up field.

The ^{13}C NMR spectrum recorded at 3.0°C shows a broad peak for the *trans* isomer and a slightly broaden peak with a shoulder for the *cis* isomer. This may be explained by the cyanide end triad of the polymer, where the configuration of the penultimate captopril moiety can split the $^{13}CN^-$ signal. So we can assign the strong peak in the *cis* region to *trans* configuration of the penultimate unit and the shoulder peak to the *cis* configuration. The *trans* cap-Au-$^{13}CN^-$ does not show the resolved signals, hence the appearance of a broad signal.

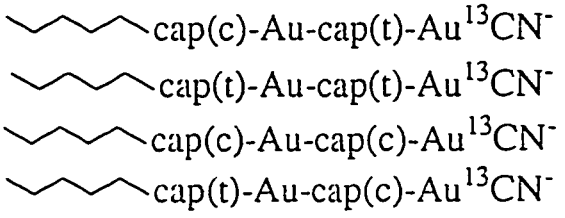

Where cap(t) represents the *trans* isomer of captopril and cap(c) represents the *cis* isomer of captopril.

As the temperature is increased, exchange rate between *trans* and *cis* isomers increases, causing further broadening. At 25.0°C, the shoulder peak disappeared from *cis* [cap-Au-^{13}CN]$^-$ signal, as the rate of exchange at this temperature is fast enough to coalesce the different configurations of the penultimate unit.

When the temperature is further increased to 45.0°C, resonance due to *cis* [cap-Au-^{13}CN]$^-$ broadens out completely to give coalescence and the average resonance is observed at 151.96 ppm.

In ^{15}N NMR measurements it was observed that at low ratio of $(Aucap)_n$: CN^- (2:1) only one resonance for ^{15}N chemical shift due to *trans* isomer is present. However when this ratio is increased to 8:1 resonances for ^{15}N chemical shift due to both *cis* and *trans* isomers of [cap-Au-CN]$^-$ are observed. Similar observation was made in ^{13}C NMR measurements, that when the CN^- concentration was increased only one resonance due to ^{13}C chemical shift of *trans* [cap-Au-CN]$^-$ was observed.

The interaction of $Se^{13}C^{15}N^-$ with $(Aucap)_n$ indicates the generation of [cap-Au-$Se^{13}C^{15}N$]$^-$ specie, as shown in equation *3.8* for [cap-Au-CN]$^-$. We have shown only the low field region of ^{13}C NMR, because the labeled $KSe^{13}C^{15}N$ was used and therefore it is easier to identify the resonances in the cyanide region. Three sets of resonances were observed. The doublet at 153.74 ppm was due to [cap(t)-Au-$Se^{13}C^{15}N$]$^-$ another doublet at 154.64 ppm due to [cap(c)-Au-$Se^{13}C^{15}N$]$^-$ and a triplet at 154.27 ppm due to [$Au(^{13}C^{15}N)_2$]$^-$ resonances. The chemical shift of [$Au(^{13}C^{15}N)_2$]$^-$ is known [16,64] and triplet is due to the virtual coupling (6.2 Hz) of trans $^{13}C^{15}N^-$ { i.e. sum of $^3J_{(^{13}C-^{15}N)}$ and $^1J_{(^{13}C-^{15}N)}$ }. Similar virtual coupling for [$Au(^{13}C^{15}N)_2$]$^-$ was observed for $R_3PAu^{13}C^{15}N$ complexes (chapter 4), which disproportionate to produce $[(R_3P)_2Au]^+$ and [$Au(^{13}C^{15}N)_2$]$^-$ species in solution. The chemical shifts of [cap(t)-$Au^{13}CN$]$^-$ and [cap(c)-$Au^{13}CN$]$^-$ are reported to be 152.18 and 143.99 ppm respectively [16], therefore, the resonances at 153.74 and 154.64 ppm must be due to the [cap(t)-Au-$Se^{13}C^{15}N$]$^-$ and [cap(c)-Au-$Se^{13}C^{15}N$]$^-$ respectively. It should be noted here that the concentration of *trans* species of captopril is always greater than *cis* at all pH ranges [132].

The ^{13}C NMR ($Se^{13}C^{15}N$) resonance of *cis* isomer of [cap-Au-$Se^{13}C^{15}N$]$^-$ species is at lower field as compared to the *trans* isomer, which is opposite to that of [cap-Au-$^{13}C^{15}N$]$^-$ in which *cis* isomer is at higher field than that of *trans* isomer [113]. This can be explained on the basis of back donation and π-bonding between gold(I) and CN^- group in [cap-Au-$^{13}C^{15}N$]$^-$ species. The *trans* isomer of captopril is a better electron donor than *cis* isomer, hence it increases the electron density on carbon centered anti bonding π* molecular orbital resulting in a down field ^{13}C NMR shift. A similar trend has been observed (chapter 4) in a series of $R_3PAu^{13}C^{15}N$ complexes in which the ^{13}C chemical shift moves down field with increase in σ-donation of phosphines, while in [cap-Au-$Se^{13}C^{15}N$]$^-$ there is less π-bonding, hence the *trans* isomer of captopril increases the electron density on carbon and results in an upfield ^{13}C NMR shift. Similar observation is made for $R_3PAuS^{13}C^{15}N$ complexes (chapter 5) in which ^{13}C chemical shift moves upfield with increase in σ-donation of phosphines.

The disproportionation of unsymmetric gold(I) complexes are known [16,19,112,113]. Similarly [cap-Au-$Se^{13}C^{15}N$]$^-$ can also under go disproportionation and redox reactions as shown in equation *3.10*.

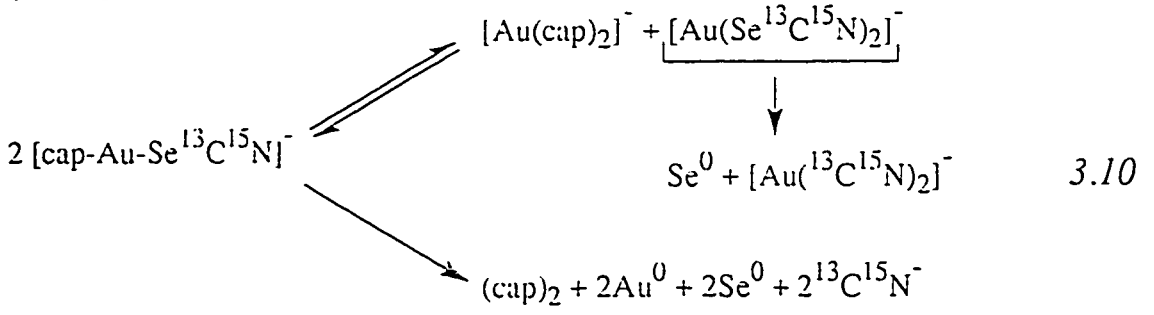

3.10

The ^{13}C NMR resonance assignment of these various species is reported previously [143-145].

As shown in Figure 3.9C, the two broad resonances at 149.82 and 143.99 ppm observed were not present in Figure 3.9B and disappeared in Figure 3.9D (after 143h), are due to [cap(t)-Au-$^{13}C^{15}N$]$^-$ and [cap(c)-Au-$^{13}C^{15}N$]$^-$ respectively [113]. It is already observed (chapter 2) that [Au(Se$^{13}C^{15}N)_2$]$^-$ is unstable in solution, as soon as it is generated, it decompose to metallic selenium and [Au($^{13}C^{15}N)_2$]$^-$. Similarly, once *trans* and *cis* [cap-Au-Se$^{13}C^{15}N$]$^-$ species were generated, they slowly decomposed to give *cis* and *trans* [cap-Au-$^{13}C^{15}N$]$^-$ as shown in equation *3.11*.

$$[\text{cap-Au-Se}^{13}\text{C}^{15}\text{N}]^- \longrightarrow [\text{cap-Au-}^{13}\text{C}^{15}\text{N}]^- + \text{Se}^0 \qquad 3.11$$

The *trans* or *cis* [cap-Au-$^{13}C^{15}N$]$^-$ complexes are supposed to be stable species, but they appeared as broad resonances at 149.82(t) and 143.99(c) ppm respectively and disappeared after 143h. It is expected that free Se$^{13}C^{15}N^-$ may be in exchange with [cap-Au-$^{13}C^{15}N$]$^-$ to form [Au(Se$^{13}C^{15}N$)($^{13}C^{15}N$)]$^-$, which then disproportionated to give [Au($^{13}C^{15}N)_2$]$^-$ and resulted in complete loss of [cap(t or c)-Au-$^{13}C^{15}N$]$^-$ as shown in equation *3.12*.

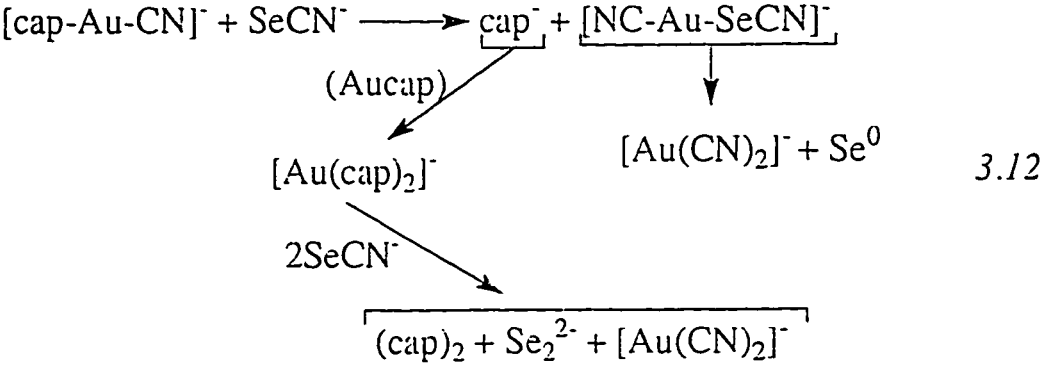

This exchange of free Se$^{13}C^{15}N^-$ with *trans* or *cis* [cap-Au-$^{13}C^{15}N$]$^-$ complexes probably caused the broadening and shifting from the

previously reported [113] chemical shifts for these species, as shown in Figure 3.9B.

The stability of [cap-Au-$Se^{13}C^{15}N$]$^-$ depends upon the ratio of 1/n[$(Aucap)_n$] : $Se^{13}C^{15}N^-$, when this ratio was 1:1, the resonances due to both *trans* or *cis* [cap-Au-$^{13}C^{15}N$]$^-$ complexes were resolved, however at a ratio of 1:0.5, the resonances due to *trans* or *cis* [cap-Au-$^{13}C^{15}N$]$^-$ complexes were not resolved. These observations indicate that the course of action of $(Aucap)_n$ with $Se^{13}C^{15}N^-$ is highly dependent upon their ratios.

Kanatzidis *et.al* [115-118] have reported the synthesis, structural characterization and reactivity of gold(I)/gold(III) polyselenide complexes. In these studies they have isolated various complexes such as $[Au_2Se_2Se_3]^{2-}$, $[Au_2Se_2Se_4]^{2-}$. These gold(I) complexes were prepared by reacting AuCN with Na_2Se_x. It is also reported that the internal transfer of electron converted gold(I) to gold(III) in some complexes as shown in equation *3.13*.

$$2Au^+ + 2Se_5^{2-} \longrightarrow [Au_2(Se_5)_2]^{2-} \qquad 3.13$$

The color of gold(I) and gold(III) polyselenides are reported as dark brown dimethylformamide.

The results presented in this study show that when $Se^{13}C^{15}N^-$ added to $(Aucap)_n$ solution, the color first changed from colorless to yellow and then to dark brown. This color change indicate that some of the selenium metal may be reduced as shown in equation *3.14*.

$$Au^+ + xSe \longrightarrow Au^{3+} + Se_x^{2-} \qquad 3.14$$

This polyselenide anion can react further with gold(I) and gold(III) to form polyselenide complexes as reported by Kanatzidis *et.al* [115-118].

Figure 3.13 shows a plot of $1/[SeCN]^-$ versus time at a 1:1 ratio, the second order rate constant was calculated for rate = $k[(Aucap)_n][SeCN^-]$ where $k= 0.014\pm 0.001$ l mol^{-1} h^{-1}. The second order rate of reaction can be explained as shown in equation *3.8*, where, $SeCN^-$ first breaks down polymer by forming $[cap\text{-}Au\text{-}SeCN]^-$, which is a rate determining step. The small 'k' value reflects that the interaction of $SeCN^-$ with $(Aucap)_n$ (high molecular weight polymer) is very slow, therefore initially the resonance due to $[cap\text{-}Au\text{-}SeCN]^-$ increases and then decreases as shown in Figure 3.9 and 3.11. This second order rate constant is an approximate value, because $SeCN^-$ not only forms complexes with $(Aucap)_n$, but also binds with $[cap\text{-}Au\text{-}CN]^-$ as shown in equation *3.12*.

The ^{13}C NMR spectra (Figure 3.12) from reaction of selenourea (SeU) with $(Aucap)_n$ indicate the formation of [cap-Au-SeU] ternary complex, before the addition of SeU the ^{13}C NMR spectrum of only $(Aucap)_n$ was very broad, but as soon as the SeU was added to it, number of resonances appeared in both low field and high field regions. The C_2 and C_3 resonances were different from that of free captopril, which suggest that these resonances are coming up from [cap-Au-SeU], because complexation of captopril to gold will have maximum effect on C_2 and C_3. The C_3 resonance of [cap-Au-SeU] is overlapped with that of $C\beta$, therefore we can monitor through only C_2 resonance. However after 20 hours the appearance of Au^0, Se^0 and resonances from both [cap-Au-SeU] and captopril disulfide $(cap)_2$ indicate that this unsymmetric complex undergoes a slow redox reaction. After 54 hours the complete disappearance of a resonance C_2 of [cap-Au-SeU] indicates

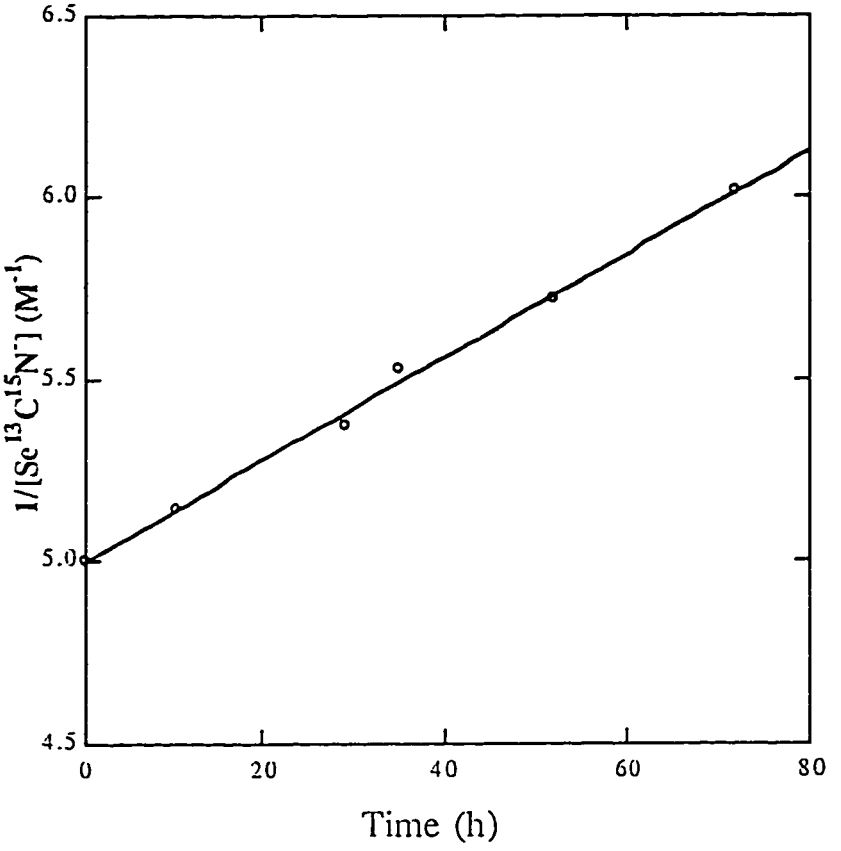

Figure 3.13 The plot of $1/[Se^{13}C^{15}N]^-$ vs time in hours, values are taken from Figure 3.11.

the completion of the reaction. We have studied (chapter 2) the interaction of $(Autm)_n$ with selenourea at pH* of 7.40, during which the formation of metallic gold and thiomalic disulfide $(tm)_2$ were observed but no metallic selenium was found. However in this study, the pH* of solution is very high, hence high concentration of OH^- ions is playing a role in the formation of selenium metal. The probable mechanism for formation of $(cap)_2$, Au^0 and Se^0 from [cap-Au-SeU] complex in presence of OH^- ions is shown below in equation *3.15*.

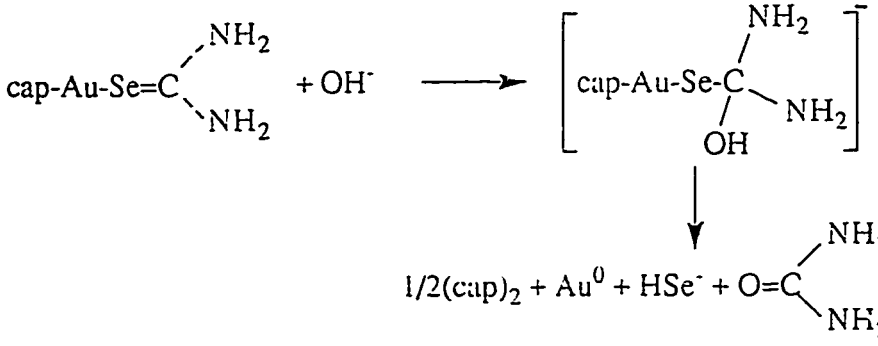

3.15

The HSe^- may undergo oxidation to produce metallic selenium. We did try to run ^{13}C NMR spectrum of free SeU at pH 12.0 but as soon as it was dissolved in D_2O, the metallic selenium was precipitated out.

During the interaction of $(Aucap)_n$ with thiourea (TU), no $(cap)_2$ and Au^0 were observed even after 70 hours, which indicate that TU interact with $(Aucap)_n$ to form stable [cap-Au-TU] ternary complex, the assignment of various resonances to [cap-Au-TU] were based on the same arguments as used in the case of [cap-Au-SeU]. Similar behavior was observed during the interaction of TU with $(Autm)_n$ in which no metallic gold or thiomalic disulfide $(tm)_2$ was observed (chapter 2).

Exchange reactions of $(Autm)_n$ with selenols have been reported [93,94] in aqueous solution, at a 1:2 ratio of $(Autm)_n$: selenols. The formation of bis(selenoate)gold(I) complex was observed with displacement of thiomalate (tm^-), which was not oxidized to thiomalic disulfide $(tm)_2$. These reactions suggests that selenols simply bind to gold(I) and no redox reaction takes place, while interaction of $(Autm)_n$ with selenone-containing ligands, selenourea and imidazolidine-2-selenone (chapter 2) resulted in redox reactions.

3.3 CONCLUSION

It is observed through viscosity measurements that $(Aucap)_n$ forms a very high molecular weight polymer as compared to that of $(Autm)_n$. The degree of polymerization is dependent upon the salts being used, normal salts (e.g. NaCl, KSCN etc.) increased polymerization, whereas π-acid ligand such as KCN breaks down the polymer. Two characteristic routs for the fragmentation of $(Aucap)_n$ have been observed from mass spectroscopy. When $^{13}CN^-$ reacts with $(Aucap)_n$, it forms *trans* and *cis* [cap-Au-^{13}CN]$^-$ complexes, which undergo disproportionation to produce $[(Aucap)_2]^-$ and $[Au(CN)_2]^-$ species. The $[Au(CN)_2]^-$ species have been detected by UV, ^{13}C and ^{15}N NMR spectroscopies. The ^{13}C NMR is also found to be sensitive to the configuration of penultimate captopril moiety in $[\text{-cap-Au-}]_n{}^{13}CN^-$. When $Se^{13}C^{15}N^-$ reacts with $(Aucap)_n$, it forms *trans* and *cis* [cap(t)-Au-$Se^{13}C^{15}N$]$^-$ complexes, which are unstable and decompose to give metallic selenium, which catalyzes various redox reactions. When

selenourea (SeU) interacts with $(Aucap)_n$ it forms unsymmetric [cap-Au-SeU] complex, which undergo redox reactions to produce $(cap)_2$, Se^0 and Au^0, while thiourea (TU) forms stable complex which does not undergo redox reactions.

CHAPTER 4

SCRAMBLING REACTIONS OF R_3PAuCN COMPLEXES

Gold(I) has a strong tendency to form two coordinate complexes as LAuX, where 'L' is frequently a neutral lewis base (e.g. phosphine, thioether etc.) and 'X' is an aryl, alkyl, halide or pseudo halide group [146-148]. Such complexes are generally neutral, but since gold(I) is usually labile there exist the possibility of ligand redistribution in solution to form the symmetrically substituted complexes $[AuL_2]^+$ and $[AuX_2]^-$ type as shown in equation *4.1*.

$$2\,L\text{-}Au\text{-}X \rightleftharpoons [AuL_2]^+ + [AuX_2]^- \qquad 4.1$$

An extreme case of ligand scrambling reaction given in equation 4.1 has been observed in (Tetrahydrothiophene)gold(I)iodide [149], which exists in the solid state as the ionic complex $[Au(THF)_2]^+[AuI_2]^-$. Several types of scrambling reactions have been studied by ^{31}P NMR and IR spectroscopy. In many cases two, three and four coordinated gold species have been observed [150]. Ligand scrambling, resulting in an increase in coordination number for gold may occur when 'L' or 'X' is present in excess. [151,152] as shown in equations *4.2* and*4.3*.

$$2\,[Ph_3PAuCN] + Ph_3P \rightleftharpoons [(Ph_3P)_3Au]^+ + [Au(CN)_2]^- \qquad 4.2$$

$$2\,[AuL_2]Cl \rightleftharpoons [AuL_3]Cl + L\text{-}Au\text{-}Cl \qquad 4.3$$

However, cyanothiolatogold(I) complexes, $[RS\text{-}Au\text{-}CN]^-$, undergo yet another type of ligand scrambling in aqueous solution [19], with retention of coordination number of gold(I). It takes place without any excess of ligands as shown in equation *4.4*.

$$2\,[RS\text{-}Au\text{-}CN]^- \rightleftharpoons [Au(RS)_2]^- + [Au(CN)_2]^- \qquad 4.4$$

Similar ligand scrambling reactions have been observed [153] for neutral alkyl or aryl phoshine gold(I) cyanide complexes in solution as shown in equation *4.5*.

$$2\,[R_3P\text{-}Au\text{-}CN] \rightleftharpoons [Au(R_3P)_2]^+ + [Au(CN)_2]^- \qquad 4.5$$

The K_{eq} of this reaction is found to be dependent upon the extrinsic factors (i.e. initial concentration, ionic strength and polarizability of the solvent) and intrinsic factors (i.e. steric hindrance and electronic properties of phosphine ligands). Previous studies [64] have demonstrated that K_{eq} increases as polarity of solvent or ionic strength of the medium increases. The phosphines selected in this study have a wide range of steric and electronic properties. Tolman [154] has used two parameters, the cone angle, 'θ' and an electronic parameter ν_{CO} to order the steric and electron donating properties of phosphines. The ν_{CO} is the frequency of the A_1 carbonyl mode of $[Ni(CO)_3L]$ dissolved in dichloromethane. In comparing two phosphines, a lower ν_{CO} value reflects a larger net electron donating ability (including σ-donating and π-accepting interactions) [154]. it has been observed that K_{eq} increases with increase in Lewis basicity of the phosphines [64]. The cone angle 'θ' is defined as the apex angle of a

cylindrical cone that is 2.28 A° from the center of phosphorous atom, as shown below.

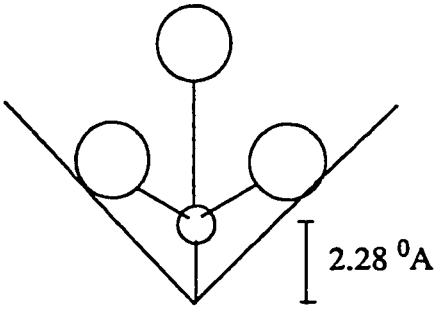

These ligand scrambling reactions of gold(I) complexes are important from biological point of view. Smokers who, are treated with various anti arthritic gold drugs have been reported to have higher concentration of gold in their red blood cells compared to the nonsmokers [20,21,155]. Tobacco smoke contains approximately o.5μg/L HCN [156] which interact with these gold drugs to form L-Au-CN (where L= thiolate or phosphine) type unsymmetric complex which readily under go disproportionation as shown in equation *4.5* to form $[Au(CN)_2]^-$ specie. The Possible mechanism by which gold in the form of $[Au(CN)_2]^-$ can enter the red blood cells is the subject of recent studies [16-19,113]. The very large formation constant for $[Au(CN)_2]^-$ with $\log\beta_2$ 36.6 [95] drives all the L-AuCN complexes to disproportionate generating $[Au(CN)_2]^-$ which can enter the red blood cells.

We have prepared labeled and unlabeled phosphine gold(I) cyanide complexes (using KCN and $K^{13}C^{15}N$) to study the various coupling constants and thermodynamic constants for these ligand scrambling reactions. The phosphines selected were $Cycl_3P$(cylohexylphosphine), *i*-Pr_3P(isopropylphosphine), Et_3P(ethylphosphine), Me_3P(methylphosphine), Ph_3P(phenylphosphine), $CyclPh_2P$ (cyclohexyldiphenylphosphine), $AllylPh_2P$ (allyldiphenylphosphine), *p*-Tol_3P(paratolylphosphine), *o*-

Tol_3P(orthotolylphosphine), *m*-Tol_3P(metatolylphosphine), *p*-$TolPh_2P$ (paratolyldiphenylphosphine), Np_3P(1-naphthylphosphine) and CEP (cyanoethylphosphine). Their cone angles, electronic parameters and ^{31}P chemical shifts are given in Table 4.1. All of the R_3PAuCN complexes were characterized by CHN elemental analysis, IR, ^{13}C, ^{15}N and ^{31}P NMR spectroscopy.

4.1 EXPERIMENTAL OVERVIEW

An overview of the synthetic methods employed, is given below the detailed procedures are presented in chapter 6.

4.1.1 Synthesis

Three methods were used to prepare R_3PAuCN complexes: (1) Double displacement of Me_2S and Cl^- from Me_2SAuCl with R_3P and CN^-(2) The displacement of Cl^- from R_3PAuCl by CN^- (3) The addition of R_3P to AuCN.

Method 1.

The reactions of Me_2SAuCl involving single displacement of Me_2S by a neutral ligand have been described in a patent [157]. However in this study double displacement of Me_2S and Cl^- from Me_2SAuCl is used to prepare R_3PAuCN complexes (equation *4.6*):

$$Me_2SAuCl + R_3P + KCN \longrightarrow R_3PAuCN + Me_2S + KCl \qquad 4.6$$

The high volatility of the Me_2S and the easy displacement of the Cl^- drive the reaction to completion. The Me_2SAuCl was prepared by the reduction of $HAuCl_4$ with an excess of Me_2S (equation *4.7*) [158].

$$HAuCl_4 + 2Me_2S + H_2O \longrightarrow Me_2SAuCl + Me_2SO + 3HCl \qquad 4.7$$

TABLE 4.1 The values of $\nu_{(CO)}$ (cm^{-1}), θ, and $\delta(^{31}P)$ (ppm) for various Phosphine ligands used in this study.

R_3P	[a]$\nu_{(CO)}$ (cm^{-1})	[a]θ	$\delta(^{31}P)$ (ppm)
$Cycl_3P$	2056.4	170	8.2
i-Pr_3P	2059.2	160	18.6
Et_3P	2061.7	132	-20.6
Me_3P	2064.1	118	-64.1
$CyclPh_2P$	2064.7	-	-6.5
o-Tol_3P	2066.6	194	-4.0
p-Tol_3P	2066.7	145	-6.8
m-Tol_3P	2067.2	-	-7.7
p-$TolPh_2P$	2068.2	145	-8.7
$AllylPh_2P$	-	-	6.4
Ph_3P	2068.9	145	-7.8
CEP	2077.9	132	-1.0

[a]values are taken from reference 154.

The reactions were carried out in a darkened room due to the decomposition of Me_2SAuCl in presence of light.

Method 2.

In this method [153] R_3PAuCN were prepared by the displacement of Cl^- with CN^- (equation *4.8*):

$$R_3PAuCl + KCN \longrightarrow R_3PAuCN + KCl \qquad 4.8$$

The R_3PAuCl was prepared by the reduction of $HAuCl_4$ with thiodiglycol at 0.0 °C followed by the addition of R_3P [159] (equation *4.9*) :

$$R_3P + HAuCl_4 + H_2O + S(CH_2CH_2OH)_2 \longrightarrow R_3PAuCl + 3HCl + OS(CH_2CH_2OH)_2 \qquad 4.9$$

The R_3PAuCl prepared in this way was washed several times to remove excess thiodiglycol to prevent further reduction of R_3PAuCl to the metallic gold.

Method 3

In this method R_3PAuCN complexes were prepared using a heterogeneous reaction. The Solution of R_3P was added to solid AuCN [64] (equation *4.10*).

$$R_3P + AuCN \longrightarrow R_3PAuCN \qquad 4.10$$

In this reaction, the R_3P was always the limiting reagent to prevent the formation of $[(R_3P)_2Au]^+$ or $[(R_3P)_3Au]^+$ species. These species have been observed by ^{31}P NMR spectroscopy in the reactions of R_3PAuX (X=halide) with the excess of R_3P [160]. The AuCN was prepared by the addition of excess H_2SO_4 (conc.) to $KAu(CN)_2$ (equation *4.11*).

$$2K[Au(CN)_2] + H_2SO_4 \longrightarrow 2AuCN + 2HCN + K_2SO_4 \qquad 4.11$$

The $KAu(CN)_2$ was prepared by the double displacement of Me_2S and Cl^- from Me_2SAuCl with two equivalents of KCN (equation *4.12*).

$$Me_2SAuCl + 2KCN \longrightarrow K[Au(CN)_2] + Me_2S + KCl \qquad 4.12$$

4.2 RESULTS

The ^{31}P, ^{13}C and ^{15}N NMR studies of the scrambling reactions of (alky/aryl)phosphine gold(I) cyanide are given below, while all experimental details are given in chapter 6.

4.2.1 ^{31}P {^{1}H} NMR studies of $R_3PAu^{13}C^{15}N$ complexes

The ^{31}P NMR spectra of 0.025 M $R_3PAu^{13}C^{15}N$ (where R_3P = Me_3P, Et_3P, *i*-Pr_3P, Cyl_3P, Ph_3P, *o*-Tol_3P, *m*-Tol_3P, *p*-Tol_3P, $CyclPh_2P$, *p*-$TolPh_2P$, $AllylPh_2P$, Np_3P and CEP) complexes were measured in CD_3OD. In all $R_3PAu^{13}C^{15}N$ complexes except *o*-$Tol_3PAu^{13}C^{15}N$, $CEPAu^{13}C^{15}N$ and $Np_3PAu^{13}C^{15}N$, two separate resonances were resolved for $R_3PAu^{13}C^{15}N$ and $[(R_3P)_2Au]^+$ species, neither of these two resonances were due to R_3P or R_3PO. The ^{31}P NMR chemical shifts of all $R_3PAu^{13}C^{15}N$ and $[(R_3P)_2Au]^+$ species are given in Table 4.2, while their $^{2}J_{(^{31}P-^{13}C)}$ and $^{3}J_{(^{31}P-^{15}N)}$ are given in Table 4.3. The ^{31}P NMR spectra of $Me_3PAu^{13}C^{15}N$, $Et_3PAu^{13}C^{15}N$ and $Ph_3PAu^{13}C^{15}N$ complexes are shown in Figure 4.1.

In all $R_3PAu^{13}C^{15}N$ complexes the resonance for $[(R_3P)_2Au]^+$ species appeared down field compared to the resonance of $R_3PAu^{13}C^{15}N$ species, which is consistent with other studies [153]. These two resonance, which were assigned on the bases of coupling constants $^{2}J_{(^{31}P-^{13}C)}$ and $^{3}J_{(^{31}P-^{15}N)}$, demonstrate that $R_3PAu^{13}C^{15}N$ complexes are undergoing ligand scrambling reactions as shown in equation *4.5*. The *m*-$Tol_3PAu^{13}C^{15}N$,

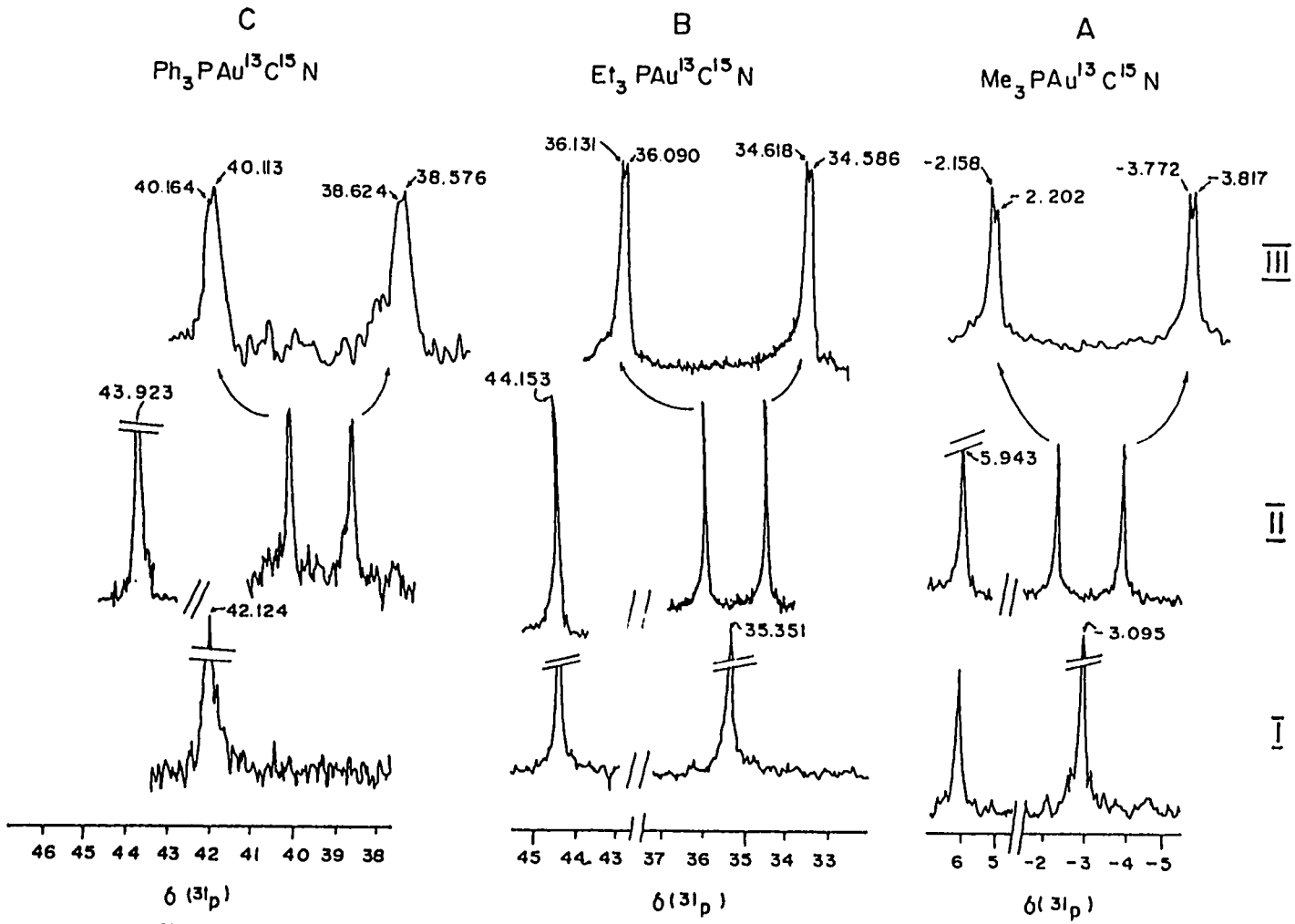

Figure 4.1 ^{31}P NMR spectra of: [A] , (I) Me_3PAuCN, (II) $Me_3PAu^{13}C^{15}N$, (III) expanded spectrum of II; [B] (I) Et_3PAuCN, (II) $Et_3PAu^{13}C^{15}N$, (III) expanded spectrum of II (all spectra were recorded at 297 K); [C] (I) $Ph_3PAu^{13}C^{15}N$ at 297 K, (II) $Ph_3PAu^{13}C^{15}N$ at 233 K (III) expanded spectrum of II.

TABLE 4.2 The Chemical shift $\delta(^{31}P)$ in ppm of $[(R_3P)_2Au]^+$ and $[R_3PAu^{13}C^{15}N]$ species.

R_3P	$[(R_3P)_2Au]^+$	$[R_3PAu^{13}C^{15}N]$
$Cycl_3P$	62.12	53.53
i-Pr_3P	79.03	65.07
Et_3P	44.17	35.35
Me_3P	5.94	-3.09
$CyclPh_2P$	51.34	44.04
o-Tol_3P	-	37.38
p-Tol_3P	40.77	34.45
m-Tol_3P	41.47	35.79
p-$TolPh_2P$	39.31	31.98
$AllylPh_2P$	40.93	35.29
Ph_3P	43.92	39.37
CEP	-	30.35
Np_3P	-	35.43

TABLE 4.3 Coupling constants $^{2}J_{(^{31}P-^{13}C)}$ and $^{3}J_{(^{31}P-^{15}N)}$ in Hz of various $R_3PAu^{13}C^{15}N$ complexes.

$R_3PAu^{13}C^{15}N$	$^{2}J_{(^{31}P-^{13}C)}$ (Hz)	$^{3}J_{(^{31}P-^{15}N)}$ (Hz)
$Cycl_3PAu^{13}C^{15}N$	115.23	2.96
i-$Pr_3PAu^{13}C^{15}N$	116.08	2.84
$Et_3PAu^{13}C^{15}N$	122.18	2.93
$Me_3PAu^{13}C^{15}N$	130.71	4.0
$CyclPh_2PAu^{13}C^{15}N$	121.96	2.57
o-$Tol_3PAu^{13}C^{15}N$	-	-
p-$Tol_3PAu^{13}C^{15}N$	126.34	2.44
m-$Tol_3PAu^{13}C^{15}N$	125.55	2.95
p-$TolPh_2PAu^{13}C^{15}N$	128.10	2.8
$AllylPh_2PAu^{13}C^{15}N$	126.00	4.42
$Ph_3PAu^{13}C^{15}N$	124.56	4.01
$CEPAu^{13}C^{15}N$	-	-
$Np_3PAu^{13}C^{15}N$	-	-

p-TolPh$_2$PAu^{13}C^{15}N and Ph$_3$PAu^{13}C^{15}N complexes gave rise to only one broad resonance at room temperature, while all other complexes gave rise to two separate resonances. However at 233 K the *m*-Tol$_3$PAu^{13}C^{15}N, *p*-TolPh$_2$PAu^{13}C^{15}N complexes gave rise to two separate resonances, while at 213 K the Ph$_3$PAu^{13}C^{15}N complex gave rise to two separate resonances for R$_3$PAu^{13}C^{15}N and [(R$_3$P)$_2$Au]$^+$ species. In all ^{31}P NMR spectra the resonance due to [(R$_3$P)$_2$Au]$^+$ appeared as a single sharp peak, whereas resonance due to R$_3$PAu^{13}C^{15}N was observed as a doublet of doublet due to $^2J_{(^{31}P-^{13}C)}$ and $^3J_{(^{31}P-^{15}N)}$ coupling constants.

4.2.2 ^{13}C {^{1}H} NMR spectra of R$_3$PAu^{13}C^{15}N complexes

The observation of two separate resonances in ^{31}P NMR spectra of RPAu^{13}C^{15}N complexes was evidence for ligand scrambling reaction. This ligand scrambling reaction was further characterized using ^{13}C NMR spectroscopy, because all three species as R$_3$PAu^{13}C^{15}N, [(R$_3$P)$_2$Au]$^+$ and [Au(^{13}C^{15}N)$_2$]$^-$ were identified very easily. A typical spectrum for one of the complex , *i*-Pr$_3$PAu^{13}C^{15}N, is shown in Figure 4.2. The ^{13}C chemical shifts for 'CN' group of all R$_3$PAu^{13}C^{15}N complexes and their $^1J_{(^{13}C-^{15}N)}$ values are given in Table 4.4. The resonance due to [Au(^{13}C^{15}N)$_2$]$^-$ species was resolved as a triplet with J(^{13}C-^{15}N) of 5.5 to 6.6 Hz due to virtual coupling at 151.70 to 152.02 ppm in all R$_3$PAu^{13}C^{15}N complexes. All coupling constants are expressed as absolute values and are comparable to other systems. The virtual coupling $^1J_{(^{31}P-^{13}C)}$ for [(R$_3$P)$_2$Au]$^+$ was only resolved in [(Cycl$_3$P)$_2$Au]$^+$ and [(*i*-Pr$_3$P)$_2$Au]$^+$ species. The ^{13}C NMR chemical shifts in all R$_3$PAu^{13}C^{15}N complexes are briefly discussed below:

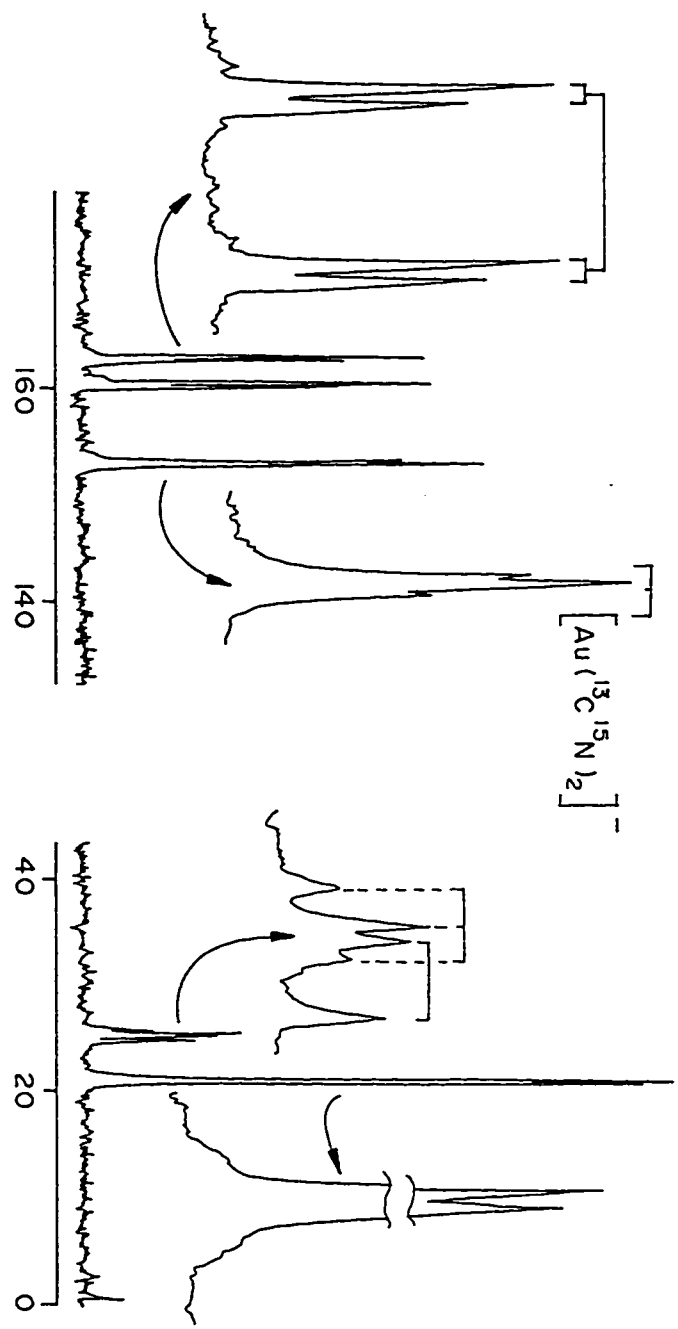

Figure 4.2 ^{13}C NMR spectrum of *i*-$Pr_3PAu^{13}C^{15}N$ complex.

TABLE 4.4 Chemical shifts in ppm $\delta(^{13}C)$ and $^{1}J_{(^{13}C-^{15}N)}$ in Hz of various $R_3PAu^{13}C^{15}N$ complexes.

$R_3PAu^{13}C^{15}N$	$\delta(^{13}C)$ (ppm)	$^{1}J_{(^{13}C-^{15}N)}$ (Hz)
$Cycl_3PAu^{13}C^{15}N$	160.7	-
i-$Pr_3PAu^{13}C^{15}N$	160.8	10.5
$Et_3PAu^{13}C^{15}N$	160.2	10.4
$Me_3PAu^{13}C^{15}N$	158.2	11.6
$CyclPh_2PAu^{13}C^{15}N$	158.8	10.7
o-$Tol_3PAu^{13}C^{15}N$	152.0	-
p-$Tol_3PAu^{13}C^{15}N$	156.9	10.6
m-$Tol_3PAu^{13}C^{15}N$	156.4	
p-$TolPh_2PAu^{13}C^{15}N$	156.7	10.7
$AllylPh_2PAu^{13}C^{15}N$	157.6	9.5
$Ph_3PAu^{13}C^{15}N$	156.6	10.3
$CEPAu^{13}C^{15}N$	157.1	-
$Np_3PAu^{13}C^{15}N$	152.06	6.8

Tricyclohexylphosphinegold(I) cyanide ($Cycl_3PAu^{13}C^{15}N$)

In high field region of ^{13}C NMR spectra number of intense resonances were observed, which were easily assigned to different carbon atoms in $Cycl_3PAu^{13}C^{15}N$ and $[(Cycl_3P)_2Au]^+$ species. In the range of 33 to 34 ppm the C_1 resonance of $Cycl_3PAu^{13}C^{15}N$ was overlapped with the C_1 resonance of $[(Cycl_3P)_2Au]^+$ species. The C_1 resonance of $Cycl_3PAu^{13}C^{15}N$ was resolved as a doublet with $^1J(^{13}C\text{-}^{31}P)$ of 30 Hz at 33.43 ppm, while sharp resonaces were observed at 31.35, 27.13 and 26.28 ppm for C_2, C_3 and C_4 respectively. In $[(Cycl_3P)_2Au]^+$ species the C_1 resonance was observed at 33.83 ppm as a triplet due to virtual coupling with $^1J(^{13}C\text{-}^{31}P)$ of 13.7 Hz, The C_2 and C_3 were resolved as sharp single resonances at 31.49 and 27.63 ppm respectively, while C_4 resonance was overlapped with C_4 resonance of $Cycl_3PAu^{13}C^{15}N$ species.

In low field region the resonance of $[Au(^{13}C^{15}N)_2]^-$ species was resolved as a triplet due to virtual coupling at 151.70 ppm with $^1J(^{13}C\text{-}^{15}N)$ of 5.5 Hz. A doublet was resolved at 160.29 ppm due to δCN of $Cycl_3PAu^{13}C^{15}N$, with $^2J_{(^{13}C\text{-}^{31}P)}$ of 118.1 Hz, while further splitting due to $^1J_{(^{13}C\text{-}^{15}N)}$ was not resolved.

Tri-i-propylphosphinegold(I) cyanide ($i\text{-}Pr_3PAu^{13}C^{15}N$)

^{13}C NMR chemical shifts and coupling constants of various species in Tri-*i*-propylphosphinegold(I) cyanide system.

$i\text{-}Pr_3PAu^{13}C^{15}N$

δC_1= 24.68 , δC_2= 20.61 and δ(CN)= 160.86 ppm

$^1J_{(^{13}C\text{-}^{31}P)}$= 28.3, $^2J_{(^{13}C\text{-}^{31}P)}$= 115.8 and $^1J_{(^{13}C\text{-}^{15}N)}$= 10.5 Hz

$[(i\text{-}Pr_3P)_2Au]^+$

δC_1= 24.68 and δC_2= 20.61 ppm.

$[Au(^{13}C^{15}N)_2]^-$

δ(CN)= 152.02 ppm and $^1J(^{13}C\text{-}^{15}N)$= 6.2 Hz

Triethylphosphinegold(I) cyanide ($Et_3PAu^{13}C^{15}N$)

^{13}C NMR chemical shifts and coupling constants of various species in Triethylphosphinegold(I) cyanide system.

$Et_3PAu^{13}C^{15}N$

δC_1= 18.11 , δC_2= 9.33 and δ(CN)= 160.24 ppm

$^1J_{(^{13}C\text{-}^{31}P)}$= 35.1, $^2J_{(^{13}C\text{-}^{31}P)}$= 122.2 and $^1J_{(^{13}C\text{-}^{15}N)}$= 10.4 Hz

$[(Et_3P)_2Au]^+$

δC_1= 18.11 and δC_2= 9.33 ppm.

$[Au(^{13}C^{15}N)_2]^-$

δ(CN)= 151.70 ppm and $^1J(^{13}C\text{-}^{15}N)$= 6.5 Hz

Trimethylphosphinegold(I) cyanide ($Me_3PAu^{13}C^{15}N$)

^{13}C NMR chemical shifts and coupling constants of various species in Trimethylphosphinegold(I) cyanide system.

$Me_3PAu^{13}C^{15}N$

δCH_3= 14.67 and δ(CN)= 158.23 ppm

$^1J_{(^{13}C\text{-}^{31}P)}$= 38.3, $^2J_{(^{13}C\text{-}^{31}P)}$= 130.0 and $^1J_{(^{13}C\text{-}^{15}N)}$= 11.6 Hz

$[(Me_3P)_2Au]^+$

δCH_3= 14.76 ppm and $^1J_{(^{13}C\text{-}^{31}P)}$= 19.3 Hz.

$[Au(^{13}C^{15}N)_2]^-$

δ(CN)= 151.24 ppm

Triphenylphosphinegold(I) cyanide ($Ph_3PAu^{13}C^{15}N$)

The ^{13}C NMR spectrum showed number of resonances for both $Ph_3PAu^{13}C^{15}N$ and $[(Ph_3P)_2Au]^+$ species in the range of 130 to 135 ppm, which cannot be identified separately. The resonance due to $[Au(^{13}C^{15}N)_2]^-$

species was resolved as a triplet due to virtual coupling at 152.05 ppm with $^{1}J_{(^{13}C-^{15}N)}$ of 6.45 Hz. The δCN of $Ph_3PAu^{13}C^{15}N$ was resolved as a doublet with $^{1}J_{(^{13}C-^{15}N)}$ of 10.3 Hz at 156.63 ppm. The $^{2}J_{(^{13}C-^{31}P)}$ was not resolved at room temperature due to fast exchange between $Ph_3PAu^{13}C^{15}N$ and $[(Ph_3P)_2Au]^+$ species.

Cyclohexyldiphenhylphosphinegold(I) cyanide (CyclPh$_2$PAu^{13}C^{15}N)

Four small resonances were resolved at 34.28, 30.55, 27.02 and 26.86 ppm due to C_1, C_2, C_3 and C_4 respectively, for both $CyclPh_2PAu^{13}C^{15}N$ and $[(CyclPh_2P)_2Au]^+$ species, while five resonances were observed in the region of 130 to 135.5 ppm for the phenyl groups of both $CyclPh_2PAu^{13}C^{15}N$ and $[(CyclPh_2P)_2Au]^+$ species. A broad resonance was resolved at 152.01 ppm for $[Au(^{13}C^{15}N)_2]^-$ species which was not resolved in a triplet. The δCN of $CyclPh_2PAu^{13}C^{15}N$ was resolved as a doublet of doublet due to $^{2}J_{(^{13}C-^{31}P)}$ of 122.8 Hz and $^{1}J_{(^{13}C-^{15}N)}$ of 10.7 Hz at 158.81 ppm.

Allyldiphenylphosphinegold(I) cyanide (AllylPh$_2$PAu^{13}C^{15}N)

In high field region a small resonance was observed at 23.97 ppm for C_1 of allyl group of both $AllylPh_2PAu^{13}C^{15}N$ and $[(AllylPh_2P)_2Au]^+$ species. In low field region the C_2 of allyl group was resolved at 129.78 and 129.40 ppm for $[(AllylPh_2P)_2Au]^+$ and $AllylPh_2PAu^{13}C^{15}N$ species, respectively, while C_3 was resolved at 122.50 ppm for both species. Five resonances were resolved in the region of 130 to 135 ppm for phenyl group of both species. The resonance due to $[Au(^{13}C^{15}N)_2]^-$ species was resolved as a triplet due to virtual coupling at 151.79 ppm with $^{1}J(^{13}C-^{15}N)$ of 6.15

Hz. The δCN of AllylPh$_2$PAu^{13}C^{15}N was resolved as a doublet of doublet due to $^2J_{(^{13}C-^{31}P)}$ of 131.0 Hz and $^1J_{(^{13}C-^{15}N)}$ of 10.8 Hz at 157.58 ppm.

Tri-p-tolylphosphinegold(I) cyanide (p-Tolyl$_3$PAu^{13}C^{15}N)

In high field region of ^{13}C NMR spectrum a single sharp resonance was observed at 21.40 ppm for CH_3 group of both *p*-Tol$_3$PAu^{13}C^{15}N and [(*p*-Tol$_3$P)$_2$Au]$^+$ species. In low field region four broad resonances were resolved at 135.24, 134.94, 131.39 and 131.12 ppm for C_1 to C4 of both species. The resonance due to [Au(^{13}C^{15}N)$_2$]$^-$ species was resolved as a triplet due to virtual coupling at 151.92 ppm with $^1J_{(^{13}C-^{15}N)}$ of 6.8 Hz. The δCN of *p*-Tol$_3$PAu^{13}C^{15}N was resolved as a doublet of doublet due to $^2J_{(^{13}C-^{31}P)}$ of 125.95 Hz and $^1J_{(^{13}C-^{15}N)}$ of 10.6 Hz at 156.88 ppm.

Tri-m-tolylphosphinegold(I) cyanide (m-Tolyl$_3$PAu^{13}C^{15}N)

The CH_3 group resonance of both *m*-Tol$_3$PAu^{13}C^{15}N and [(*m*-Tol$_3$P)$_2$Au]$^+$ species in ^{13}C NMR spectrum was observed at 21.33 ppm, while five broad resonances were resolved at 140.96, 134.11, 135.65, 130.54 and 132.31 ppm for C_1, C_2, C_3, C_4 and C_6 respectively of both species. The resonance due to [Au(^{13}C^{15}N)$_2$]$^-$ species was resolved as a triplet due to virtual coupling at 151.70 ppm with $^1J_{(^{13}C-^{15}N)}$ of 6.6 Hz. The δCN of *m*-Tol$_3$PAu^{13}C^{15}N was resolved as a doublet with $^1J_{(^{13}C-^{15}N)}$ of 10.3 Hz at 156.55 ppm. The $^2J_{(^{13}C-^{31}P)}$ was not resolved at room temperature due to fast exchange between *m*-Tol$_3$PAu^{13}C^{15}N and [(*m*-Tol$_3$P)$_2$Au]$^+$ species.

p-tolyldiphenylphosphinegold(I) cyanide
(p-TolylPh$_2$PAu^{13}C^{15}N)

In high field region of ^{13}C NMR spectrum a single sharp resonance was observed at 21.38 ppm for CH_3 group of both *p*-TolPh$_2$PAu^{13}C^{15}N and

[(*p*-TolPh$_2$P)$_2$Au]$^+$ species. In low field region number of resonances were observed in the region of 130 to 135 ppm for carbons of *p*-Tollyl and Phenyl groups in both species, which were difficult to assign separately. The resonance due to [Au(^{13}C^{15}N)$_2$]$^-$ species was resolved as a triplet due to virtual coupling at 151.94 ppm with $^1J_{(^{13}C\text{-}^{15}N)}$ of 6.8 Hz. The δCN of *p*-TolPh$_2$PAu^{13}C^{15}N was resolved as a doublet with $^1J_{(^{13}C\text{-}^{15}N)}$ of 10.7 Hz at 156.64 ppm. The $^2J_{(^{13}C\text{-}^{31}P)}$ was not resolved at room temperature due to fast exchange between *p*-TolPh$_2$PAu^{13}C^{15}N and [(*p*-TolPh$_2$P)$_2$Au]$^+$ species.

Tris(cyanoethyl)phosphinegold(I) cyanide (CEPAu^{13}C^{15}N)

Two sharp resonances were observed at 14.04 and 21.97 ppm for C_2 and C_1 respectively of CEPAu^{13}C^{15}N in ^{13}C NMR spectrum. The resonance for CN group, not coordinated to gold(I) was observed at 122.27 ppm, While δCN for CN group coordinated to gold(I) was observed at 152.12 ppm

Tri-o-tolylphosphinegold(I) cyanide (o-Tolyl$_3$PAu^{13}C^{15}N)

In high field region of ^{13}C NMR spectrum a single sharp resonance was observed at 22.07 ppm for CH_3 group, while in low field region number of resonances were observed in the region of 126 to 134 ppm which were difficult to assign The δCN was resolved as a triplet at 152.15 ppm with $^1J_{(^{13}C\text{-}^{15}N)}$ of 6.8 Hz.

Tri-1-naphthylphosphinegold(I) cyanide (Np$_3$PAu^{13}C^{15}N)

Number of resonances were observed in the region of 124 to 140 ppm for naphthyl group which were difficult to assign. The δCN was resolved as a triplet at 152.03 ppm with $^1J_{(^{13}C\text{-}^{15}N)}$ of 6.8 Hz.

4.2.3 ^{15}N {^{1}H} NMR spectra of $R_3PAu^{13}C^{15}N$ complexes

^{15}N NMR spectra of $Cycl_3PAu^{13}C^{15}N$, *i*-$Pr_3PAu^{13}C^{15}N$, $Et_3PAu^{13}C^{15}N$, $Me_3PAu^{13}C^{15}N$ and *p*-$TolPh_2PAu^{13}C^{15}N$ complexes were recorded, while in other complexes due to low sensitivity of the instrument and low solubility of the complexes we were unable to get their ^{15}N NMR spectra. The ^{15}N chemical shift difference between $R_3PAu^{13}C^{15}N$ and $[Au(^{13}C^{15}N)_2]^-$ species is very small therefore in most of the cases only one resonance was observed. A typical ^{15}N NMR spectra of $Et_3PAu^{13}C^{15}N$ complex is shown in Figure 4.3. The chemical shifts for ^{15}N NMR spectra of all $R_3PAu^{13}C^{15}N$ complexes are given in Table 4.5.

In case of $Et_3PAu^{13}C^{15}N$ complex two separate resonances were observed for $Et_3PAu^{13}C^{15}N$ and $[Au(^{13}C^{15}N)_2]^-$ species. The resonance due to $[Au(^{13}C^{15}N)_2]^-$ species was resolved as a triplet due to virtual coupling with $^{1}J_{(^{15}N-^{13}C)}$ of 6.90 Hz at 266.79 ppm. The $\delta^{15}N$ of $Et_3PAu^{13}C^{15}N$ was resolved as a doublet of doublet due to $^{1}J_{(^{15}N-^{13}C)}$ of 10.4 Hz and $^{3}J_{(^{15}N-^{31}P)}$ of 3.48 Hz at 265.54 ppm.

In case of $Me_3PAu^{13}C^{15}N$, separate resonances were resolved for $Me_3PAu^{13}C^{15}N$ and $[Au(^{13}C^{15}N)_2]^-$ species. The resonance of $[Au(^{13}C^{15}N)_2]^-$ species was resolved as a triplet with $^{1}J_{(^{15}N-^{13}C)}$ of 6.66 Hz at 267.38 ppm. The $\delta^{15}N$ of $Me_3PAu^{13}C^{15}N$ was resolved as a doublet of doublet due to $^{1}J_{(^{15}N-^{13}C)}$ of 10.35 Hz and $^{3}J_{(^{15}N-^{31}P)}$ of 4.0 Hz at 267.35 ppm.

In case of all other complexes a single broad resonance was resolved for both $R_3PAu^{13}C^{15}N$ and $[Au(^{13}C^{15}N)_2]^-$ species.

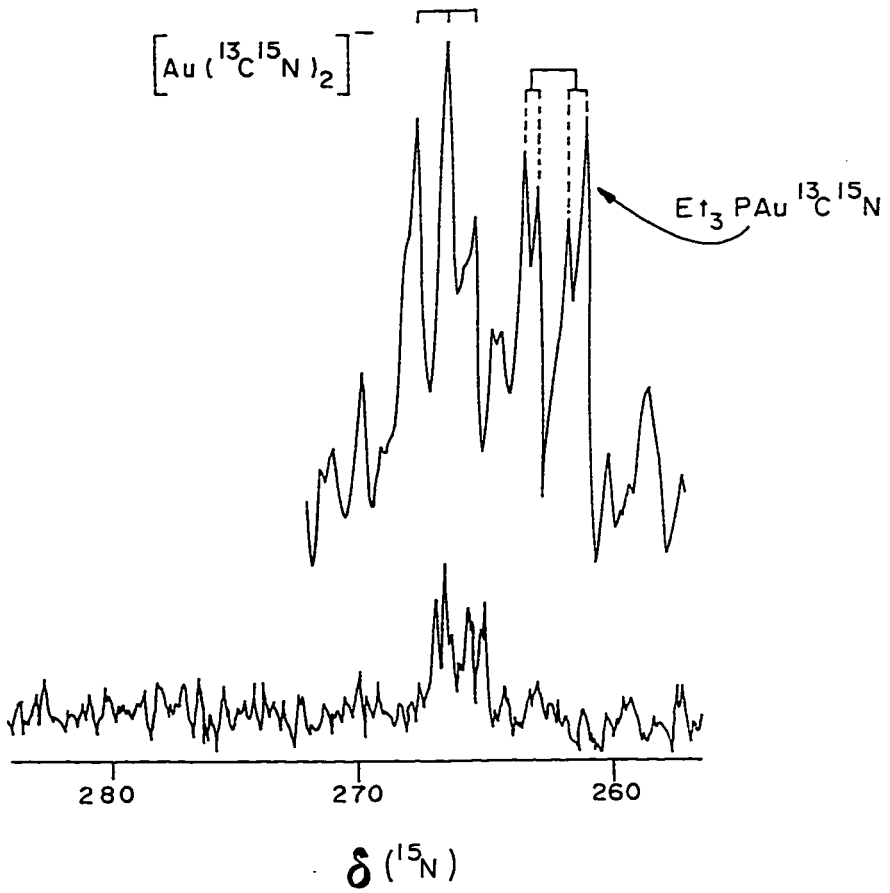

Figure 4.3 ^{15}N NMR spectrum of $Et_3PAu^{13}C^{15}N$ complex.

TABLE 4.5 Chemical shift in ppm $\delta(^{15}N)$ of various $R_3PAu^{13}C^{15}N$ complexes.

$R_3PAu^{13}C^{15}N$	$\delta(^{15}N)$
$Cycl_3PAu^{13}C^{15}N$	264.35
i-$Pr_3PAu^{13}C^{15}N$	264.61
$Et_3PAu^{13}C^{15}N$	265.54
$Me_3PAu^{13}C^{15}N$	267.35
p-$Tol_3PAu^{13}C^{15}N$	270.06

4.2.4 Calculation of activation parameters

Proton decoupled ^{31}P NMR spectra of $R_3PAu^{13}C^{15}N$ complexes were recorded over various temperature ranges for different complexes to measure their free activation energy, at low temperatures the two resonances due to $R_3PAu^{13}C^{15}N$ and $[(R_3P)_2Au]^+$ species were very sharp, as the temperature was increased these resonances started to broaden out and in some cases coalesced peak was observed at higher temperature.

The integration of ^{31}P NMR resonances gave relative concentration for both species and then K_{eq} was calculated. The simulation of exchange broadened ^{31}P NMR spectra were carried out using a library program [162]. Where non-coupled two site exchange with unequal population was considered. The matching of simulated and experimental spectra were carried out by superimposition of calculated and experimental spectra.

The activation parameters $\Delta H^{\#}$ and $\Delta S^{\#}$ were calculated from the Eyring plot of ln(k/T) versus 1/T. The values of $\Delta H^{\#}$, $\Delta S^{\#}$ and $\Delta G^{\#}_{273}$ for all $R_3PAu^{13}C^{15}N$ complexes are given in Table 4.6. The determination of $\Delta H^{\#}$ and $\Delta S^{\#}$ by dynamic NMR is known to be not very accurate due to large systematic errors. However these errors in $\Delta H^{\#}$ and $\Delta S^{\#}$ are often mutually compensatory, so that $\Delta G^{\#}$ is better defined near coalescence temperature.

The calculations are shown below.

$$2\,R_3PAuCN \rightleftharpoons [(R_3P)_2Au]^+ + [Au(CN)_2]^-$$

$$k_{eq} = \frac{[(R_3P)_2Au]^+_{eq}[Au(CN)_2]^-_{eq}}{[R_3PAuCN]^2_{eq}}$$

The equilibrium concentrations of these species can be obtained from the integration of ^{31}P NMR spectra as below:

TABLE 4.6 The $\Delta H^{\#}$, $\Delta S^{\#}$ and $\Delta G^{\#}_{273}$ of different $R_3PAu^{13}C^{15}N$ complexes

$R_3PAu^{13}C^{15}N$	$\Delta H^{\#}$ (kJ/mol)	$\Delta S^{\#}$ (J/mol K)	$\Delta G^{\#}_{273}$ (kJ/mol)
i-$Pr_3PAu^{13}C^{15}N$	14.19±0.29	-195.02±0.54	67.43±0.29
$Me_3PAu^{13}C^{15}N$	4.41±0.06	-215.65±0.16	63.28±0.06
$Ph_3PAu^{13}C^{15}N$	53.1±0.50	49.00±0.50	39.7±0.50
$AllylPh_2PAu^{13}C^{15}N$	45.27±0.97	-53.67±2.75	59.9±0.97
m-$Tol_3PAu^{13}C^{15}N$	33.87±0.73	50.42±2.28	47.64±0.73
p-$Tol_3PAu^{13}C^{15}N$	60.01±1.33	10.66±3.49	57.10±1.33
p-$TolPh_2PAu^{13}C^{15}N$	28.33±0.07	-54.99±0.22	43.33±0.07

$$[R3PAuCN]_{eq} = \frac{I_{(R_3PAuCN)} * [R_3PAuCN]_0}{I_{(R_3PAuCN)} * 1/2I_{(R_3P)_2Au^+}}$$

$$[(R_3P)_2Au]^+_{eq} = \frac{1/2I_{(R_3P)_2Au^+} * [R_3PAuCN]_0}{I_{(R_3PAuCN)} * 1/2I_{(R_3P)_2Au^+}}$$

Where 'I' indicates the ^{31}P NMR integration of that species.

$$\text{Rate} = 2k[R_3PAuCN]^2_{eq} \quad \text{and} \quad k = 1/[2[R_3PAuCN]_{eq} * \tau]$$

Eyring equation $k = \frac{k_B.T}{h} e^{-\Delta H^{\#}/RT} e^{\Delta S^{\#}/R}$

$$\ln(k/T) = \ln(k_B/h) - \Delta H^{\#}/RT + \Delta S^{\#}/R$$

$$\ln(k/T) = -\Delta H^{\#}/RT + [\ln(k_B/h) + \Delta S^{\#}/R]$$

When we plot 'ln(k/T)' versus '1/T' then,

$$\text{Slope} = -\Delta H^{\#}/R \quad \text{and} \quad \Delta H^{\#} = -\text{slope} * R$$

$$\text{Intercept} = \Delta S^{\#}/R + \ln(k_B/h) \quad \text{and} \quad \Delta S^{\#} = (\text{Intercept} - 23.76) * R$$

$$\Delta G^{\#} = \Delta H^{\#} - T\Delta S^{\#}$$

The measurement of activation parameters in different complexes is briefly discussed below.

Tri-i-propylphosphinegold(I) cyanide (i-Pr3PAuCN)

The proton decoupled ^{31}P NMR spectra of 0.025 M *i*-Pr_3PAuCN in DMSO-d_6 were recorded in the temperature range of 293.0 to 453.0 K. At 293 K two sharp resonances were observed for *i*-Pr3PAuCN and $[(i\text{-}Pr_3P)_2Au]^+$ species. Which started to broaden out at higher temperature. At 408 K both peaks were collapsed, but no coalescence resonance was observed upto 453 K, at which metallic gold was observed in the solution due to decomposition of the complex, therefore no further spectra were recorded at higher temperatures. The 'τ' values were calculated at 370.5,

385.5 and 401.8 K and are given in Table 4.7 with their rate constants. The $\Delta H^{\#}$ was found to be 14.19±0.29KJ/Mol, The $\Delta S^{\#}$ was -195.02±0.54 J/Mol K and the $\Delta G^{\#}_{273}$ was obtained as 67.43±0.29 KJ/Mol.

Trimethylphosphinegold(I) cyanide (Me_3PAuCN)

The proton decoupled ^{31}P NMR spectra of 0.0256 M Me_3PAuCN in CD_3OD were recorded in the temperature range of 293.0 to 333.0 K. Two sharp resonances were observed for Me_3PAuCN and $[(Me_3P)_2Au]^+$ species at 293.0 K, which started to broaden out at higher temperature. Even at 333.0 K broad peaks were observed. Since the boiling point of solvent (CD_3OD) is 338 K, hence we stopped recording spectra at higher temperatures. The 'τ' values were measured at 296.0, 316.8, 322.0 and 339.0 ^0C and are given in Table 4.8 with their rate constants. The $\Delta H^{\#}$ was found to be 4.41±0.06KJ/Mol, The $\Delta S^{\#}$ was -215.65±0.16 J/Mol K and the $\Delta G^{\#}_{273}$ was obtained as 63.28±0.06 KJ/Mol.

The proton decoupled ^{31}P NMR spectra of 0.025 M Me_3PAuCN were also recorded in DMSO-d_6 in the temperature range of 293.0 to 388.0 K. Two sharp resonances were observed for Me_3PAuCN and $[(Me_3P)_2Au]^+$ species at 293.0 K, which started to broaden out at higher temperature and at 338.0 K both peaks had collapsed, while no coalescence resonance was observed even upto 388.0 K. The 'τ' values were measured at 294.0, 308.4, and 322.0 K and are given in Table 4.8 with their rate constants. The $\Delta H^{\#}$ was found to be 12.20±0.19KJ/Mol, The $\Delta S^{\#}$ was -189.51±0.45 J/Mol K and the $\Delta G^{\#}_{273}$ was obtained as 63.94±0.19 KJ/Mol.

Triphenylphosphinegold(I) cyanide (Ph_3PAuCN)

The proton decoupled ^{31}P NMR spectra of 0.006 M Ph_3PAuCN in CD_3OD were recorded in the temperature range of 168 to 301 K. Two

TABLE 4.7 Life time and rate constant data for the redistribution reaction of 0.0254 M *i*-$Pr_3PAu^{13}C^{15}N$ in DMSO.

Temperature (K)	τ_a (s)	k (L mol^{-1} s^{-1})
370.5	0.200	163
385.5	0.080	408
401.8	0.012	2,723

TABLE 4.8 Life time and rate constant data for the redistribution reaction of 0.025 M $Me_3PAu^{13}C^{15}N$ in CD_3OD and DMSO.

Solvent	Temperature (K)	τ_a (s)	k (L mol^{-1} s^{-1})
CD_3OD	296.0	0.100	266
	316.8	0.035	760
	322.0	0.020	1330
	339.2	0.009	2955
DMSO	294.0	0.040	206
	308.0	0.010	823
	322.0	0.001	8235

sharp resonances were observed for Ph_3PAuCN and $[(Ph_3P)_2Au]^+$ species at 168 K. Which started to broaden out at higher temperatures and coalesced around 223 K. Above 223 K the average peak started to become sharper. The 'τ' values were measured at 233.0, 243.0, 253.0 263.0 and 273 K and are given in Table 4.9 with their rate constants. The $\Delta H^{\#}$ was found to be 53.1±0.50KJ/Mol, The $\Delta S^{\#}$ was +49±0.5 J/Mol K and the $\Delta G^{\#}_{273}$ was obtained as 39.7 ± 0.5 KJ/Mol.

Allyldiphenylphosphinegold(I) cyanide (AllylPh2PAuCN)

The proton decoupled ^{31}P NMR spectra of 0.026 M $AllylPh_2PAuCN$ in CD_3OD were recorded in the temperature range of 293.0 to 333.0 K. Two sharp resonances were observed for $AllylPh_2PAuCN$ and $[(AllylPh_2P)_2Au]^+$ species at 293.0 K, which started to broaden out at higher temperatures. We did not observe coalescence peak upto 333.0 K, but due to the boiling point of solvent (CD_3OD) we were unable to record the spectra at higher temperatures. The 'τ' values were measured at 293.0, 308.0, 338.0 and 354.0 K and are given in Table 4.10 with their rate constants. The $\Delta H^{\#}$ was found to be 45.27±0.97KJ/Mol, The $\Delta S^{\#}$ was -53.67±2.75 J/Mol K and the $\Delta G^{\#}_{273}$ was obtained as 59.9 ± 0.97 KJ/Mol.

Tri-m-tolylphosphinegold(I) cyanide (m-Tol3PAuCN)

The proton decoupled ^{31}P NMR spectra of 0.0257 M *m*-Tol_3PAuCN in CD_3OD were recorded in the temperature range of 233.0 to 333.0 K. Two sharp resonances were observed for *m*-Tol_3PAuCN and $[(m\text{-}Tol_3P)_2Au]^+$ species at 233.0 K, which started to broaden out at higher temperatures. The broad coalescence peak was also observed at 333.0 K. The 'τ' values were measured at and 231.3, 245.9, 260.5 and 354.3 K and are given in Table 4.11 with their rate constants. The $\Delta H^{\#}$ was found to be

TABLE 4.9 Life time and rate constant data for the redistribution reaction of 0.010 M $Ph_3PAu^{13}C^{15}N$ in CD_3OD.

Temperature (K)	τ_a (s)	k (L mol^{-1} s^{-1})
233.0	0.00790	1840
243.0	0.00240	6056
253.0	0.00063	23,071
263.0	0.00030	48,450
273.0	0.00012	121,124

TABLE 4.10 Life time and rate constant data for the redistribution reaction of 0.026 M $AllylPh_2PAu^{13}C^{15}N$ in CD_3OD.

Temperature (K)	τ_a (s)	k (L mol^{-1} s^{-1})
293.0	0.25	95
308.0	0.20	119
322.0	0.03	794
338.0	0.02	1,190
354.0	0.01	2,380

TABLE 4.11 Life time and rate constant data for the redistribution reaction of 0.0257 M *m*-$Tol_3PAu^{13}C^{15}N$ in CD_3OD

Temperature (K)	τ_a (s)	k (L mol^{-1} s^{-1})
231.3	0.2500	109
245.9	0.0180	1,509
260.5	0.0090	3,019
354.3	0.0002	135,869

33.87±0.73KJ/Mol, the $\Delta S^{\#}$ was 50.42±2.28 J/Mol K and the $\Delta G^{\#}_{273}$ was obtained as 47.64 ± 0.73 KJ/Mol.

Tri-p-tolylphosphinegold(I) cyanide (p-Tol$_3$PAuCN)

The proton decoupled ^{31}P NMR spectra of 0.0248 M *p*-Tol$_3$PAuCN in CD_3OD were recorded in the temperature range of 293.0 to 333.0 K. Two sharp resonances were observed for *p*-Tol$_3$PAuCN and [(*p*-Tol$_3$P)$_2$Au]$^+$ species at 293.0 K, which started to broaden out at higher temperatures. The 'τ' values were measured at 294.2, 308.4, 316.8 and 322.5 K and are given in Table 4.12 with their rate constants. The $\Delta H^{\#}$ was found to be 60.01±1.33KJ/Mol, The $\Delta S^{\#}$ was 10.66±3.49 J/Mol K and the $\Delta G^{\#}_{273}$ was obtained as 57.10 ± 1.33 KJ/Mol.

p-tolyldiphenylphosphinegold(I) cyanide (p-TolPh$_2$PAuCN)

The proton decoupled ^{31}P NMR spectra of 0.0269 M *p*-TolPh$_2$PAuCN in CD_3OD were recorded in the temperature range of 203.0 to 333.0 K. Two sharp resonances were observed for *p*-TolPh$_2$PAuCN and [(*p*-TolPh$_2$P)$_2$Au]$^+$ species at 203.0 K. Which started to broaden out at higher temperatures. A broad coalescence peak was observed at 294.0, which started to become sharper at higher temperatures. The 'τ' values were measured at 229.3, 295.9, 308.4, 322.0 and 339.7 K and are given in Table 4.13 with their rate constants. The $\Delta H^{\#}$ was found to be 28.33±0.07KJ/Mol, The $\Delta S^{\#}$ was -54.99±0.22 J/Mol K and the $\Delta G^{\#}_{273}$ was obtained as 43.33 ± 0.07 KJ/Mol.

TABLE 4.12 Life time and rate constant data for the redistribution reaction of 0.0248 M *p*-$Tol_3PAu^{13}C^{15}N$ in CD_3OD.

Temperature (K)	τ_a (s)	k (L mol^{-1} s^{-1})
294.2	0.0450	565
308.4	0.0200	1271
316.8	0.0100	2543
322.5	0.0042	6054

TABLE 4.13 Life time and rate constant data for the redistribution reaction of 0.0269 M *p*-$TolPh_2PAu^{13}C^{15}N$ in CD_3OD.

Temperature (K)	τ_a (s)	k (L mol^{-1} s^{-1})
229.3	0.01100	2,273
295.9	0.00030	83,333
308.4	0.00020	125,000
322.0	0.00010	250,000
339.7	0.00006	416,667

4.3 DISCUSSION

The K_{eq} of ligand redistribution reaction in alkyl/aryl phosphine cyanide complexes (equation *4.5*) is known to depend upon various factors as discussed in the beginning of chapter , however basicity of the phosphine ligands has been observed to be the most important factor during this study. The $R_3PAu^{13}C^{15}N$ complexes in which phosphine ligands have ν_{CO} value equal to or less than 2066.7 cm^{-1} exhibit this equilibrium at room temperature and show separate resonances for all three $R_3PAu^{13}C^{15}N$, $[(R_3P)_2Au]^+$ and $[Au(^{13}C^{15}N)_2]^-$ species in ^{13}C, ^{31}P and ^{15}N NMR spectra. However the *m*-Tol_3P, *p*-tol_3P and Ph_3P have ν_{CO} value higher than that of 2066.7 cm^{-1}, therefore K_{eq} in their complexes has lower value and all species are in fast exchange with each other at room temperature. When this temperature is decreased the exchange become slow and at 233K the *m*-$Tol_3PAu^{13}C^{15}N$ and *p*-$Tol_3PAu^{13}C^{15}N$ complexes yielded two separate resonances on ^{31}P NMR spectrum for $R_3PAu^{13}C^{15}N$ and $[(R_3P)_2Au]^+$ species. The $Ph_3PAu^{13}C^{15}N$ and $[(Ph_3P)_2Au]^+$ species were still in fast exchange at this temperature and gave only average resonance, however at 213K two separate resonances were resolved for these species. In case of CEPAuCN even at this temperature average resonance was observed due to its very low basicity. At 200K the sample was completely frozen all signals were lost , therefore we were unable to resolve separate resonances for this complex. In case of *o*-$Tol_3PAu^{13}C^{15}N$ and $Np_3PAu^{13}C^{15}N$ complexes, the steric factor i.e. cone angle 'θ' of phosphine ligands is playing important role. The ortho tolyl phosphine has a cone angle of 194°. This large cone angle is some how responsible to prevent the *o*-$Tol_3PAu^{13}C^{15}N$ complex

from disproportionation. Same is true for $Np_3PAu^{13}C^{15}N$ complex because the cone angle of 1-naphthyl phosphine is also comparable to that of orthotolyl phosphine. Hence *o*-$Tol_3PAu^{13}C^{15}N$ and $Np_3PAu^{13}C^{15}N$ complexes did not undergo ligand redistribution reaction and only one resonance was observed in ^{31}P NMR and in 'CN' region of ^{13}C NMR spectrum even at 213K.

Figure 4.4 shows the plot of $\delta(^{31}P)$ of $R_3PAu^{13}C^{15}N$ versus $\delta(^{31}P)$ of $[(R_3P)_2Au]^+$ species. Until now the theory behind interpretation of ^{31}P NMR chemical shift is poorly understood. This is largely due to the fact that ^{31}P NMR chemical shifts are influenced by number of factors including the nature of metal, phosphine ligands and other ligands, geometry of the complex, coordination number of the central metal, oxidation state of the central metal etc. Since all these factors are almost same in both $R_3PAu^{13}C^{15}N$ and $[(R_3P)_2Au]^+$ species, therefore their $\delta(^{31}P)$ exhibit linear relationship with each other.

Theoretical interpretations of ^{13}C chemical shifts for π-bonded ligands in metal complexes are not completely satisfactory. In much of the literature, changes in chemical shifts of atoms with 2p-π electrons have been attributed to the changes in paramagnetic term σ_p [144]. the magnitude of 'σ_p' depends upon three interrelated factors which are not often easily separated.

1. The carbon electron density and radial extension of 2p orbitals.
2. Energies of electronic states of the molecule.
3. π-bond order between carbon and adjacent atoms.

The molecular orbital calculations [163] for several arene carbonyl complexes of the type $[(C_6H_6)M(CO)_3]$ have shown that the product of all

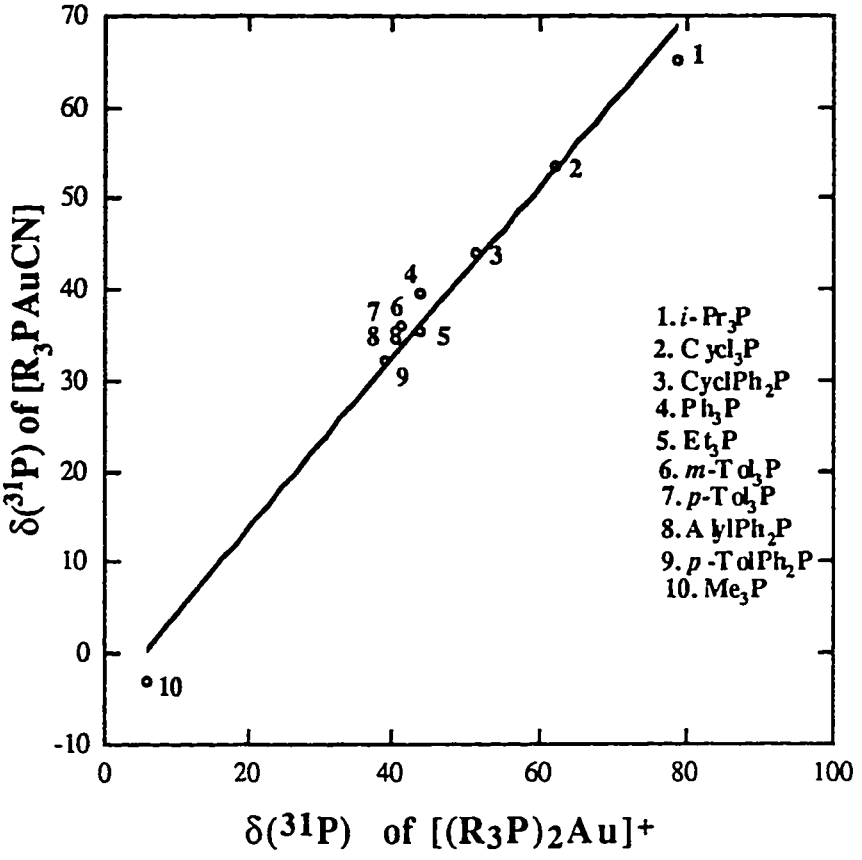

Figure 4.4 Plot of $\delta(^{31}P)$ of $[R_3PAu^{13}C^{15}N]$ vs $\delta(^{31}P)$ of $[(R_3P)_2Au]^+$ species.

these factors must be considered together in determining ^{13}C chemical shifts of 'CO'. In this study we have observed the opposite dependence of $\delta(^{15}N)$ and $\delta(^{13}C)$ on the basicity of phosphine ligands as shown in Figure 4.5. There is upfield shift in ^{15}N chemical shift, while down field shift in ^{13}C chemical shift with increase in basicity of the phosphine ligands. This opposite behavior can be explained on the bases of π-bonding or back bonding between gold(I) and CN ligand as shown in Fig. 1.10.

The π-bonded species involves transfer of electron density from a filled metal d-orbital in to the carbon centered member of the cyanide π^* anti bonding molecular orbitals, most of the electron density donated from the metal to the cyanide ligand would be expected to reside on the cyanide carbon. Thus, stabilization of the π-bonded species by increased electron donation across a series of axial ligands should shift the cyanide ^{13}C chemical shift down field as observed. Similarly the reduction in 'C-N' bond order in the π-bonded species, would be expected to be accompanied by an upfield shift of the ^{15}N resonance.

This opposite dependence of ^{15}N and ^{13}C chemical shifts on the basicity of *trans* axial ligands is common in other metal cyanide systems. Brown et al. [141,142] have reported this behavior in a series of cyano(ligand)cobaloxime system.

Figure 4.6 shows a plot of $^2J_{(^{31}P-^{13}C)}$ in $R_3PAu^{13}C^{15}N$ complexes versus $\nu_{(CO)}$ of phosphine ligands. It is observed that $^2J_{(^{31}P-^{13}C)}$ increases with increase in $\nu_{(CO)}$ of phosphine ligands. The theory behind $^2J_{(^{31}P-^{13}C)}$ is not well understood but empirical corelations have been observed. Studies of metal carbonyl complexes with phosphine ligands *trans* to the carbonyl demonstrates that $^2J_{(^{31}P-^{13}C)}$ increases as the electronegativity of the

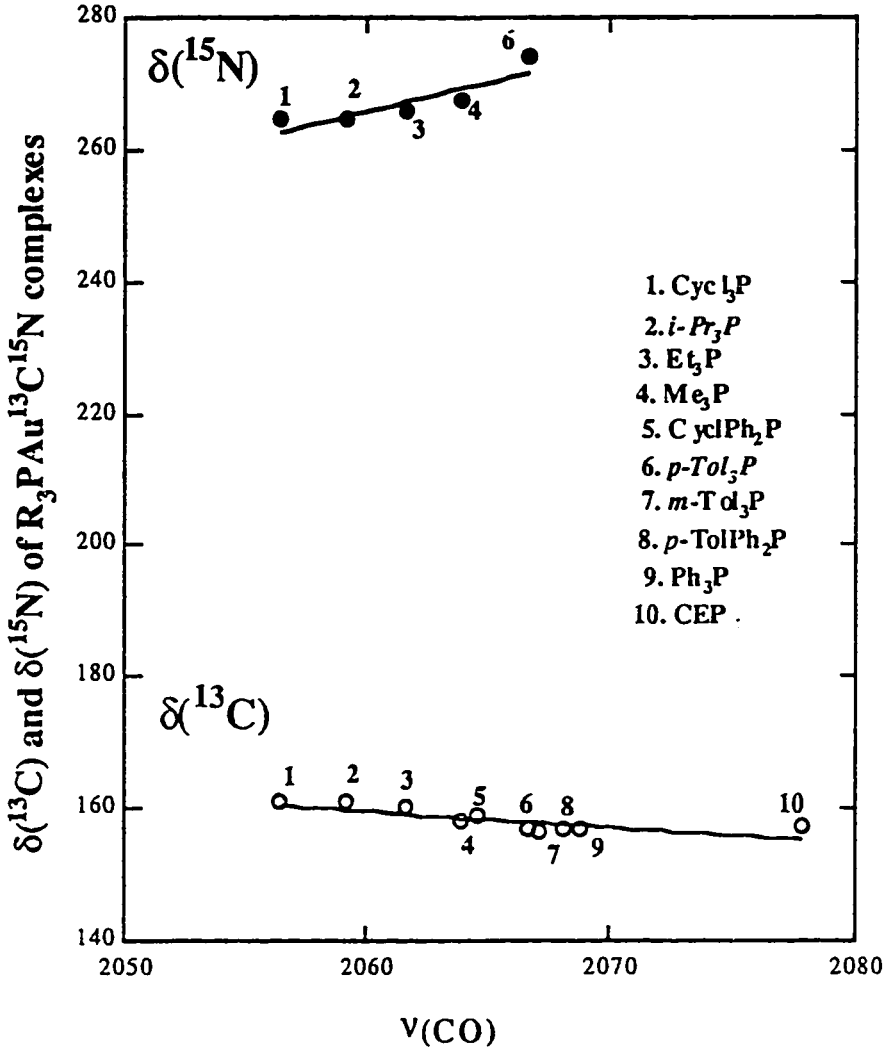

Figure 4.5 Plot of $\delta(^{13}C)$ and $\delta(^{15}N)$ of [R3PAu13C15N] complexes vs $\nu_{(CO)}$ of phosphines.

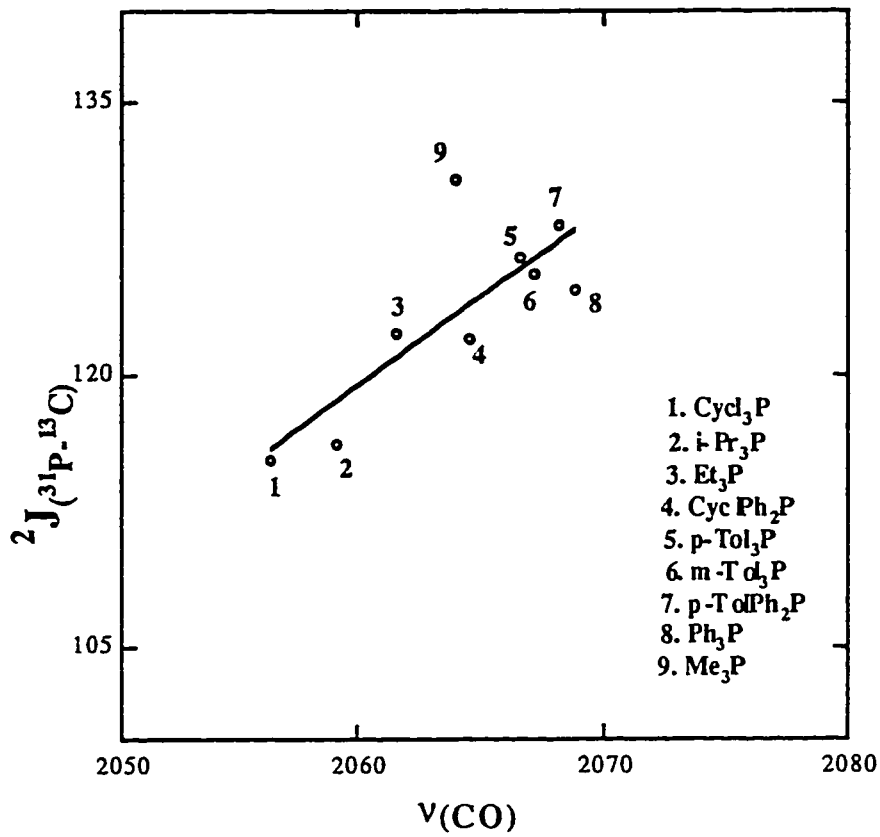

Figure 4.6 Plot of $^2J_{(31P\text{-}13C)}$ of $R_3PAu^{13}C^{15}N$ complexes vs $\nu_{(CO)}$ of phosphines.

phosphine substituent increases [164]. Similar trend is observed here because $\nu_{(CO)}$ represents the basicity or electronegativity of phosphines. Increase in $\nu_{(CO)}$ value indicate decrease in basicity or increase in electronegativity of phosphine ligands. The increase in electronegativity of the phosphine substituents causes increase in the effective nuclear charge on the phosphorous atom, which causes phosphorous to withdraw electron density from the metal resulting in increase in $^2J_{(^{31}P-^{13}C)}$ value.

Figure 4.7 shows an increase in $^2J_{(^{31}P-^{13}C)}$ of $R_3PAu^{13}C^{15}N$ complexes with the decrease in $\delta(^{13}C)$ of cyanide group in series of $R_3PAu^{13}C^{15}N$ complexes. The decrease in chemical shift of ^{13}C means shift towards high field is due to increase in effective nuclear charge on carbon atom, which is responsible for increase in $^2J_{(^{31}P-^{13}C)}$ like that of Phosphorous.

Possible mechanism for ligand redistribution

The first aspect that should be considered is that whether the reaction proceeds via associative or dissociative mechanism. Numerous examples are present in the literature where gold(I) complexes undergo ligand exchange by an associative mechanisms [88,160]. The other d^{10} metals are also known to react via associative mechanism [165]. A dissociative mechanism has been reported for the thermal decomposition of CH_3AuPPh_3, but the nature of the reaction and its products are different than those observed in this study. Therefore it seems more probable that ligand redistribution for these $R_3PAu^{13}C^{15}N$ complexes follow associative mechanism. This associative mechanism is also supported by the anomalous behavior of $Cycl_3PAu^{13}C^{15}N$ complex. The cone angle of cylohexyl phosphine is 170° and it took several weeks to establish the equilibrium [64]. for redistribution

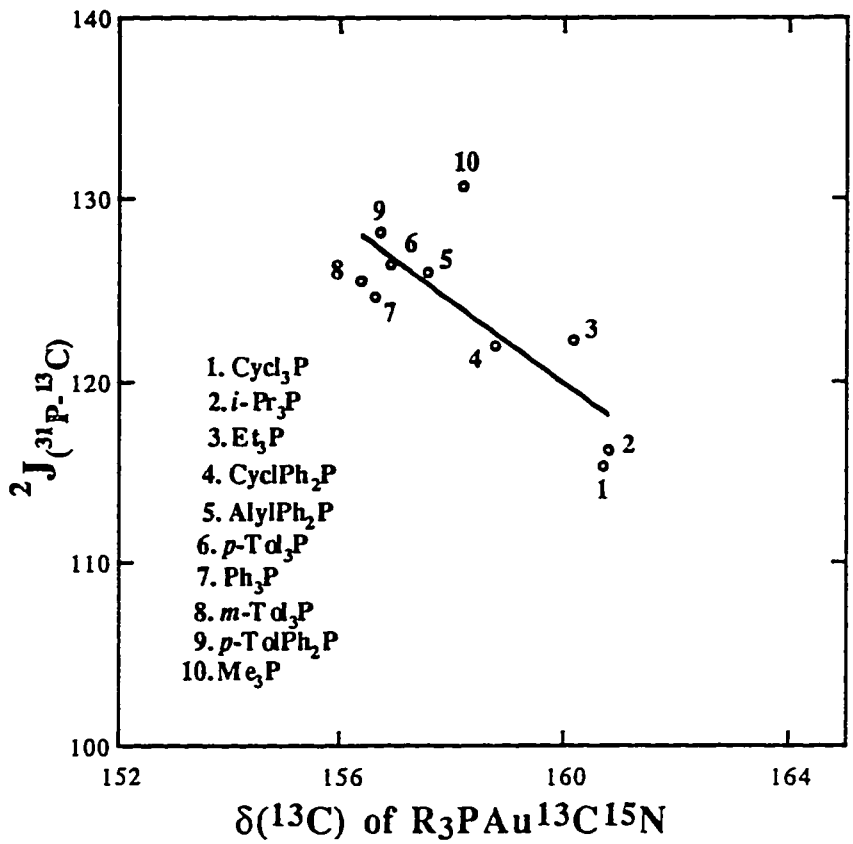

Figure 4.7 Plot of $^2J_{(31P-13C)}$ vs $\delta(^{13}C)$ of $R_3PAu^{13}C^{15}N$ complexes.

reaction. If the exchange occurred by a dissociative mechanism then the large steric hindrance of cylohexylphosphine ligand would not have an effect on the time required to reach the equilibrium.

Three reasonable intermediates are possible for associative mechanism, which are shown in scheme 4.1. All intermediates contain bridging cyanide. In intermediates I and II, the cyanide forms a linear bridge with the gold(I). Similar cyanide bridging is observed in AuCN [166] and Me_2AuCN] [167] complexes. In intermediate III cyanide bridges through only carbon atom like carbonyl in number of metal carbonyl complexes e.g. $[Fe_2(CO)_9]$ etc. This type of bridging has not been observed for gold complexes but is observed in CuCN complexes.

Fig 4.8 shows an increase in $\Delta G\#_{273}$ (for redistribution reactions of R_3PAuCN complexes as shown in eq *4.5*) with increase in basicity (i.e. decrease in $\nu_{(CO)}$) of phosphine ligands in R_3PAuCN complexes. This trend can be explained on the bases of mechanism 4.1A. When the basicity of phosphine increases it causes more electron donation to the gold(I) and results in more stronger bond between gold(I) and phosphine. Therefore intermediate complex has to pass through a large activation barrier, which results in large value of $\Delta G\#_{273}$.

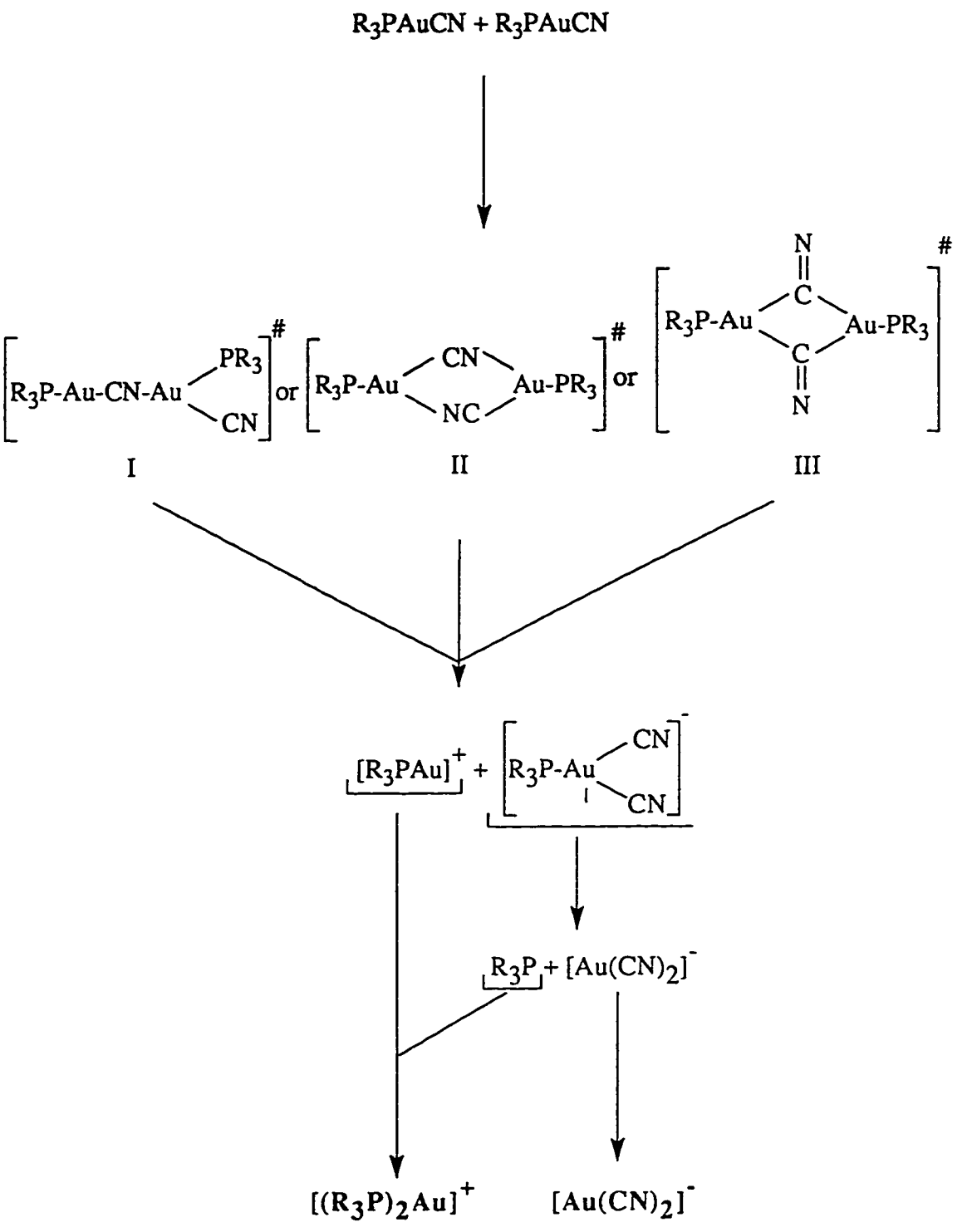
R3PAuCN + R3PAuCN
R3P-Au-CN-Au
PR3
CN
or
R3P-Au
CN
NC
Au-PR3
or
N
C
R3P-Au
Au-PR3
C
N
#
I
II
III
[R3PAu]+ +
R3P-Au
CN
CN
R3P + [Au(CN)2]-
[(R3P)2Au]+
[Au(CN)2]-

Scheme 4.1

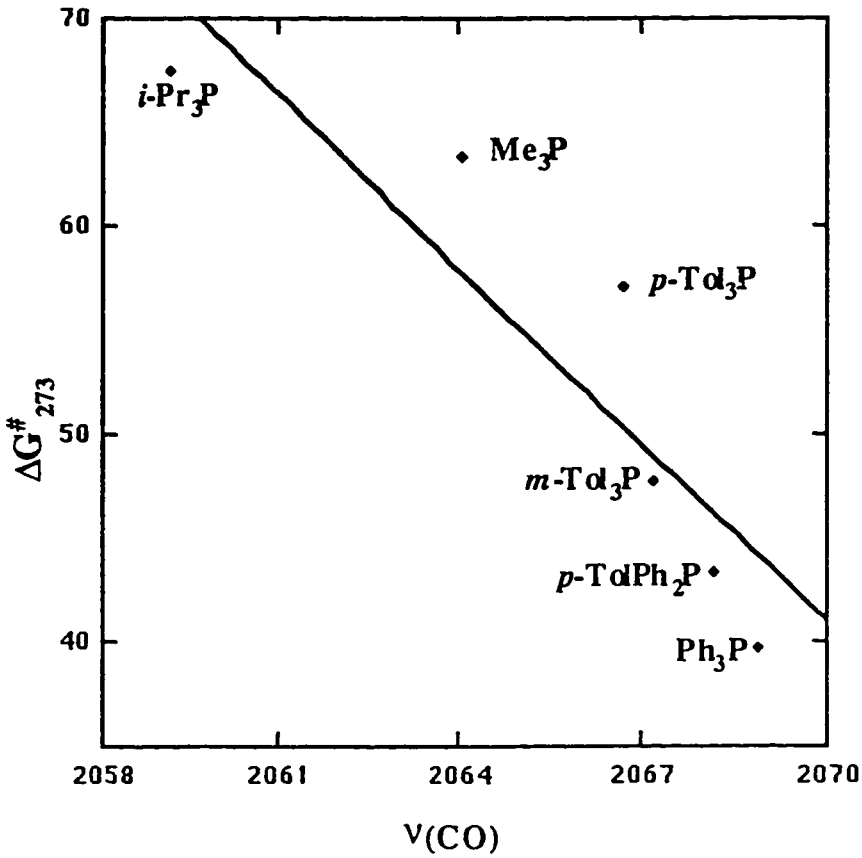

Figure 4.8 Plot of $\Delta G^{\#}_{273}$ for redistribution of R3PAuCN complexes vs $\nu_{(CO)}$ of phosphines.

CHAPTER 5

SPECTROSCOPIC STUDIES OF THE $R_3PAuSCN$ COMPLEXES

In order to study the electronic control of the bonding mode of ambidentate ligands such as SCN^- and $SeCN^-$ using Spectroscopic techniques, the linearly dicoordinated gold(I) complexes offer a number of advantages over the complexes of other class (b) metals that have square planar geometry, such as Pt(II), Pd(II), Ir(II) and Rh(I). Since the ligands are on opposite sides of the molecule there can be no steric control [169-171] of the bonding mode of the thiocyanate and selenocyanate ions. The ligands are also in proper position to investigate a *trans* influence [170-172] on the bonding mode. Since most of these Au(I)-thiocyanate complexes are neutral, they would not be susceptible to counter ion control [170,171,173] of the bonding mode. Another advantage would be that the infrared spectra of the complexes should be relatively simple to analyze because only two ligands are present.

The concept of anti symbiotic trans influence predicts [172] that the site *trans* to a strong *trans* directing ligand will become harder in complexes of class (b) metals. Unfortunately, much of the work previously reported

[170,171] has involved the use of bulky ligands, such as alkyl and aryl phosphines, in square planar thiocyanate and selenocyanate complexes. Separation of the steric and electronic control variables becomes quite difficult in these cases and tends to destroy the usefulness of the thiocyanate and selenocyanate ions as probes to determine if a particular coordination site is hard or soft. Indeed, the question of electronic versus steric control of the thiocyanate's bonding mode, especially in phosphine containing complexes of Pd(II) and Pt(II) has been the source of considerable controversy [170,171] for almost two decades. Fortunately, the linear gold(I) thiocyanate complexes utilized in this study are free of these complications, and serve as an ideal testing ground for probing the anti symbiotic *trans* influence theory [172]. It has been found [174,175] that in solid state, thiocyanate is bonded only via 'S' to gold atom. However Burmeister and Melpolder [176,177] have observed this anti symbiotic trend in series of solutions of linear L-Au-SCN complexes using infrared spectroscopy; the L-Au-NCS/L-Au-SCN ratio increases as the *trans* effect of the 'L' phosphine ligand increases.

In present study we have prepared a series of doubly labeled $R_3PAuS^{13}C^{15}N$ (where R_3P= Me_3P, Et_3P, *i*-Pr_3P, *p*-$TolPh_2P$, Ph_3P and cyanoethylphosphine CEP) complexes to see whether ligand redistribution reactions and anti symbiotic *trans* effect is observed in these type of gold(I) complexes using ^{13}C, ^{31}P and ^{15}N NMR and infrared spectroscopy.

5.1 EXPERIMENTAL OVERVIEW

An overview of the synthetic method is given below, the detailed procedures for the synthesis of all $R_3PAuSCN$ complexes are given in chapter 6.

5.1.1 Synthesis

The $R_3PAuSCN$ complexes were prepared by the replacement of halide group with thiocyanate ligand in R_3PAuX (where X= Cl^- or Br^-) complexes as shown below in equation *5.1*:

$$R_3PAuX + NaSCN \longrightarrow R_3PAuSCN + NaX \qquad 5.1$$

5.2 RESULTS

The ^{31}P, ^{13}C, ^{15}N NMR and I.R.spectroscopic studies of $R_3PAuSCN$ complexes are given below, while instrumentation is given in chapter 6.

5.2.1 ^{31}P NMR spectra of $R_3PAuS^{13}C^{15}N$ complexes

The ^{31}P-{^1H} NMR spectra of $R_3PAuS^{13}C^{15}N$ (where R_3P= Me_3P, Et_3P, *i*-Pr_3P, *p*-Tol.Ph_2P, Ph_3P and cyanoethylphosphine CEP) complexes were measured in their methanolic solution. In each case a single sharp resonance was observed. There was no splitting due to $^3J_{(^{31}P-^{13}C)}$ or $^4J_{(^{31}P-^{15}N)}$. The ^{31}P chemical shifts for all $R_3PAuS^{13}C^{15}N$ complexes are given in Table 5.1.

5.2.2 ^{13}C NMR spectra of $R_3PAuS^{13}C^{15}N$ complexes

The ^{13}C-{^1H} NMR spectra of $R_3PAuS^{13}C^{15}N$ complexes were recorded with the same solutions used for ^{31}P NMR studies. Two broad resonances were observed in low field region of almost all complexes for -$AuS^{13}C^{15}N$ and -$Au^{15}N^{13}CS$ linkage isomers. The $^1J_{(^{13}C-^{15}N)}$ was not

TABLE 5.1. The ^{13}C, ^{15}N, ^{31}P NMR chemical shifts in ppm and $\nu_{(CO)}$ in cm^{-1} for $R_3PAuS^{13}C^{15}N$ complexes.

$R_3PAuS^{13}C^{15}N$	$\delta(^{31}P)$	$\delta(^{13}C)$ of S-bonded	$\delta(^{13}C)$ of N-bonded	$\delta(^{15}N)$	$\nu_{(CO)}$[a]
i-$Pr_3PAuS^{13}C^{15}N$	68.14	119.42	119.14	233	2059.2
$Et_3PAuS^{13}C^{15}N$	36.37	119.89	119.61	232	2061.7
$Me_3PAuS^{13}C^{15}N$	-4.64	120.28	120.01	231	2064.1
p-$TolPh_2PAuS^{13}C^{15}N$	30.54	124.83	124.76	-	2068.2
$Ph_3PAuS^{13}C^{15}N$	35.00	126.48	126.48	-	2068.9
$CEPAuS^{13}C^{15}N$	47.54	129.53	129.30	-	2077.9

[a] taken from reference 154.

resolved in these complexes except in *p*-Tol.$Ph_2PAuS^{13}C^{15}N$ due to exchange between S-bonded and N-bonded isomers. The resonance due to S-bonded isomer was more intense and was at low field as compared to the N-bonded isomer. The ^{13}C chemical shifts for all $R_3PAuS^{13}C^{15}N$ complexes are given in Table 5.1 and 5.2.

5.2.3 ^{15}N NMR spectra of $R_3PAuS^{13}C^{15}N$ complexes

The ^{15}N-{^1H} NMR spectra of same solutions of $R_3PAuS^{13}C^{15}N$ complexes was also recorded, but due to low sensitivity of instrument, low solubility of complexes and only 50% labeled ^{15}N the signal to noise ratio was very poor. We were able to get the resonances for *i*-$Pr_3PAuS^{13}C^{15}N$, $Et_3PAuS^{13}C^{15}N$ and $Me_3PAuS^{13}C^{15}N$ complexes only, in the region of 231 to 233 ppm. In case of *i*-$Pr_3PAuS^{13}C^{15}N$ two broad resonances were resolved for S-bonded and N-bonded linkage isomers. The $^1J_{(^{13}C-^{15}N)}$ was not resolved due to exchange between linkage isomers, while in other complexes only one broad resonance was resolved without any splitting for both isomers. The ^{15}N chemical shifts for $R_3PAuS^{13}C^{15}N$ complexes are given in Table 5.1. The typical ^{31}P, ^{13}C and ^{15}N NMR spectra of *i*-$Pr_3PAuS^{13}C^{15}N$ are shown in Figure 5.1.

5.2.4 The infrared spectroscopy of $R_3PAuS^{13}C^{15}N$ complexes

The solution infrared spectra of all $R_3PAuSCN$ complexes except CEPAuSCN, in dichloromethane yielded two separate absorption bands in the region of 2122-to-2129 cm^{-1} for S-bonded isomer, while other in the region of 2082-to-2091 cm^{-1} for N-bonded isomer [177], which are given in Table 5.3. In case of CEPAuSCN due to very low solubility, solution infrared spectrum was not very good and two separate absorption bands were not resolved. A typical solution infrared spectrum of *i*-$Pr_3PAuSCN$ in

TABLE 5.2. The ^{13}C chemical shifts of $R_3PAuS^{13}C^{15}N$ complexes.

$R_3PAuS^{13}C^{15}N$	δC_1 (ppm)	δC_2 (ppm)	δC_3 (ppm)	δC_4 (ppm)	$^1J(^{31}P\text{-}^{13}C)$ (Hz)
i-$Pr_3PAuS^{13}C^{15}N$	24.93	20.70	-	-	30.8
$Et_3PAuS^{13}C^{15}N$	18.60	9.51	-	-	35.7
$Me_3PAuS^{13}C^{15}N$	15.22	-	-	-	38.8
$Ph_3PAuS^{13}C^{15}N$	135.20	133.45	130.74	130.64	-
$CEPAuS^{13}C^{15}N$	24.09	10.08	124.00	-	-
p-$TolPh_2PAuS^{13}C^{15}N$	δCH_3 21.44	δC_{1a} 135.29	δC_{2a} 133.36	δC_{3a} 130.66	δC_{4a} 135.02
	δC_{1b} 135.09	δC_{2b} 133.36	δC_{3b} 129.94	δC_{4b} 129.70	

Where R_3P are $(^1CH_3)_3P$, $(^2CH_3\text{-}^1CH_2)_3P$,

$[(^2CH_3)_2{}^1CH]_3P$, $(^3CN\text{-}^2CH_2\text{-}^1CH_2)_3P$,

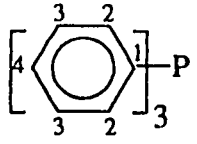

,

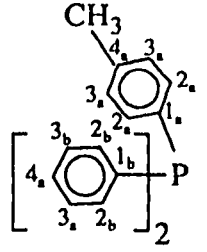

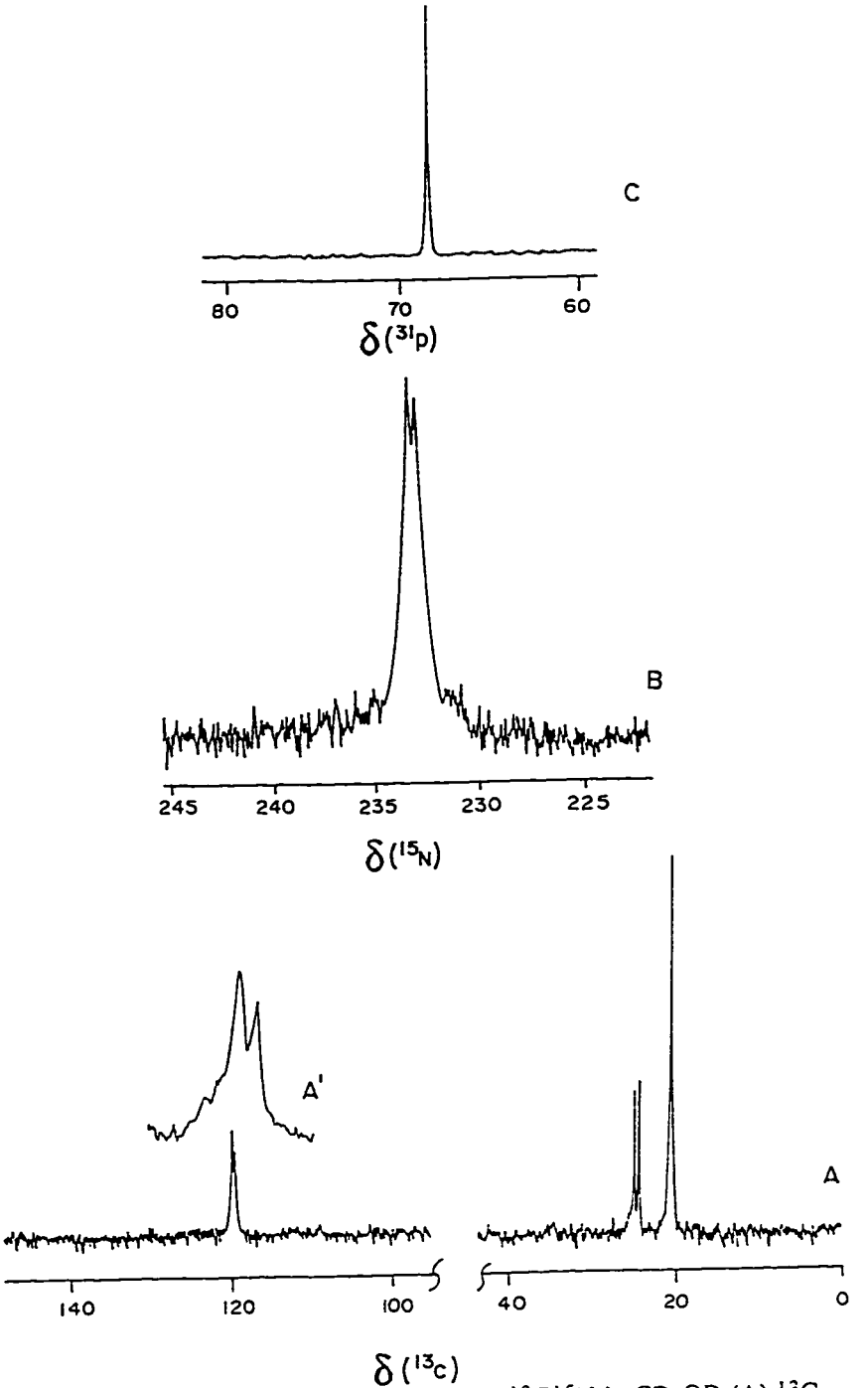

Figure 5.1 NMR spectra of 0.45 M *i*-$Pr_3PAuS^{13}C^{15}N$ in CD_3OD (A) ^{13}C NMR, (A') expansion of ^{13}C NMR spectrum in 'SCN' region, (B) ^{15}N NMR and (C) ^{31}P NMR spectrum.

TABLE 5.3. The ν_{SCN}, ν_{NCS}, Au-NCS/Au-SCN ratio and % N-bonded isomer in $R_3PAuSCN$ complexes from their infrared spectra of solution .

$R_3PAuS^{13}C^{15}N$	ν_{SCN} (cm^{-1})	ν_{NCS} (cm^{-1})	Au-NCS/Au-SCN	% N-bonded isomer
i-$Pr_3PAuS^{13}C^{15}N$	2124.3	2085.7	0.224	2.2
$Et_3PAuS^{13}C^{15}N$	2126.0	2084.3	1.570	5.7
$Me_3PAuS^{13}C^{15}N$	2122.0	2091.7	1.112	10.0
$Ph_3PAuS^{13}C^{15}N$	2129.5[a]	2082.7	0.470	4.5[a]
$CEPAuS^{13}C^{15}N$	2125.8	-	-	-
p-$TolPh_2PAuS^{13}C^{15}N$	2125.9	2089.5	1.851	15.6

[a]=Reference 177

the ν_{CN} region is shown in Figure 5.2. It was observed that the N-bonded isomer was a minor component in all of $R_3PAuSCN$ complexes, since the integrated absorption intensity of the ν_{CN} band of an N-bonded thiocyanate is generally an order of magnitude larger [170] than that of an S-bonded thiocyanate. However, it is clear that proportion of N-bonded isomer increases as the *trans* influence of phosphine ligand increases. If the assumption is made that the intensity of the N-bonded isomer is exactly ten times that of S-bonded isomer, then the percent of N-bonded isomer present at equilibrium can be calculated [177] as follows:

10X/(1-X) = Au-NCS/Au-SCN ratio;

Where 100X is the percent of the N-bonded isomer present in the solution. The ratios of integrated absorption intensities of ν_{CN} infrared absorption bands and percent of N-bonded isomer present in the solution of all $R_3PAuSCN$ complexes are given in Table 5.3.

The solid state infrared spectra of all $R_3PAuSCN$ complexes showed that only the S-bonded isomer is present in solid form. Apparently the crystal packing favors the geometry of this isomer [174,175].

5.3 DISCUSSION

In chapter 4 we have shown that the ^{31}P NMR spectra of R_3PAuCN complexes give two separate resonances for $[(R_3P)_2Au]^+$ and R_3PAuCN species due to ligand redistribution reaction as shown below in equation *5.2*:

$$2R_3PAuCN \text{ ----------> } [(R_3P)_2Au]^+ + [Au(CN)_2]^- \qquad 5.2$$

However, in present studies for all $R_3PAuS^{13}C^{15}N$ complexes only one ^{31}P NMR resonance is observed. Which indicates that there is no ligand

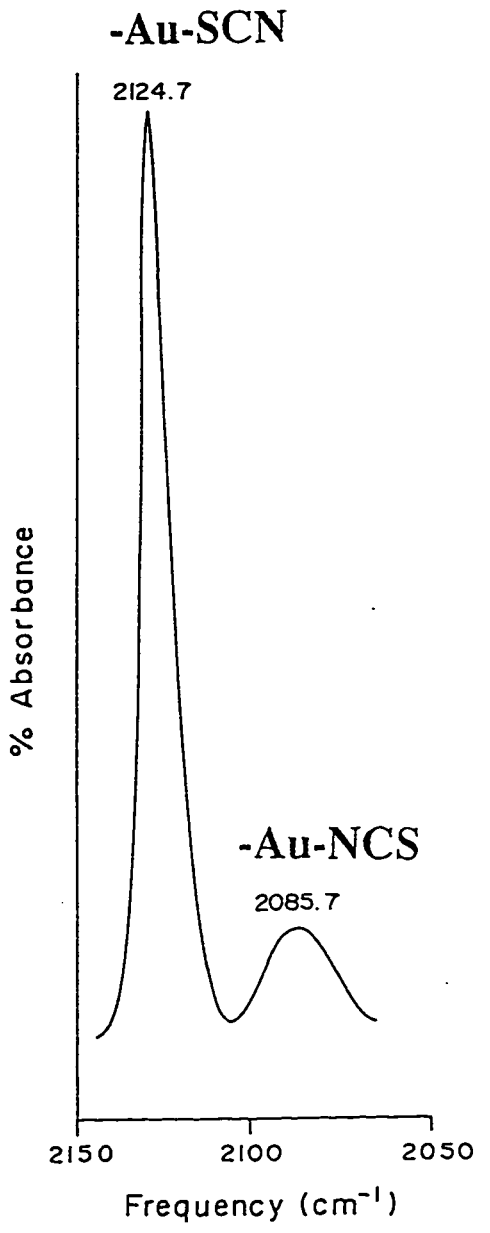

Figure 5.2 The infra red spectrum of 0.50 M *i*-$Pr_3PAuS^{13}C^{15}N$ in dichloromethane in absorption mode for 'SCN' group.

redistribution reaction in $R_3PAuS^{13}C^{15}N$ complexes or it is so fast that cannot be resolved on NMR time scale. In case of $R_3PAu^{13}C^{15}N$ complexes we have measured $^2J_{(^{31}P-^{13}C)}$ and $^3J_{(^{31}P-^{15}N)}$ coupling constants, but in this case we were unable to find any splitting due to $^3J_{(^{31}P-^{13}C)}$ or $^4J_{(^{31}P-^{15}N)}$, which means that in $R_3PAuS^{13}C^{15}N$ complexes the exchange between 'S' bonded and 'N' bonded 'SCN' is so fast that this splitting is not resolved.

The $^{13}C-\{^1H\}$ NMR studies are also consistent with the observations of ^{31}P NMR studies. The ^{13}C NMR gave rise to two broad resonances for linkage isomers but the resonance due to $[Au(S^{13}C^{15}N)_2]^-$ was not observed, which indicate that there is no ligand redistribution reaction as shown in equation *5.2*.

The ^{15}N NMR spectra of $R_3PAuS^{13}C^{15}N$ complexes was considered to be the most important technique to probe the S-bonded and N-bonded 'SCN' ligand in this series of complexes. However, due to low sensitivity of the instrument only one broad resonance was resolved in the region of 231 to 233 ppm for both S-bonded and N-bonded linkage isomers. However, a single resonance in ^{15}N NMR spectra of $R_3PAuS^{13}C^{15}N$ complexes supports the results of ^{13}C and ^{31}P NMR studies that ligand redistribution reactions do not occur in this series of complexes otherwise ^{15}N resonances due to $R_3PAuS^{13}C^{15}N$ and $[Au(S^{13}C^{15}N)_2]^-$ species would have been observed as shown in equation *5.2*.

The formation constants ($\log\beta_2$) for $[Au(CN)_2]^-$ and $[Au(SCN)_2]^-$ are reported [178] to be 39.0 and 17.0 respectively. The R_3PAuCN complexes readily undergo ligand redistribution reactions as shown in equation *5.2* due to large formation constant of $[Au(CN)_2]^-$, while this ligand redistribution

reaction is not favorable in $R_3PAuSCN$ complexes due to small formation constant of $[Au(SCN)_2]^-$.

A correlation that is frequently used to determine the relative basicity of phosphines is the electronic parameter $\nu_{(CO)}$ for $[R_3PNi(CO)_3]$ complexes (values tabulated by Tollman [154]). A decrease in $\nu_{(CO)}$ value indicates a net increase in the electron donating ability of a phosphine. Figure 5.3 shows an opposite behavior of dependence of $\delta(^{13}C)$ of 'CN' and 'SCN' groups of $R_3PAu^{13}C^{15}N$ and $R_3PAuS^{13}C^{15}N$ respectively on $\nu_{(CO)}$ values of different phosphines. In $R_3PAu^{13}C^{15}N$ complexes $\delta(^{13}C)$ decreases with increase in $\nu_{(CO)}$ value of phosphines due to the involvement of π-bonding between gold(I) and 'CN' group. While in $R_3PAuS^{13}C^{15}N$ complexes there is no π-bonding between gold(I) and 'SCN' group, therefore basicity of phosphine is effecting $\delta(^{13}C)$ directly i.e. increase in basicity of phosphine causes more donation of electron towards gold(I) which in turn increase the effective nuclear charge on 'C' atom causing an upfield shift of $\delta(^{13}C)$.

The solution infrared spectroscopy has been observed to be the most successful technique for the study of anti symbiotic *trans* effect in $R_3PAuSCN$ complexes. Figure 5.4 shows a linear relationship between the *trans* effect (basicity) of phosphines and the % N-bonded isomer in all complexes except that of $Ph_3PAuSCN$. As the trans effect of phosphines increases (basicity decreases) it causes decrease in the strength of 'Au-P' bond, which intern favors the 'NCS' bonded isomer [177].

This linkage isomerism can be explained on the basis of bridging of 'SCN' group between two gold species. The '-Au-SCN' bond undergo cleavage and a new '-Au-NCS' bond with 'SCN' group of other species is

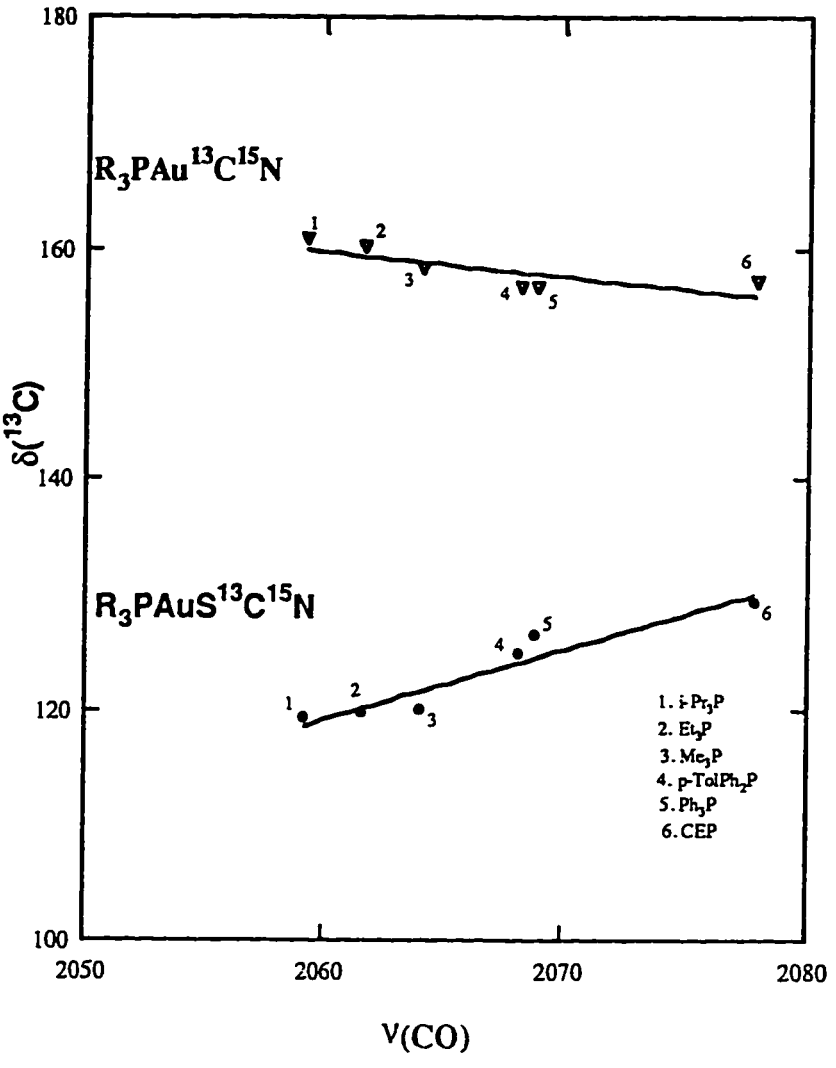

Figure 5.3 Plot of $\delta(^{13}C)$ of $R_3PAu^{13}C^{15}N$ and $R_3PAuS^{13}C^{15}N$ complexes vs $\nu_{(CO)}$ of phosphines. The solid lines are regression lines.

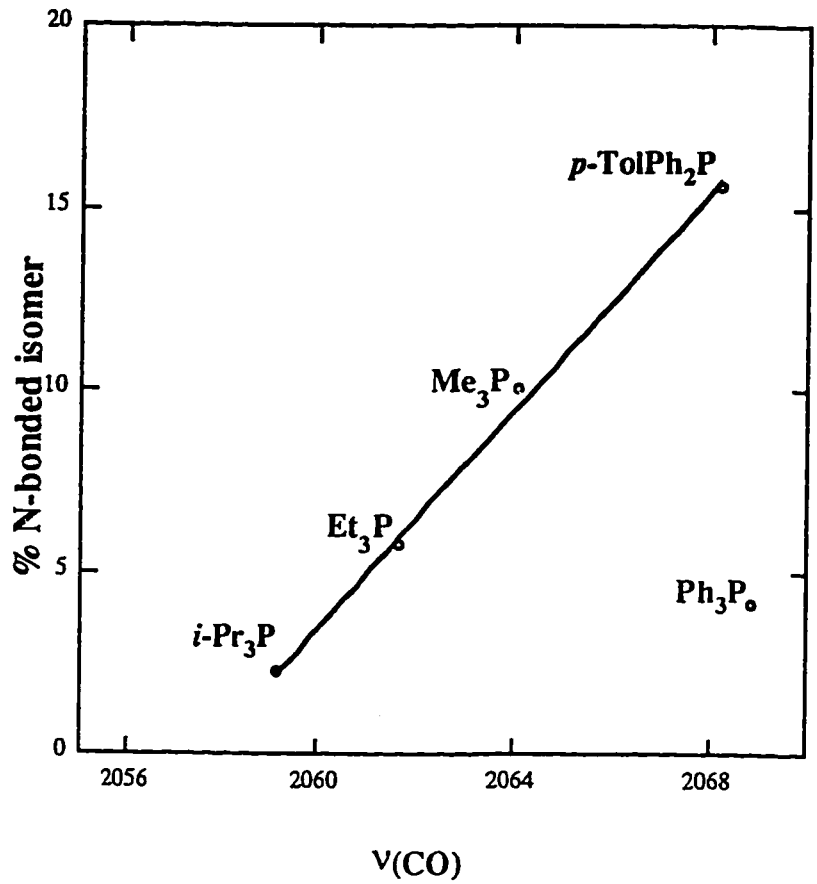

Figure 5.4 Plot of %-N bonded isomer in $R_3PAuSCN$ complexes vs $\nu_{(CO)}$ of phosphines. The solid line is regression line.

[Note: The value of $Ph_3PAuSCN$ is not included in the regression.]

formed. In this way $R_3PAuSCN$ complexes do not undergo disproportionation during linkage isomerism as is observed in R_3PAuCN complexes. The anomalous behavior of $Ph_3PAuSCN$ in *trans* effect relationship can be explained on the basis of our previous observation in R_3PAuCN complexes. In which all other complexes exhibited equilibrium for redistribution reaction at room temperature as shown in equation *5.1* and all species were characterized using ^{13}C, ^{31}P and ^{15}N NMR spectroscopy, however, in case of Ph_3PAuCN this equilibrium was very fast and separate resonances for all species were resolved at -60 ^0C. In the similar way the bond formation and breakage in $Ph_3PAuSCN$ for linkage isomerism might be very fast and results in less % N-bonded isomer than expected.

The results of this study follow the results exhibited by other class (b) metal systems [170,171] and add further support to the concept of the anti symbiotic *trans* influence [172] as being the primary electronic effect which causes certain coordination sites on class (b) metals to exhibit class (a) behavior. When a soft ligand is placed *trans* to thiocyanate, as in LAuSCN, the stronger the *trans* director L-ligand becomes, the more N-bonding is observed, which is exactly what would be expected. In this case steric control of the bonding mode of the thiocyanate does not interfere with the interpretation of the results. The ^{13}C, ^{31}P and ^{15}N NMR spectroscopy shows that these complexes do not undergo ligand redistribution reactions as in the case of R_3PAuCN complexes.

CHAPTER 6

EXPERIMENTAL

Experimental work of all four objectives is given in detail in this chapter.

6.1 INSTRUMENTATION

6.1.1 I.R. spectroscopy

The solid state infra red spectra of R_3PAuCN and $R_3PAuSCN$ complexes were recorded on Perkin Elmer IR 180 spectrophotometer using KBr pellets.

While a Perkin Elmer 1600 FT series was used to measure solution infrared spectra in the ν_{CN} regionof $R_3PAuSCN$ complexes

The ratios of the ν_{CN} integrated absorption intensities of N-bonded/S-bonded thiocyanate were calculated as follows [177]. The infrared stretching region was recorded using the linear absorbance mode rather than the linear transmittance mode. The low energy tail of the high energy absorption band was drawn in (an estimate) and the resulting envelops were traced on paper, which were carefully cut out and weighed

on a Mettler balance. The weight of the N-bonded band was divided by that of S-bonded band giving an N-bonded/S-bonded ratio.

6.1.2 pH measurements

All pH measurements were made at 22°C with a Fisher Accumet pH meter model 620 equipped with a Fischer microprobe combination pH electrode. The pH* is used to indicate the actual meter reading for D_2O solutions without any correction for deuterium isotope effects.

6.1.3 Mass spectroscopy

Gold(I) captopril was subjected to electron impact mass spectrometry using high resolution, JEOL JMS-HX100 mass spectrometer. The mass spectrometer was scanned from 35-450 amu. The sample was introduced into the spectrometer using the direct insertion probe. The probe temperature was programmed from 40.0°C to 250.0°C at 32°C/minute with the ion source temperature at 250.0°C. The electron energy was 70 ev and the emission was 100 μA.

6.1.4 Viscosity measurements

In order to measure the viscosity of gold(I) captopril solution Ubbelohde KPG viscometer was used with a capillary constant of K=0.03120. All viscosity measurement were made at 26°C.

6.1.5 UV visible spectroscopy

The UV visible spectra were recorded on the Perkin Elmer l-5 UV spectrophotometer, with path length of 1 cm.

6.1.6 ^{13}C NMR spectroscopy

The ^{13}C NMR spectra were recorded at 50.30 MHz on a Varian XL-200 spectrometer operating in the pulsed Fourier transform mode. The measurements were carried out with broad-band ^{1}H decoupling and in

some cases with coherent off-resonance ^{1}H decoupling. Chemical shifts were measured relative to internal reference dioxane (67.40) or glycerol (63.33) up field from $SiMe_4$. All spectra were recorded using 20,000-30,000 scans.

6.1.7 ^{15}N NMR spectroscopy

The ^{15}N NMR spectra were obtained at 20.284, MHz on a XL-200 NMR spectrometer . The chemical shifts were measured using a sealed external reference $NH_4{}^{15}NO_3$ which has a resonance at 375.11 ppm relative to neat $CH_3{}^{15}NO_2$ which resonates at 380.2 ppm.[139] The spectral conditions were 5.0 s delay time, 16K data points, spectral width 10,000 Hz, pulse width 5.0 μs (20°), 10 mm multinuclear probe. Approximately 60,000 scans were accumulated for each sample.

6.1.8 ^{31}P NMR Spectroscopy

The ^{31}P NMR spectra were obtained at 80.98 MHz on a Varian XL-200 spectrometer using above solutions at the probe temperature of 297 K. The ^{31}P NMR chemical shifts are measured from external reference 1% TMP [161]. The spectral conditions were: 1.0 s delay time, 32 K data points, spectral width 4,000 Hz, pulse width 5.0 μs, 10 mm multinuclear probe. Approximately 10,000 scans were accumulated for each sample.

6.2 CHEMICALS

The compounds $(Autm)_n$, KSCN KSeCN and $AuBr.2H_2O$ were obtained from ICN K & K Labs., Plainview, New York. were obtained from Fluka Chemical Co. The $K^{13}CN$, $KC^{15}N$ $K^{13}C^{15}N$ (99% labeled), $NaS^{13}C^{15}N$ (50% labeled), $KSe^{13}CN$ was obtained from Merck, Sharp and

Dohme, Canada. The $KSe^{13}C^{15}N$ was obtained from Isotec Ohio, USA. The imidazolidine-2-selone (SeImt) was prepared as described in the literature [99]. Captopril and captopril disulfide were a gift from the Bristol Myers-Squibb Institute for medical research, Princeton, NJ. U.S.A. The The 99.7% D_2O, 40% NaOD in D_2O 35% DCl in D_2O, thiomalic acid (Htm), KCN, thiourea (TU), selenourea (SeU), Methanol, absolute ethanol, anhydrous ether, chloroform, acetone, dimethylsulfide, concentrated sulfuric acid, acetonitrile, dichloromethane and thiodiglycol were obtained from Fluka Chemical Co. Sodium tetrachloroaurate dihydrate ($NaAuCl_4.2H_2O$), auric acid ($HAuCl_4.4H_2O$), tricyclohexylphosphine($Cycl_3P$), tri-*i*-propylphosphine (*i*-Pr_3P), triethylphosphine(Et_3P), trimethylphosphine(Me_3P), cyclohexyldiphenylphosphine($CyclPh_2P$), tri-*o*-tolylphosphine(*o*-Tol_3P), tri-*p*-tolyl phosphine (*p*-Tol_3P), tri-*m*-tolyl phosphine (*m*-Tol_3P), *p*-tolyldiphenylphosphine(*p*-$TolPh_2P$), allyldiphenyl phosphine ($AllylPh_2P$), triphenylphosphine(Ph_3P), *tris*(cyanoethyl)phosphine (CEP), tri-1-naphthyl phosphine(Np_3P), NaSCN and $AgNO_3$ were obtained from Stream Chemical Co.

6.3 SYNTHESIS OF VARIOUS GOLD COMPLEXES

The detailed synthetic procedure of all complexes prepared in this study is given in this chapter. The synthesis has been grouped as follow:

1. Precursor complexes
2. R_3PAuCN complexes
3. $R_3PAuSCN$ complexes

4. Gold(I) captopril complex.

All reactions were carried out at room temperature unless specified. Phosphines and potassium cyanide were handled after wearing gloves in the fume hood, while reactions involving Me_2SAuCl were carried out in the darkened room due to its decomposition in presence of sunlight.

6.3.1 Precursor complexes

Synthesis of different precursor complexes of gold(I) which were used to prepare R_3PAuCN and $R_3PAuSCN$ complexes is given below.

6.3.1.1 Synthesis of R_3PAuX (X= Cl^- or Br^-) complexes

The synthesis of R_3PAuX complexes is given below:

Tri-iso-propylphosphine gold(I) chloride (i-Pr$_3$PAuCl) [168]

A solution of *i*-propylphosphine (0.75 ml, 0.63 g, 3.9 mmol) in 20.0 ml acetone was added to the solution of $HAuCl_4.4H_2O$ (0.81 g, 2.0 mmol) in 10.0 ml of a 1:1 acetone/ethanol mixture with continuous stirring under flow of nitrogen gas. The golden yellow color of solution was turned light yellow, as the solvent started to evaporate due to nitrogen gas, a white precipitate was formed. The mixture was cooled in the ice bath and the precipitates were separated by centrifugation. The *i*-Pr_3PAuCl (0.66 g, 86%) was washed with liberal excess of cold absolute ethanol and was dried under vacuum. The analysis calculated for $C_9H_{21}PAuCl$ was C=27.52% and H=5.35%, while found was C=27.45% and H=5.40%.

Triethylphosphine gold(I) chloride (Et$_3$PAuCl) [168]

A solution of ethylphosphine (0.85 ml, 0.68 g, 5.8 mmol) in 20.0 ml chloroform was added to the solution of Me_2SAuCl (1.69 g, 5.8 mmol) in 10.0 ml of chloroform with continuous stirring under flow of nitrogen gas.

After half an hour the chloroform was removed by using rotary evaporator, which gave rise to brown colored Et_3PAuCl (1.69 g, 83.7%). which was washed with cold ethanol and anhydrous ether and was dried under vacuum. The analysis calculated for $C_6H_{15}PAuCl$ was C=20.54% and H=4.28%, while found was C=20.61% and H=4.30%.

Trimethylphosphine gold(I) chloride (Me3PAuCl) [159]

The $HAuCl_4.4H_2O$ (1.59 g, 3.86 mmol) was dissolved in 20.0 ml of ethanol and was cooled in an ice bath. A cold solution of thiodiglycol (1.1 ml, 0.94 g, 7.7 mmol) in 10.0 ml of ethanol was added slowly. After stirring for 10 minutes the solution was still yellow indicating the presence of Au(III) instead of Au(I). The solution was removed from the ice bath and was stirred at room temperature. Within half an hour the solution became colorless indicating the formation of Au(I). Then a cold solution of trimethyl phosphine (0.40 ml, 0.29 g, 3.9 mmol) in ethanol was added to the gold(I) solution slowly. After stirring for 20 minutes, solution was placed in refrigerator over night. White precipitates of Me_3PAuCl (1.01 g, 85.0%) were formed, which were washed with liberal excess of cold ethanol and anhydrous ether and were dried under vacuum. The analysis calculated for C_3H_9PAuCl was C=11.67% and H=2.92%, while found was C=11.72% and H=2.87%.

Triphenylphosphine gold(I) chloride (Ph3PAuCl)

A solution of triphenylphosphine (0.89 g, 3.4 mmol) in 15.0 ml of chloroform was added to a solution of $HAuCl_4.4H_2O$ (0.70 g, 1.7 mmol) in 10.0 ml of a 1:1 acetone/ethanol mixture with continuous stirring under flow of nitrogen gas. The golden yellow colored solution turned light yellow. As the solvent started to evaporate due to nitrogen gas, a white

precipitate was formed. The mixture was cooled in ice bath and Ph_3PAuCl (0.71 g, 85%) was isolated by centrifugation, which was washed with absolute ethanol and was dried in vacuum. The analysis calculated for $C_{18}H_{15}PAuCl$ was C=43.70% and H=3.06%, while found was C=43.82% and H=3.17%.

Tri-o-tolylphosphine gold(I) bromide (o-Tol$_3$PAuBr)

A solution of gold(I) bromide (0.39 g, 1.4 mmol) in 20.0 ml of de ionized water was added to the solution of *o*-tolylphosphine (0.43 g, 1.4 mmol) in 15.0 ml of acetone with continuous stirring. Reaction took place immediately and the color of the solution changed from reddish brown to pale yellow with the formation of orange colored precipitates. The solution was stirred continuously for half an hour. The orange colored *o*-Tol_3PAuBr (0.50 g, 61%) was filtered off, washed with cold ethanol and dried under vacuum. The analysis calculated for $C_{21}H_{21}PAuBr$ was C=43.38% and H=3.62%, while found was C=43.64% and H=3.84%.

p-tolyldiphenylphosphine gold(I) bromide (p-TolPh$_2$PAuBr)

A solution of gold(I) bromide (0.86 g, 3.1 mmol) in 50.0 ml of double distilled water was added to the solution of *p*-tolyldiphenylphosphine (0.85 g, 3.1 mmol) in 20.0 ml of acetone with continuous stirring. Reaction took place immediately and the color of solution was changed from reddish brown to pale yellow with formation of yellow colored precipitates. The solution was stirred continuously for half an hour. The yellow colored *p*-$TolPh_2PAuBr$ (1.00 g, 58.5%) was filtered off, washed with liberal excess of cold ethanol and dried under vacuum. The analysis calculated for $C_{19}H_{17}PAuBr$ was C=41.24% and H=3.07%, while found was C=41.23% and H=3.08%.

Tris(cyanoethyl)phosphine gold(I) bromide (CEPAuBr)

A solution of gold(I) bromide (0.65 g, 2.4 mmol) in 30.0 ml of $CH_3CN:CH_2Cl_2$ (2:3) was added to a solution of *tris* (cyanoethyl)phosphine (0.46 g, 2.4 mmol) in 20.0 ml of $CH_3CN:CH_2Cl_2$ (2:3) with continuous stirring. The color of the solution was changed from reddish brown to yellowish orange and was stirred continuously for half an hour. Finally 40.0 ml of ethyl ether was added to the solution which gave rise to the white colored solid. The white crystalline CEPAuBr (0.43 g, 39%) was filtered off, washed with liberal excess of cold ethanol and dried under vacuum. The analysis calculated for $C_9H_{12}N_3PAuBr$ was C=22.99% and H=2.55%, while found was C=23.01% and H=2.59%.

6.3.1.2 Synthesis of dimethylsulfide gold(I) chloride (Me_2SAuCl)

In a darkened room, dimethylsulfide (0.50 ml, 6.8 mmol) was added to a solution of $HAuCl_4$ (0.62 g, 1.5 mmol) in 15.0 ml of 95% ethanol. There was a transient red color, followed by immediate formation of a white precipitate. Nitrogen gas was passed through the solution to remove excess of dimethylsulfide. After stirring for 10 minutes the solvent was light yellow, this yellow color persisted even upon addition of more dimethylsulfide. The mixture was cooled in ice bath, the precipitates were filtered, washed with liberal excess of absolute ethanol and dried under vacuum. White shiny crystalline Me_2SAuCl (0.42 g, 95%) was obtained. The analysis calculated for C_2H_6SAuCl was C=8.15% and H=2.04%, while found was C=8.20% and H=2.21%.

6.3.1.3 Synthesis of gold(I) cyanide (AuCN)

In a darkened room, Me_2SAuCl (0.37 g, 1.3 mmol) was dissolved in 20.0 ml of acetone. Under nitrogen gas, an aqueous solution of KCN (0.17 g, 2.7 mmol) was added dropwise with continuous stirring. After 10 minutes, the colorless solution was filtered to remove solid impurities. Then concentrated H_2SO_4 was added dropwise to the $K[Au(CN)_2]$ solution in fume hood due to the generation of HCN. Lemon yellow precipitates of AuCN were formed immediately, which were allowed to settle down and were separated by centrifugation. It was washed several times with double distilled water, with liberal excess of absolute ethanol, with anhydrous ether and dried in vacuum. The yellow AuCN (0.16 g, 74%) was dried under vacuum. The analysis calculated for AuCN was C=5.38% and N=6.27%, while found was C=5.39% and N=6.29%.

6.3.2 Synthesis of R_3PAuCN complexes

Synthesis of all labeled and unlabeled R_3PAuCN complexes is given below. Their C,H, N analysis, melting points, and % yields are given in Table 6.1.

Tricyclohexylphosphine gold(I) cyanide ($Cycl_3PAuCN$) [160]

Tricyclohexylphosphine (0.21 g, 0.75 mmol) was dissolved in 40.0 ml methanol at 50°C and the solution was purged with nitrogen gas. Then solid AuCN(0.18 g, 0.80 mmol) was added to the solution and was stirred continuously for one hour under nitrogen gas. The solution was then filtered to remove unreactive AuCN, while clear colorless filtrate was placed in fume hood for slow evaporation of the solvent. The white needle

TABLE 6.1 The elemental analysis, melting points and % yield of $R_3PAu^{13}C^{15}N$ complexes.

$R_3PAu^{13}C^{15}N$	Found(calcd.) (%)			M.pt. (°C)	Yield (%)
	C	H	N		
$Cycl_3PAu^{13}C^{15}N$	44.8 (45.45)	6.7 (6.55)	2.6 (2.77)	135.0	78
i-$Pr_3PAu^{13}C^{15}N$	31.64 (31.27)	5.77 (5.47)	3.80 (3.91)	108.0	54
$Et_3PAu^{13}C^{15}N$	25.08 (24.58)	4.54 (4.39)	4.16 (4.39)	109.0	41
$Me_3PAu^{13}C^{15}N$	15.94 (16.00)	2.97 (3.0)	3.86 (5.0)	201.0	80
$CyclPh_2PAu^{13}C^{15}N$	46.45 (46.42)	4.26 (4.25)	3.04 (2.95)	165.0	82
o-$Tol_3PAu^{13}C^{15}N$	51.16 (50.10)	4.12 (3.97)	3.13 (2.84)	240.0	81
p-$Tol_3PAu^{13}C^{15}N$	50.10 (50.08)	3.97 (3.94)	2.84 (2.81)	55.0	85
m-$Tol_3PAu^{13}C^{15}N$	50.10 (50.05)	3.97 (3.90)	2.84 (2.75)	137.0	86
p-$TolPh_2PAu^{13}C^{15}N$	48.11 (47.95)	3.39 (3.31)	2.95 (2.80)	68.0	69
$AllylPh_2PAu^{13}C^{15}N$	43.12 (42.89)	3.43 (3.33)	3.03 (3.11)	135.0	75
$Ph_3PAu^{13}C^{15}N$	46.23 (46.93)	3.29 (3.08)	2.81 (3.08)	205.0	90
$CEPAu^{13}C^{15}N$	29.7 (28.95)	2.9 (2.87)	14.1 (13.64)	114.0	71
$Np_3PAu^{13}C^{15}N$	58.56 (57.68)	3.30 (3.25)	2.35 (2.42)	248.0	75

like crystalline $Cycl_3PAuCN$ was recovered on complete evaporation of solvent (0.33 g, 0.66 m mol, 88%).

Tricyclohexylphosphine gold(I) cyanide ($Cycl_3PAu^{13}C^{15}N$) *[157]*

Me_2SAuCl (0.18 g, 0.62 mmol) was dissolved in 20.0 ml of acetone in darkened room. Then solid tricyclohexylphosphine (0.17 g, 0.62 mmol) was added to the solution under nitrogen gas. The tricyclohexylphosphine was dissolved readily. Then solid $K^{13}C^{15}N$ (0.04 g, 0.62 mmol) was added to the above solution and was stirred continuously for two hours under nitrogen gas. The $Cycl_3PAu^{13}C^{15}N$ was precipitated out by addition of de ionized water to the solution. These precipitates were separated by filtration and were washed with liberal excess of de ionized water to remove KCl and unreactive $K^{13}C^{15}N$. The $Cycl_3PAu^{13}C^{15}N$ precipitates were dried under vacuum (0.19 g, 59%).

Tri-i-propylphosphine gold(I) cyanide ($i\text{-}Pr_3PAuCN$) *[153]*

Tri-*i*-propylphosphine (0.04 ml, 0.2 mmol) was dissolved in 15.0 ml of acetone under continuous flow of nitrogen gas. The AuCN (0.06 g, 0.3 mmol) was then added as a solid to the above solution and was stirred continuously for one hour. The unreactive AuCN was removed by centrifugation and colorless solution was placed in fume hood for slow evaporation of solvent. The white needle like crystalline *i*-Pr_3PAuCN was recovered on complete evaporation of solvent (0.07 g, 80 %), which was washed with liberal excess of ethyl ether.

Tri-i-propylphosphine gold(I) cyanide ($i\text{-}Pr_3PAu^{13}C^{15}N$)

The *i*-Pr_3PAuCl (0.22 g, 0.56 mmol) was dissolved in 20.0 ml of acetone. The aqueous solution of $AgNO_3$ (0.10 g, 0.56 mmol) was added

dropwise to the above solution, which caused the precipitation of AgCl. The white precipitates of AgCl were removed by centrifugation and aqueous solution of $K^{13}C^{15}N$ (0.04 g, 0.56 mmol) was added to the above clear solution and was stirred continuously for one hour. The solution was then left in refrigerator overnight, after which white needle like crystalline *i*-$Pr_3PAu^{13}C^{15}N$ (0.15 g, 70%) was isolated, washed with de ionized water, ethyl ether and dried under vacuum.

Triethylphosphine gold(I) cyanide (Et$_3$PAuCN) *[64]*

The Et_3PAuCl (0.11 g, 0.30 mmol) was dissolved in 10 ml of ethanol. The aqueous solution of $AgNO_3$ (0.05 g, 0.3 mmol) was added dropwise to the above solution, which caused the precipitation of AgCl. The white precipitates of AgCl were removed by centrifugation and aqueous solution of KCN (0.02 g, 0.3 mmol) was added to the above clear solution and was stirred continuously for one hour. The solution was left in the refrigerator overnight, after which white needle like crystalline Et_3PAuCN (0.08 g, 73%) was isolated, which was washed with de ionized water, ethyl ether and dried under vacuum.

Triethylphosphine gold(I) cyanide (Et$_3$PAu^{13}C^{15}N)

Same procedure was used to prepare doubly labeled $Et_3PAu^{13}C^{15}N$ complex using $K^{13}C^{15}N$ with 75.0% yield.

Trimethylphosphine gold(I) cyanide (Me$_3$PAuCN) *[153]*

The Me_3PAuCl (0.10 g, 0.31 mmol) was dissolved in 10 ml of ethanol. The aqueous solution of $AgNO_3$ (0.05 g, 0.3 mmol) was added dropwise to the above solution, which caused the precipitation of AgCl. The white precipitates of AgCl were removed by centrifugation and aqueous solution of KCN (0.02 g, 0.3 mmol) was added to the above clear

solution and was stirred continuously for one hour. The solution was then left in refrigerator over night, after which white needle like crystalline Me_3PAuCN (0.08 g, 90%) was isolated, which was washed with de ionized water, ethyl ether and dried under vacuum.

Trimethylphosphine gold(I) cyanide ($Me_3PAu^{13}C^{15}N$)

Same procedure was used to prepare doubly labeled $Me_3PAu^{13}C^{15}N$ complex using $K^{13}C^{15}N$ with 78% yield.

Cylohexyldiphenylphosphine gold(I) cyanide ($CyclPh_2PAu^{13}C^{15}N$)

Me_2SAuCl (0.36 g, 0.12 mmol) was dissolved in 20.0 ml of acetone in darkened room under nitrogen gas. Then cyclohexyldiphenylphosphine (0.03g, 0.1 mmol) was dissolved in 10.0 ml of acetone and was then added to the above solution of Me_2SAuCl under nitrogen gas. Then aqueous solution of $K^{13}C^{15}N$ (0.01 g, 0.1 mmol) was added to the above solution and was stirred continuously for two hours under Nitrogen gas. The $CyclPh_2PAu^{13}C^{15}N$ was obtained as white precipitates on the addition of small amount of de ionized water to the solution. These precipitates were separated by filtration and were washed with liberal excess of de ionized water to remove KCl and unreactive $K^{13}C^{15}N$. The $CyclPh_2PAu^{13}C^{15}N$ (0.05 g, 85%) precipitates were dried in vacuum.

Tri-o-tolylphosphine gold(I) cyanide ($o\text{-}Tol_3PAu^{13}C^{15}N$)

The *o*-Tol_3PAuBr (0.04 g, 0.08 mmol) was dissolved in 10.0 ml of acetone. The aqueous solution of $AgNO_3$ (0.01 g, 0.08 mmol) was added dropwise to the above solution, which caused the precipitation of AgBr. The dark colored precipitates of AgBr were removed by centrifugation and aqueous solution of $K^{13}C^{15}N$ (0.01 g, 0.08 mmol) was added to the above

clear solution, which immediately gave rise to colloidal solution. It was stirred continuously for one hour. The solution was then placed under vacuum to remove the solvent completely, which gave rise to *o*-$Tol_3PAu^{13}C^{15}N$ (0.03 g, 80%) as white solid, which was washed with with liberal excess of de ionized water and ethyl ether .

Tri-p-tolylphosphine gold(I) cyanide (p-$Tol_3PAu^{13}C^{15}N$)

The Me_2SAuCl (0.07 g, 0.02 mmol) was dissolved in 20.0 ml of acetone in darkened room under nitrogen gas. Then tri-*p*-tolylphosphine (0.07 g, 0.02 mmol) was dissolved in 10.0 ml of acetone and was then added to the above solution of Me_2SAuCl under Nitrogen gas. The aqueous solution of $K^{13}C^{15}N$ (0.02 g, 0.02 mmol) was then added to the above solution and was stirred continuously for two hours under nitrogen gas. The *p*-$Tol_3PAu^{13}C^{15}N$ (.0.10 g, 76%) was obtained as white precipitate on addition of small amount of de ionized water to the solution. These precipitates were separated by filtration and were washed with liberal excess of de ionized water to remove KCl and unreactive $K^{13}C^{15}N$ then dried under vacuum.

Tri-m-tolylphosphine gold(I) cyanide (m-$Tol_3PAu^{13}C^{15}N$)

The Me_2SAuCl (0.10 g, 0.03 mmol) was dissolved in 20.0 ml of acetone in darkened room under nitrogen gas. Then tri-*m*-tolylphosphine (0.10 g, 0.03 mmol) was dissolved in 10.0 ml of acetone and was then added to the above solution of Me_2SAuCl under nitrogen gas. The aqueous solution of $K^{13}C^{15}N$ (0.02 g, 0.03 mmol) was then added to the above solution and was stirred continuously for two hours under nitrogen gas. The *m*-$Tol_3PAu^{13}C^{15}N$ (0.159 g, 84%) was obtained as white precipitate on addition of small amount of de ionized water to the solution. These

precipitates were separated by filtration and were washed with liberal excess of de ionized water to remove KCl and unreactive $K^{13}C^{15}N$, then dried under vacuum.

p-tolyldiphenylphosphine gold(I) cyanide (p-TolPh$_2$PAu^{13}C^{15}N)

The Me_2SAuCl (0.08 g, 0.03 mmol) was dissolved in 20.0 ml of acetone in darkened room under nitrogen gas. Then *p*-tolyldiphenyl phosphine (0.07 g, 0.03 mmol) was dissolved in 10.0 ml of acetone and was then added to the above solution of Me_2SAuCl under nitrogen gas. The aqueous solution of $K^{13}C^{15}N$ (0.02 g, 0.03 mmol) was then added to the above solution and was stirred continuously for two hours under nitrogen gas. The *p*-$TolPh_2PAu^{13}C^{15}N$ (.0.09 g, 70%) was obtained as white precipitate on addition of small amount of de ionized water to the solution. These precipitates were separated by filtration and were with liberal excess of de ionized water to remove KCl and unreactive $K^{13}C^{15}N$, then dried under vacuum.

Allyldiphenylphosphine gold(I) cyanide (AllylPh$_2$PAuCN)

The allyldiphenylphosphine(0.14 ml, 0.50 mmol) was dissolved in 20.0 ml of acetone and solution was purged with nitrogen gas. Then solid AuCN(0.12 g, 0.55 mmol) was added to the solution and was stirred continuously for one hour under nitrogen gas. The solution was then filtered to remove unreactive AuCN, while clear colorless filtrate was placed in fume hood for slow evaporation of the solvent. The $AllylPh_2PAuCN$ was recovered as a white solid on complete evaporation of solvent (0.21 g, 95%), which was washed with liberal excess of de ionized water, ethyl ether and dried under vacuum.

Allyldiphenylphosphine gold(I) cyanide (AllylPh$_2$PAu^{13}C^{15}N)

The Me_2SAuCl (0.13 g, 0.45 mmol) was dissolved in 20.0 ml of acetone in darkened room under nitrogen gas. Then allyldiphenylphosphine (0.13 ml, 0.45 mmol) was dissolved in 10.0 ml of acetone and was then added to the above solution of Me_2SAuCl under nitrogen gas. The aqueous solution of $K^{13}C^{15}N$ (0.03 g, 0.5 mmol) was then added to the above solution and was stirred continuously for two hours under nitrogen gas. The $AllylPh_2PAu^{13}C^{15}N$ (.0.18 g, 88%) was obtained as white precipitates on addition of small amount of de ionized water to the solution. These precipitates were separated by filtration and were washed with liberal excess of de ionized water to remove KCl and unreactive $K^{13}C^{15}N$ then dried under vacuum.

Triphenylphosphine gold(I) cyanide (Ph$_3$PAu^{13}C^{15}N)

The Ph_3PAuCl (0.15 g, 0.30 mmol) was dissolved in 20.0 ml of acetone at high temperature. The aqueous solution of $AgNO_3$ (0.05 g, 0.3 mmol) was added dropwise to the above solution, which caused the precipitation of AgCl. The white precipitates of AgCl were removed by centrifugation and aqueous solution of $K^{13}C^{15}N$ (0.02 g, 0.3 mmol) was added to the above clear solution and was stirred continuously for one hour. The solution was then cooled in ice bath, which gave rise to white needle like crystalline $Ph_3PAu^{13}C^{15}N$ (0.11 g, 75%), which was washed with de ionized water, ethyl ether and dried under vacuum.

Tris(cyanoethyl)phosphine gold(I) cyanide (CEPAu^{13}C^{15}N)

The CEPAuBr (0.09 g, 0.2 mmol) was dissolved in 20.0 ml of acetone. The aqueous solution of $AgNO_3$ (0.03 g, 0.2 mmol) was added

dropwise to the above solution, which caused the precipitation of AgBr. The white precipitates of AgBr were removed by centrifugation and aqueous solution of $K^{13}C^{15}N$ (0.01 g, 0.2 mmol) was added to the above clear solution and was stirred continuously for one hour. The solution was then cooled in ice bath, which gave rise to white needle like crystalline $CEPAu^{13}C^{15}N$ (0.06 g, 70%) was isolated, which was washed with de ionized water, ethyl ether and dried under vacuum.

Tri-1-naphthylphosphine gold(I) cyanide ($Np_3PAu^{13}C^{15}N$)

The Me_2SAuCl (0.05 g, 0.2 mmol) was dissolved in 20.0 ml of acetone in darkened room under Nitrogen gas. Then 1-naphthylphosphine (0.06 g, 0.2 mmol) was dissolved in 10.0 ml of hot acetone and was then added to the above solution of Me_2SAuCl under nitrogen gas. The aqueous solution of $K^{13}C^{15}N$ (0.01 g, 0.2 mmol) was then added to the above solution and was stirred continuously for one hour under nitrogen gas. The $Np_3PAu^{13}C^{15}N$ (.0.08 g, 75%) was obtained as white precipitates on addition of small amount of de ionized water to the solution. These precipitates were separated by filtration and were washed with liberal excess of de ionized water to remove KCl and unreactive $K^{13}C^{15}N$ then dried under vacuum.

6.3.3 Synthesis of R3PAuSCN complexes

Synthesis of all $R_3PAuS^{13}C^{15}N$ complexes, prepared during this research, is given below. Their C, H, N analysis, melting points and percent yields are given in Table 6.2.

TABLE 6.2. The elemental analysis, melting points and % yield of $R_3PAuS^{13}C^{15}N$ complexes.

$R_3PAuS^{13}C^{15}N$	Found (Calcd.) (%)				M.Pt. (°C)	Yield (%)
	C	H	N	S		
i-$Pr_3PAuS^{13}C^{15}N$	28.0 (29.0)	5.0 (5.0)	3.1 (3.5)	7.4 (7.7)	72.0	56
$Et_3PAuS^{13}C^{15}N$	21.2 (22.6)	3.9 (4.0)	3.6 (3.9)	8.7 (8.6)	50.0	65
$Me_3PAuS^{13}C^{15}N$	14.6 (14.6)	2.6 (2.7)	3.9 (4.4)	9.6 (9.6)	123.0-125.0	70
p-$TolPh_2PAuS^{13}C^{15}N$	46.9 (47.2)	3.7 (3.8)	2.4 (2.6)	5.8 (5.7)	50.0-52.0	75
$Ph_3PAuS^{13}C^{15}N$	43.2 (44.1)	2.8 (2.9)	2.8 (2.8)	5.9 6.2)	165.0	65
$CEPAuS^{13}C^{15}N$	26.7 (26.8)	2.7 (2.7)	12.9 (12.6)	7.2 (7.1)	124.0-126.0	55

Tri-i-propylphosphine gold(I) thiocyanate (i-Pr$_3$PAuS^{13}C^{15}N)

The *i*-Pr$_3$PAuCl (0.08 g, 0.2 mmol) was dissolved in 20.0 ml of acetone. The aqueous solution of $AgNO_3$ (0.03 g, 0.2 mmol) was then added to the above solution, which immediately gave rise to white precipitates of AgCl, that were filtered off. Then aqueous solution of NaS^{13}C^{15}N (50% labeled, 0.02 g, 0.2 mmol) was added to the clear filtrate and was stirred continuously for an hour. The solution was then left in fume hood to evaporate the solvent slowly. On complete evaporation of solvent white crystalline *i*-Pr$_3$PAuS^{13}C^{15}N (0.07 g, 89%) was isolated, which was washed with liberal excess of ether.

Triethylphosphine gold(I) thiocyanate (Et$_3$PAuS^{13}C^{15}N)

The Et$_3$PAuCl (0.10 g, 0.29 mmol) was dissolved in 20.0 ml of acetone. Then solid NaS^{13}C^{15}N (50% labeled, 0.02 g, 0.3 mmol) was added to above solution and was stirred continuously for half an hour. It gave rise to white precipitates of NaCl, which were filtered off and clear filtrate was placed in rotary evaporator to remove the solvent completely. Then chloroform was added to the residue, which dissolved the Et$_3$PAuS^{13}C^{15}N complex and unreactive NaS^{13}C^{15}N was left undissolved, which was filtered off and the clear filtrate was placed under vacuum to remove the solvent. The Et$_3$PAuS^{13}C^{15}N complex (0.10 g, 90%) was obtained as white solid.

Trimethylphosphine gold(I) thiocyanate (Me$_3$PAuS^{13}C^{15}N)

The Me$_3$PAuCl (0.09 g, 0.3 mmol) was dissolved in 20.0 ml of acetone. Then solid NaS^{13}C^{15}N (50% labeled, 0.03 g, 0.3 mmol) was added to above solution and was stirred continuously for half an hour. It

gave rise to white precipitates of NaCl, which were filtered off and clear filtrate was placed in rotary evaporator to remove the solvent completely. Then chloroform was added to the residue, which dissolved the $Me_3PAuS^{13}C^{15}N$ complex and unreactive $NaS^{13}C^{15}N$ was left undissolved, which was filtered off and the clear filtrate was placed under vacuum to remove the solvent. The $Me_3PAuS^{13}C^{15}N$ complex (0.08 g, 90%) was obtained as white solid.

Triphenylphosphine gold(I) thiocyanate ($Ph_3PAuS^{13}C^{15}N$)

The Ph_3PAuCl (0.07 g, 0.1 mmol) was dissolved in 20.0 ml of acetone at high temperature. The aqueous solution of $AgNO_3$ (0.02 g, 0.1 mmol) was then added to the above solution, which immediately gave rise to white precipitates of AgCl, that were filtered off. Then aqueous solution of $NaS^{13}C^{15}N$ (50% labeled, 0.01 g, 0.1 mmol) was added to the clear filtrate and was stirred continuously for an hour. The solution was then left in fume hood to evaporate the solvent slowly. On complete evaporation of solvent, white $Ph_3PAuS^{13}C^{15}N$ (0.05 g, 65%) was isolated, which was washed with liberal excess of ether.

p-tolyldiphenylphosphine gold(I) thiocyanate (p-$TolPh_2PAuS^{13}C^{15}N$)

The p-$TolPh_2PAuBr$ (0.08 g, 0.1 mmol) was dissolved in 20.0 ml of acetone. The aqueous solution of $AgNO_3$ (0.03 g, 0.1 mmol) was then added to the above solution, which immediately gave rise to dark colored precipitates of AgBr, that were filtered off. Then aqueous solution of $NaS^{13}C^{15}N$ (50% labeled, 0.01 g, 0.1 mmol) was added to the clear filtrate and was stirred continuously for an hour. The solution was then left in fume hood to evaporate the solvent slowly. On complete evaporation of

solvent cream colored *p*-TolPh$_2$PAuS^{13}C^{15}N (0.06 g, 75%) was isolated, which was washed with liberal excess of ether.

Tris(cyanoethyl)phosphine gold(I) thiocyanate (CEPAuS^{13}C^{15}N)

The CEPAuBr (0.12 g, 0.27 mmol) was dissolved in 20.0 ml of acetone. The aqueous solution of $AgNO_3$ (0.05 g, 0.3 mmol) was then added to the above solution, which immediately gave rise to dark colored precipitates of AgBr, that were filtered off. Then aqueous solution of NaS^{13}C^{15}N (50% labeled, 0.02 g, 0.3 mmol) was added to the clear filtrate and was stirred continuously for an hour. The solution was then left in fume hood to evaporate the solvent slowly. On complete evaporation of solvent white crystalline CEPAuS^{13}C^{15}N (0.08 g, 65%) was isolated, which was washed with liberal excess of ether.

6.3.4 Synthesis of gold(I) captopril

The $NaAuCl_4$ (0.12 g, 0.33 mmol) was dissolved in 20.0 ml of de ionized water and was cooled down to 0.0°C in ice bath. The aqueous solution of thiodiglycol (0.07 ml, 0.7 mmol) was added dropwise to the above solution and was stirred for half an hour, during which the color of solution was changed from golden yellow to colorless (i.e. gold(III) was reduced to gold(I)). Then aqueous solution of captopril (0.07 g, 0.3 mmol) was added dropwise to the gold(I) solution, which immediately gave rise to the white precipitate of gold(I) captopril, however solution was stirred continuously for half an hour. The white precipitate of gold(I) captopril were filtered off, washed several times with de ionized water and dried in vacuum. The melting point was found to be. 245.0°C. The analysis

calculated for $C_9H_{13}NAuNaO_3S$ is C=24.85%, H=3.00%, N=3.20% and S=7.35% while found is C=24.95%, H=3.20%, N=3.50% and S=7.62%.

REFERENCES

1. G. B. Kaufman, *Gold. Bull.* 1983, **16**, 21.
2. G. Allen *"Gold"*, Thomas Y. Cromwell & Co., New York, 1964, pp. 105-106, 228-249.
3. G. B. Kaufman, *Gold. Bull.* 1958, **18**, 31.
4. C. F. ShawIII, *Inorg. Perspect. Biol. Med.*, 1979, **2**, 287.
5. J. Forestier, *Bull. Mem. Soc. Med. Hop. Paris*, 1929, **53**, 323.
6. R. L. Kaye and R. E. Pemberton, *Arch. Int. Med.*, 1976, **136**, 1023.
7. J. W. Swingler, G. B. Bluhm and H. Duncan, *Arthritis Rheum.*, 1973, **15**, 125.
8. M. A. Mazid, M. T. Razi, P. J. Sadler, G. N. Greaves, S. J. Gurman, M. H. J. Koch and J. C. Phillips, *J. Chem. Soc., Chem. Commun.*, 1980, 1261.
9. D. T. Hill and B. M. Sutton, *Cryst. Struct. Commun.*, 1980, **9**, 679.
10. B. Vermon-Roberts, J. L. Dore, J. D. Jessop and W. J. Henderson, *Ann. Rheum. Dis.*, 1976, **35**, 477.
11. A. J. Lewis and D. T. Walz, *Prog. Med. Chem.*, 1982, **19**, 1.
12. A. Larber and T. M. Simon, *Gold. Bull.* 1979, **12**, 149.
13. M. J. DiaMartino and D. T. Walz, *Inflamation,* 1977, **2**, 131.
14. D. H. Brown and W. E. Smith, *Chem. Soc. Rev.*, 1980, **9**, 217.
15. C. F. Shaw III, *Comments Inorg. Chem.*, 1989, **8**, 233.

16. G. G. Graham, J. R. Bales, M. C. Grootveld and P. J. Sadler, *J. Inorg. Biochem.*, 1985, **25**, 163.
17. A. A. Isab, A. L. Horman, M. T. Coffer and C. F. Shaw III, *J. Amer. Chem. Soc.*, 1988, **110**, 3278.
18. A. A. Isab, *J. Inorg. Biochem.*, 1992 **45**, 145.
19. G. Lewis and C. F. Shaw III, *Inorg. Chem.*, 1986, **25**, 58.
20. G. G. Graham, T. M. Haavisto, H. M. Jones and G. D. Champion, *Biochem. Pharmacol.*, 1984 **33**, 1257.
21. D. W. James, N. W. Ludvigsen, L. G. Cleland and S. C. Milazzo, *J. Rheum.*, 1982, **9**, 532.
22. D. Lewis, H. A. Capell, C. J. Mcneil, M. S. Iqbal, D. H. Brown and W. E. Smith, *Ann. Rheum. Dis.*, 1983, **42**, 566.
23. N. S. Pennys, W. E. Eaglestein and P. Frost, *Arch. Dermatol.*, 1976, **112**, 1467.
24. N. S. Pennys, W. E. Eaglestein and P. Frost, *Arch. Dermatol.*, 1976, **112**, 185.
25. N. S. Pennys, W. E. Eaglestein, S. Indigin and P. Frost, *Arch. Dermatol.*, 1973, **108**, 56.
26. W. D. Block, O. H. Buchanan and R. H. Freyberg, *J. Pharm. Exp. Ther.*, 1941, **73**, 200.
27. W. D. Block, O. H. Buchanan and R. H. Freyberg, *J. Pharm. Exp. Ther.*, 1942, **74**, 355.
28. E. G. McQueen and P. W. Dykes, *Ann. Rheum. Dis.* 1969, **28**, 437.
29. H. A. Wartz, J. E. Christiansen and F. N. Andrews, *Am. J. Physiol.* 1960, **199**, 67.
30. J. S. Lawrence, *Ann. Rheum. Dis.* 1961, **20**, 341.

31. R. H. Freyberg, W. D. Block and S. Levy, *Ann. Rheum. Dis.* 1942, **1**, 77.

32. E. A. Tonna, G. Brecker, E. P. Cronkite and I. L. Schwartz, *Arthr. Rheum.*, 1963, **6**, 1.

33. J. J. Bertrand, H. Waine and C. A. Tobias, *J. Lab. Clin. Med.*, 1948, **33**, 1133.

34. R. C. Gerber, H. E. Paulus and M. Lederer, *Arthr. Rheum.*, 1972, **15**, 622.

35. F. E. Krusius, A. Markkanen and P. Peltola., *Ann. Rheum. Dis.* 1970, **29**, 232.

36. N. L. Gottlieb, P. M. Smith and E. M. Smith, *Arthr. Rheum.*, 1972, **15**, 16.

37. P. M. Smith, E. M. Smith and N. L. Gottlieb, *J. Lab. Clin. Med.*, 1973, **82**, 930.

38. E. S. Botzvadza, L. M. Movlishvili and E. N. Ghinturi, *Phys. Med. Biol.*, 1969, **14**, 19.

39. A. Loorber, R. L. Cohen, C. Chang and H. E. Anderson, *Arthr. Rheum.*, 1968, **11**, 170.

40. W. E. Spiar, A. H. Sommer and J. G. White, *Phys. Rev.*, 1959, **115**, 57.

41. J. Knecht, R. Fischer, H. Overhof and F. J. Hensel, *J. Chem. Soc., Chem. Commun.* 1978, **21**, 905.

42. W. J. Peer and J. J. Logwski, *J. Am. Chem. Soc.* 1978, **100**, 6260.

43. A. M. Manzany and J. P. Fackler, *J. Am. Chem. Soc.* 1984, **106**, 801.

44. H. Schmidbaur, J. R. Mnadl, A. Frank and G. Huttner, *Chem. Ber.*, 1976, **109**, 466.

45. K. Leary, A. Zalkin and N. Batlett, *Inorg. Chem.*, 1974, **14**, 775.

46. P. J. Sadler, *Struct. Bonding*, 1976, **29**, 171.

47 P. G. Jones, J. J. Guy and G. M. Sheldrick, *Acta Cryst.* 1975, **B31**, 2687.

48. M. R. Caira, L. R. Nassimbeni and A. L. Rodgers, *Acta Cryst.* 1975, **B31**, 112.

49. G. Bandolini, D. A. Cemente and G. Marangoni, *J. Chem. Soc. Dalton Trans.*, 1973, 886.

50. G. E. Glass, J. H. Konnert, M. G. Miles and R. S. Tobias, *J. Am. Chem. Soc.* 1970, **90**, 1131.

51. S. Komiya, J. C. Huffman and J. K. Kochi, *Inorg. Chem.*, 1977, **16**, 1253.

52. E. S. Clark, D. H. Templeton and C. M. McGillavry, *Acta Cryst.* 1958, **11**, 284.

53. V. F. Duckworth and N. C. Stephenson, *Inorg. Chem.*, 1969, **8**, 1661.

54. R. Timkovich and A. Tulinsky, *Inorg. Chem.*, 1977, **16**, 962.

55. W. T. Robinson and E. Sinn, *J. Chem. Soc. Dalton Trans.*, 1975, 726.

56. G. E. Coates, C. Kowala and J. M. Swan, *Austr. J. Chem.*, 1966, **19**, 539.

57. H. A. Brown, *J. Am. Chem. Soc.*, 1927, **49**, 958.

58. H. Reuben, A. Zalkin, M. D. Faltens and D. H. Templeton, *Inorg. Chem.*, 1974, **13**, 1836.

59. J. deP.Teresa, *An. Fis. Quim.*, 1944, **40**, 66.

60. C. Kowala and J. M. Swan, *Austr. J. Chem.*, 1966, **19**, 208.

61. P. A. Duddel, J. G. Evans, P. L.Goggin, R. J. Goodfellow, A. J. Rest and J. G. Smith, *J. Chem Soc. A*, 1969, 2134.

62. P. G. Jones, *Gold Bull.*, 1981, **14**, 3.

63. P. L. Bellon, M. Manassero and M. Sansoni, *Ric. Sci.*, 1969, **39**, 173.

64. A. L. Hermann-Arendt and C. F. Shaw III, *Inorg. Chem.*, 1990, **29**, 4683.

65. A. K. H. Al-Saady, K. Moss, C. A. McAuliffe and R. V. Parish, *J. Chem. Soc. Dalton Trans.*, 1984, 1609.

66. R. Heese and P. Jennische, *Acta Chem. Scand.*, 1972, **26**, 3855.

67. W. S. Crane and H. Beall, *Inorg. Chim. Acta*, 1978, **31**, L469.

68. N. C.Baenziger, K. T. Dittmore and J. R. Doyle, *Inorg. Chem.*, 1974, **13**, 805.

69. P. G. Jones, *Acta Cryst.* 1980, **B36**, 3105.

70. R. C. Elder, E. H. K. Zeiher, M. Onady and R. R. Whittle, *J. Chem. Soc., Chem. Commun.*, 1981, 900.

71. P. G. Jones, A. G. Maddock, M. J. Mays, M. M. Mir and A. F. Williams, *J. Chem. Soc. Dalton Trans.*, 1977, 1434.

72. H. A. Bent, *Chem. Rev.*, 1961, **61**, 275.

73. J. K. Kochi "*Organometallic Mechanisms and catalysis*" Academic Press, New York, 1978, pp. 534,566.

74. L. E. Orgel, *J. Chem. Soc.* 1958, 4186.

75. G. M. Bancroft, T. Chan, R. J. Puddephatt and J. S. Tse, *Inorg. Chem.*, 1982, **21**, 2946.

76. S. K. Chastian and R. W. Mason, *Inorg. Chem.*, 1982, **21**, 3717.

77. F. N. Ghadially, *Ann. Rheum. Dis.*, 1976, **35**, 67.

78. B. V. Roberts, *Ann. Rheum. Dis.*, 1976, **35**, 477.

79. W. E. Smith and J. Reglinski, *Perspect. Bioinorg. Chem.*, 1991, **1**, 183.

80. R. C. Elder, M. K.Eidsness, C. F. Sahaw III and N. A. Schaffer, *ACS Symp. Ser.*, 1983, No.209,385.

81. W. F. Keen, C.J. L. Lock, P. J. Rooney and W. W. Buchanan, *Clin. Exp. Rheum.*, 1984, **2**, 321.

82. A. A. Isab and P. J. Sadler, *J. Chem. Soc. Dalton Trans.* 1981, 1657.

83. R. C. Elder and M. K.Eidsness, *Chem. Rev.*, 1987, **87**, 1027.

84. R. C. Elder, K. Ludwing, J. N. Cooper and M. K.Eidsness, *J. Am. Chem. Soc.*, 1987, **107**, 5024.

85. G. Lewis and C. F. Shaww III, *Inorg. Chem.*, 1986, **25**, 58.

86. J. Reglinski, S. Hoey and W. Smith., *Inorg. Chim. Acta*, 1988, **152**, 261.

87. A. A. Isab and P. J. Sadler, *J. Chem. Soc., Chem. Commun.*, 1976, 1051.

88. A. A. Isab and P. J. Sadler, *J. Chem. Soc. Dalton Trans.*, 1982, 135.

89. A. A. Isab, *J. Chem. Soc. Dalton Trans.*, 1986, 1049.

90. A. A. Isab, *Inorg. Chim. Acta*, 1987, **135**, 19.

91. C. F. Shaww III, N. A. Schaeffer, R. C. Elder, M. K.Eidsness, J. M. Trooster and G. H. M. Callis, *J. Am. Chem. Soc.*, 1984, **106**, 3511.

92. G. Otiko, M. T. Razi, P. J. Sadler, A. A. Isab and D. L. Rabenstein, *J. Inorg. Biochem.*, 1983, **19**, 227.

93. A. A. Isab and A. P. Arnold, *J. Coord. Chem.*, 1989, **20**, 95.

94. A. A. Isab, *Transition Met. Chem.*, 1994, **19**, 495.

95. R. D. Hancock, N. P. Finklestein and A. J. Avers, *Inorg. Nucl. Chem.*, 1972, **34**, 3747.

96. A. R. Pettitgrew and G. S. Fell, *Clin. Chem.*, 1973, **19**, 466.

97. J. Chaudiere and A. L. Tappel, *J. Inorg. Biochem.*, 1984, **20**, 313.

98. C. J. Dillard and A. L. Tappel, *J. Inorg. Biochem.*, 1986, **28**, 13.

99. F. A. Devillanova and G. Verani, *Rend. Sem. Fac. Sci. Univ. Cagliari*, 1977, **47**, 255.

100. A. A. Isab and P. J. Sadler, *Biochem. Biophys. Acta*, 1977, **492**, 322.

101. D. R. Goddadrd, B. D. London, S. O. Ajaysi and M. J. Cambell, *J. Chem. Soc. A*, 1969, 506.

102. D. R. Goddadrd and S. O. Ajaysi, *J. Chem. Soc. A*, 1971, 2673.

103. A. A. Isab, *Inorg. Chim. Acta*, 1984, **91**, L35.

104. A. A. Isab, *Transition Metal Chem.*, 1989, **14**, 235.

105. M. T. Fairhurst and D. L. Rabenstein, *Inorg. Chem.*, 1975, **14**, 13.

106. A. A. Isab and A. P. Arnold, *J. Coord. Chem.* 1985, **14**, 73.

107. W. E. Smith, J. Reglinski, S. Hoey, D. H. Brown and R. D. Sturrock, *Inorg. Chem.*, 1990, **29**, 5190.

108 A. P. Arnold, K. S. Tan and D. L. Rabenstein, *Inorg. Chem.*, 1986, **25**, 2433.

109 D. L. Rabenstein, M. C. Tourangeau and C. A. Evans, *Can. J. Chem.*, 1976, **54**, 2518.

110 A. J. Carty, S. F. Malone, N. J. Taylor and A. J. Canty, *J. Inorg. Biochem.*, 1983, **18**, 291.

111. V. V. Skopenko, G. V. Tsintsadze and E. I. Ivanova, *Russ. Chem. Rev.*, 1982, **51**, 21.

112. A. A. Isab, *J. Inorg. Biochem.*, 1992, **46**, 145.

113. A. A. Isab , I. H. Gazi and A. Al-Arfaj, *J. Chem. Soc. Dalton Trans.*, 1993, 841.

114. M. G. Kanatzidis and S. P. Haung, *Inorg. Chem.*, 1989, **28**, 4467.

115. A. A. Isab , I. H. Gazi, M. I. M. Wazeer and H. Perzanowski, *J. Inorg Biochem.*, 1993, **50**, 299.

116. Y. Park and M. G. Kanatzidis, *Angew. Chem. Intl. Ed. Engl.*, 1990, **29**, 914.

117. M. G. Kanatzidis, *Comments Inorg. Chem.*, 1990, **10**, 161.

118. S. P. Haung and M. G. Kanatzidis, *Inorg. Chem.*, 1991, **30**, 3572.

119. M. A. Ondetti, B. Rubin and D. W. Cushman, *Science*, 1977, **196**, 441.

120. D. W. Cushman, H. S. Cheung, E. F. Sabo and M. A. Ondetti, *Prog. Cardiovasc. Dis.*, 1978, **21**, 176.

121. L. T. Skeggs, F. E. Dorer, J. R. Kahn, K. E. Lentz and M. Levine, *Am. J. Med.*, 1976, **60**, 737.

122. B. H. Migdalof, K. K. Wong, S. J. Lan, K. J. Kripalani and S. M. Singhvi, *Fed. Proc., Fed. Am. Soc. Exp. Biol.*, 1980, **39**, 757.

123. S. J. Lan, S. H. Weinstein and B. H. Migdalof, *Drug. Metab. Dispos.*,1982, **10**, 306.

124. B. K. Park, P. S. Garbowski, J. H. K. Yeung and A. M. Breckenridge, *Biochem. Pharmacol.*, 1982, **31**, 1755.

125. M. F. R. Martin, F. McKenna, H. A. Bird, K. E. Surrall, J. S. Dixon and V. Wright, *Lancet*, 1984, **1**, 1325.

126. F. Sicuteri, *Adv. Exp. Med. Biol.*, 1983, **156B**, 1141.

127. V. Madison and J. Schellman, *Biopolymers*, 1970, **9**, 511.

128. J. T. Gerig, *Biopolymers*, 1971, **10**, 2435.

129. W. E. Stewart and T. H. Siddal III, *Chem. Rev.*, 1970, **70**, 517.

130. C. H. Hassall, A. Krohn, C. J. Moody and W. A. Thomas, *J. Chem. Soc., Perkin Trans.*, 1984, **1**, 155.

131. C. A. Evans and D. L. Rabenstein, *J. Am. Chem. Soc.*, 1974, **96**, 7312.

132. D. L. Rabenstein and A. A. Isab, *Anal. Chem.*, 1982, **54**, 526.

133. M. A. Hughes, G. L. Smith and D. R. Williams, *Inorg. Chim. Acta*, 1985, **107**, 247.

134. G. L. Christie, M. A. Hughes, S. B. Rees and D. R. Williams, *Inorg. Chim. Acta*, 1988, **151**, 215.

135. A. A. Isab, *J. Chem. Soc. Dalton Trans.*, 1991, 449.

136. D. H. Brown, G. McKlinely and W. E. Smith, *J. Chem. Soc., Dalton Trans.*, 1977, 1874.

137. D. T. Hill, B. M. Sutton, A. A. Isab, T. Razi, P. J. Sadler, J. M. Trooster and G. H. M. Callis, *Inorg. Chem.*, 1983, **22**, 2936.

138. L. F. Larkworthy and D. Sattari, *J. Inorg. Nucl. Chem.*, 1980, **42**, 551.

139. P. R. Srinivasan and R. L. Lichter, *J. Magn. Resonance*, 1977, **28**, 227

140. G. B. Butler, U. S. Patent No.3288770, 1966.

141. K. L. Brown and S. Satyanarayana, *Inorg. Chem.*, 1992, **31**, 1366.

142. K. L. Brown and S. Satyanarayana, *J. Am. Chem. Soc.*, 1992, **114**, 5674.

143. D. A Keire and D. L. Rabenstein, *Bioorg. Chem.*, 1989, **17**, 257.

144. J. J. Pesek and W. R. Mason, *Inorg. Chem.*, 1979, **18**, 924.

145. M. Sano, Y. Yoshikawa and H. Yamtera, *Inorg. Chem.*, 1982, **21**, 2521.

146. P. L. Bellon, M. Manassero and M. Sansoni, *Ric. Sci.*, 1969, **39**, 173.

147. P. D. Gavens, J. J. Guy, M. J. Mays and G. M. Sheldrick, *Acta Cryst.* 1977, **B33**, 137.

148. N. C. Baenziger, W. E. Bennett and D. M. Soboroff, *Acta Cryst.*, 1976, **B32**, 962.

149. S. Ahrland, B. Noren and A. Oskarsson, *Inorg. Chem.*, 1985, **24**, 1330.

150. S. Al-Baker, W. E. Hill and C. A. McAuliffe, *J. Chem. Soc., Dalton Trans.*, 1977, 8.

151. R. V. Parish, O. Parry and C. A. McAuliffe, *J. Chem. Soc., Dalton Trans.*, 1981, 2098.

152. E. L. Muetterties and C. W. Allegranti, *J. Am. Chem. Soc.*, 1970, **92**, 4114.

153. A. L. Hormann, C. F. Shaw III, D. W. Bennett and W. M.Reiff, *Inorg. Chem.*, 1986, **25**, 3953.

154. C. A. Tolman, *Chem. Rev.*, 1977, **77**, 313.

155. G. G. Graham, T. M. Havisto, P. J. McNaught, C. D. Brown and G. D. Champion, *J. Rheum.*, 1982, **4**, 527.

156. P. W. Derby and J. Wilson, *J. Ophthalmol.*, 1967, **51**, 336.

157. L. G. Vaughan, U. S. Patent 3,661,959, May 9, 1972.

158. C. F. Shaw III, M. P. Cancro and I. S. Butler, *J. Labelled Compd. Radiopharm.*, 1979, **16**, 827.

159. J. A. Muir, M. M. Mariel and L. B. Pulgar, *Acta Cryst.*, 1985, **C41**, 1174.

160. S. Al-Baker, W. E. Hill and C. A. McAuliffe, *J. Chem. Soc., Dalton Trans.*, 1986, 1297.

161. A. A. Isab, C. F. Shaw III, J. D. Hoeschele and J. Locke, *Inorg. Chem.*, 1988, **27**, 3588.

162. The NMR program liberary, The Science and Engineering Research Council, Daresbury Lab., Cheshire, U. k.

163. D. A. Brown, J. P. Chester, N. J. Fitzpatrick and I. J. King, *Inorg. Chem.*, 1977, **16**, 2497.

164. E. O. Fischer, R. L. Keiter, L. Krauss and J. G. Verkade, *J. Organomet. Chem.*, 1972, **C7**, 37.

165. S. Otsuka and T. Yoshida, *J. Am. Chem. Soc.*, 1977, **99**, 2134.

166. G. S. Zhdanov and E. A. Shugan, *Acta Physiochem. U.S.S.R.* 1945, **20**, 253.

167. F. Stocco, G. C. Stocco, W. M. Scovell and R. S. Tobias, *Inorg. Chem.* 1971, **10**, 2639.

168. C. A. McAuliffe, R. V. Parish and P. D. Randall, *J. Chem. Soc. Dalton Trans.* 1979, 1730.

169. F. Basolo, W. H. Baddley and J. L. Burmeister, *Inorg. Chem.*, 1964, **3**, 1202.

170. J. L. Burmeister, *The Chemistry and Biochemistry of Thiocyanic Acid and its derivatives'*, A. A. Newman, Ed., Academic Press,

pp. 68-130 (1975).

171. A. H. Norbury, *Adv. Inorg. Chem. Radiochem.*, 1975, **17**, 231.

172. R. G. Pearson, *Inorg. Chem.*, 1973, **12**, 712.

173. J. L. Burmeister and J. C. Lim, *J. Chem. Soc. Chem. Comm.*, 1968, 1346.

174. N. J. DeStefano and J. L. Burmeister, *Inorg. Chem.*, 1971, **10**, 998.

175. M. M. El-Etri and W. M. Scovell, *Inorg. Chem.*,, 1990, **29**, 480.

176. J. L. Burmeister and J. B. Melpolder, *J. Chem Soc. Chem. Comm.*, 1973, 613.

177. J. B. Melpolder and J. L. Burmeister, *Inorg. Chim. Acta*, 1981, **49**, 115.

178. P. N. Dickson, A. Wehlri and G. Geier, *Inorg. Chem.*, 1988, **27**, 2921.